ithreeinstitute

Connecting the dots of the bacterial cell cycle: a potential role for Spo0J in Z ring positioning

Isabella Veronica Hajduk

A thesis submitted in fulfilment of the requirements for the degree of Doctor of Philosophy

February 2018

UTS
UNIVERSITY OF TECHNOLOGY SYDNEY

Certificate of Authorship/Originality

I, Isabella Veronica Hajduk, certify that the work in this thesis has not previously been submitted for a degree nor has it been submitted as part of requirements for a degree except as fully acknowledged within the text.

I also certify that the thesis has been written by me. Any help that I have received in my research work and the preparation of the thesis itself has been acknowledged. In addition, I certify that all information sources and literature used are indicated in the thesis.

This research is supported by an Australian Government Research Training Program Scholarship.

Production Note:
Signature removed prior to publication.

_____

Isabella Hajduk, February 2018

Acknowledgements

What a journey this has been. I have so many people to thank that have come along on this ride with me. First and foremost, my supervisor, mentor and inspiring friend and woman, Liz Harry. Thank you for all your guidance, love and support over all these years on all fronts: scientific, mental and emotional. Thank you for picking me up on the bad days and showering me with praise on the good ones. Thank you for also introducing me to the cutest kitties in the world!

Thank you to my co-supervisor and original lab mentor back in the day, Chris Rodrigues. You are an absolute force to be reckoned with. Thank you for keeping me on my toes scientifically, and for igniting in me the fire for science both in the past and the present. Also thank you to both Liz and Chris for all your feedback and drafting of this thesis.

Thank you to all the Harry lab family: immediate and extensive, past and present. Thank you for accepting my high expectations for morning tea, but my goodness, we've had some good food over the last few years! Thank you for the laughs, love and support, both in and out of the lab. Also special thank you to Kevin, my first honours student, and the best student anyone could ask for – thanks mate!

Thank you to my PhD crew. Thank you for all the caffeine over the years, but mostly thank you for listening to me vent and sharing in my PhD woes. A special thanks to Kate, Jacqueline and Krish, my immediate PhD family, for all the laughs and food (especially from Krish)! Thank you to Cyn, Jen and Sue for cheering me on and providing priceless advice over the last few years. To my non-PhD friends, I'm sorry for being so MIA over the years, but thank you for still sticking by me and I promise my ghosting days are coming to an end!

A huge thanks to my family including mum, Rob, dad, and Ciocia for always trying to understand what I do, but also for your patience and support. I especially thank my mum for being the bestest buddy and mum anyone could ask for. You have been an absolute champion with your love and support over all these years.

To my darling partner Michael, I could not ask for a better person to have by my side through this adventure. I can't put into words what you mean to me, and I will be forever grateful for our time together. I can't wait to explore the post-PhD life with you <3 >|0

Finally, I would also like to thank the Australian Commonwealth Government Department of Industry for the Australian Postgraduate Award Scholarship I received throughout my PhD candidature.

Abstract

Cell division is of utmost importance for the propagation of all living organisms. In bacteria, the earliest stage of cell division is the formation of the cytokinetic Z ring at the division site at the cell centre (midcell), which must be tightly co-ordinated with chromosome replication and segregation to ensure that each newborn cell receives a full complement of the genetic material. What still eludes us is how bacterial cells position their division site so precisely at the cell centre to enable the production of two genetically identical daughter cells.

The current understanding of how bacterial cells position their division site is that it occurs via the combination of two negative regulators, the Min system and nucleoid occlusion mediated by the protein Noc. These two systems act by preventing the Z ring from forming at incorrect positions, either at the cell poles or within the vicinity of the chromosome, respectively. The overall result is that the two systems prevent the Z ring from forming anywhere other than the cell centre. However, as discovered recently, they do not define the division site, suggesting the existence of other regulatory mechanisms for midcell Z ring assembly. So what does define the division site? It has been shown in *Bacillus subtilis* that Z ring assembly may be coupled with the early stages of DNA replication and recent work in this area has led to the proposed Ready-Set-Go model.

The Ready-Set-Go model proposes a putative link between Z ring positioning and DNA replication such that the progress through the initiation phase of DNA replication promotes an increase in ability of the Z ring to assemble midcell. Specifically, mutants blocked at an early stage of initiation lead to fewer midcell Z rings than those blocked at later stages of initiation. Importantly, this correlation between DNA replication initiation progression and Z ring position is only observed in *noc* mutants. Interestingly the observations that led to this model also hinted at an alternative possibility: mechanisms linked to chromosome organisation may also impact Z ring positioning. Thus the primary objective of the work presented in this

thesis was to obtain a better understanding of the link between the early stages of DNA replication and cell division in the model organism *B. subtilis*, and how chromosome organisation plays into this link. To explore this possibility further, and ultimately test the validity of the Ready-Set-Go model, this thesis examined the role of Soj and Spo0J, two players with distinct roles in the regulation of DNA replication initiation and chromosome organisation, in Z ring positioning using the same conditions that led to the Ready-Set-Go model. Surprisingly, a *spo0J noc* double mutant, but not a *soj noc* double mutant, allows for wild-type levels of midcell Z ring assembly, regardless of the block imposed at the initiation stage of DNA replication. This suggests that the ability to assemble a Z ring at midcell is not linked to the progression of the initiation stage of DNA replication, thus challenging the idea of a link between DNA replication initiation and Z ring position. Importantly, this result and others, also suggest a role for Spo0J in the regulation of Z ring position.

To start to elucidate how Spo0J plays into the regulation of Z ring position, Z ring positioning was examined in cells blocked at an early event of DNA replication initiation that also harbor point mutants of Spo0J impacting its function in DNA replication initiation through *soj* or points mutants that impact its function in the recruitment of SMC (required to organise the chromosome). Interestingly, this data and others support two models for how Spo0J may function in Z ring positioning: Spo0J, like Noc, is a nucleoid occlusion protein or Spo0J-mediated chromosome organisation blocks midcell Z ring assembly by a generating a nucleoid morphology that inhibits midcell Z ring assembly. Both models are discussed and contrasted in detail in light of recent advances in the understanding of bacterial chromosome organisation.

Collectively, this thesis challenges the long-standing idea of a link between DNA replication initiation and Z ring positioning and creates a solid foundation for future studies examining how chromosome organisation impacts Z ring positioning.

Table of Contents

Table of Figures and Tables

Table of Figures

Table of Tables

Publications

Journal articles

Monahan LG, Hajduk IV, Blaber SP, Charles IG, Harry EJ (2014) Coordinating Bacterial Cell Division with Nutrient Availability: a Role for Glycolysis. *mBio* **5**

Hajduk IV, Rodrigues CDA, Harry EJ (2016) Connecting the dots of the bacterial cell cycle: Coordinating chromosome replication and segregation with cell division. *Seminars in Cell & Developmental Biology* **53:** 2-9

Conference proceedings

Poster presentation 2014
Australian Society for Microbiology Annual Scientific Meeting

Poster presentation 2014
Gordon Research Conference, Vermont

Poster presentation 2013
BacPath 12

Poster presentation 2013
Federation of European Microbiology Societies

Oral presentation 2012
12th East Coast Bacillus Meeting

Poster presentation 2012
29th RNSH/UTS/USYD Scientific Research Meeting

Poster presentation 2011
28th RNSH/UTS/USYD Scientific Research Meeting

Abbreviations

AGRF	Australian Research Genome Facility
Ab	antibody
B.	*Bacillus*
bp	base pair(s)
BP	band pass
BSA	bovine serum albumin
cat	chloramphenicol
CFP	cyan fluorescent protein
cm	centimetres
CCD	charged coupled device
DAPI	4'6-diamidino-2-phenylindole
DNA	deoxyribonucleic acid
E.	*Escherichia*
erm	Erythromycin
et al.	and others
FRAP	fluorescence recovery after photobleaching
fts	filamentation temperature sensitive
g	centrifugal force
g	gram(s)
GFP	green fluorescent protein
GMD	germination medium defined
IFM	immunofluorescence microscopy
IgG	Immunoglobulin G
IPTG	isopropyl-1-thio-β-D-galactopyranoside
kan	Kanamycin
L	litre(s)
LP	long pass
M	moles per litre
MQW	Milli-Q purified water
MSA	mineral salts A
NA	numerical aperture
N/A	not applicable

neo	Neomycin
OD_x	optical density at (x refers to the wavelength in nm)
P	probability
P_{xyl}	xylose-inducible promoter
PAB	penassay antibiotic medium 3 broth
PAGE	polyacrylamide gel electrophoresis
PBP	penicillin binding protein
PBS	phosphate buffered saline
PCR	polymerase chain reaction
pH	power of Hydrogen
phleo	phleomycin
RNA	ribonucleic acid
ROW	reverse osmosis purified water
rpm	revolutions per minute
RT	room temperature
SDS	sodium dodecyl sulfate
SEM	standard error of the mean
spp.	species
spc	spectinomycin
TBAB	tryptose blood agar base
tet	tetracycline
thy^-	thymine auxotroph
Tris	tris(hydroxymethyl)methylamine
Trp	L-Tryptophan
ts	temperature sensitive
U	units (enzyme activity)
UV	ultraviolet
V	volt(s)
v/v	volume per volume
w/v	weight per volume
YFP	yellow fluorescent protein
µ	micro- (10^{-6})

UNIVERSITY OF TECHNOLOGY SYDNEY

Chapter 1.
Introduction

ithreeinstitute

1.1 Preface

Cell division (or cytokinesis) is a process central to the continued survival of all living organisms. While the eukaryotic cell cycle has been well defined, the mechanisms by which bacterial cells divide to generate viable, newborn cells is more complex than originally thought, and many aspects have yet to be elucidated. In bacteria, cell division occurs via the coordinated in-growth of the cell envelope layers, including the peptidoglycan (PG; cell wall) and membrane layers to form a septum in the middle of the cell (midcell). This ultimately leads to the splitting of the progenitor cell into two identical daughter cells (Adams & Errington, 2009; Haeusser & Margolin, 2016; Harry et al, 2006). Septum formation is tightly regulated, as this process must be temporally and spatially coupled with the replication of the genetic material to guarantee the production of viable offspring. Unlike the eukaryotic cell, the bacterial cell has been long been perceived to lack internal structure or organisation. Yet continued advances in microscopy have revealed otherwise. For example, despite not being enclosed by a nuclear membrane, the chromosome exists in a compact conformation, occupying a defined location within the cell, similar to that of the eukaryotic nucleus, hence the name nucleoid (Thanbichler et al, 2005).

What still eludes us is how bacterial cells regulate the division process. How do they position the division site at midcell, and how do they coordinate this with chromosome replication to ensure equal partitioning of genetic material into newborn cells? Answering these questions is important. With the continued emergence of antibacterial resistance around the world, the search for novel antibacterial targets is crucial. By understanding the mechanisms behind bacterial cell division, it allows us to discover and identify essential cell division proteins which have not been targeted by antibacterial drugs (Margalit et al, 2004; Tan et al, 2012; Vollmer, 2006). Also, it is a fundamental biological process that is worth studying in its own right.

This thesis focuses on the processes and regulation of cell division in bacteria, specifically in its coordination with DNA replication and chromosome segregation. Recent studies have proposed that the ability of bacterial cells to position the Z ring (a prerequisite for septation) precisely at the division site at midcell is linked to the early stages of DNA replication (Harry et al, 1999; Moriya et al, 2010). This led to the proposed 'Ready-Set-Go' model, which suggests that as initiation of DNA replication progresses, leading up to the assembly of the replication machinery, the cell has an increase in potential to form a Z ring at midcell (Moriya et al, 2010). The current question is how does this link between DNA replication and positioning the division site at midcell come about? Given the close relationship between DNA replication and chromosome segregation, it is likely that chromosome segregation, or proteins involved in this process play into this link. Therefore, the aim of the thesis is to shine light onto whether, and how, chromosome segregation proteins might play into this link.

Declaration

I declare that the following publication included in this thesis in lieu of a chapter meets the following criteria:

- The majority of the content in the following publication included in this chapter has been planned, executed and prepared for publication by me. For detailed contribution, please refer to statement below.
- The work presented here has been peer reviewed and accepted for publication.
- The initial draft of the work has been written by me and any subsequent changes in response to co-authors and editors reviews were performed by me.

Publication title: Connecting the dots of the bacterial cell cycle: Coordinating chromosome replication and segregation with cell division

Authors: Isabella V Hajduk, Christopher D Rodrigues, Elizabeth J Harry

Author's contributions: Isabella wrote the paper and edited all drafts of the paper. Elizabeth and Christopher both read and provided comments on the drafts. Christopher also created the paper figures.

Journal name: Seminars in Cell & Developmental Biology
Volume/ page numbers: Volume 53, pages 2-9
Status: Published May 2016
DOI: 10.1016/j.semcdb.2015.11.012

I declare that the publication above meets the requirements to be included in the thesis.

Candidate's name: Isabella Hajduk

Candidate's signature:

Date (dd/mm/yy):

1.2 Introduction

Survival of any cellular organism relies on the efficient coordination of chromosome replication with cell division to produce viable daughter cells. The ordering of distinct events of cell growth, chromosome replication, chromosome segregation and cytokinesis (cell division) is fundamental to the cell cycle in actively dividing eukaryotic cells and occurs through checkpoints that ensure completion of a prior event before initiation of a subsequent event. However, in the cell cycle of bacteria dividing under high nutrient or high growth conditions, the events of cell growth, chromosome replication, chromosome segregation and the assembly of the division machinery at the division site occur simultaneously. The chromosome begins a subsequent round of replication prior to the completion of the first, a mechanism termed multifork replication. As the round of replication nears completion, the division machinery accumulates and assembles at the division site in preparation for septation, although the subsequent splitting of the daughter cells is held off until midcell has been cleared of DNA. The simultaneous nature of these cell cycle events in bacteria makes advances in this area challenging due to the difficulty in separating these processes and, despite intense investigation over several decades, the exact mechanism as to how bacteria spatially and temporally couple septum formation with the replication and segregation of the genetic material is not yet clearly understood. This review focuses on the current evidence of a coordinating link between these processes in *Bacillus subtilis* (Gram-positive model system) and *Escherichia coli* (Gram-negative model system), and the latest advances in chromosome conformation capture techniques to bring us one step closer to answering this fundamental question.

1.3 DNA replication

DNA replication is a tightly regulated and ordered process divided into three main stages: initiation, synthesis (or elongation) and termination. A key regulatory molecule for ensuring that replication occurs only once per cycle and in synchrony with cell growth and division is initiator DnaA, an AAA+ ATPase (ATPases Associated with various cellular Activities) found in virtually all bacteria (Kaguni, 2006; Katayama

et al, 2010): levels of DnaA are stringently controlled. Means of its control vary amongst bacteria and have been recently reviewed (Katayama et al, 2010; Wolanski et al, 2015; Wolański et al, 2014). In its ATP-bound form DnaA exists as a helical oligomer that binds to specific AT-rich sequences (DnaA-boxes) within *oriC*. It is the binding of DnaA to the single chromosome origin of replication, *oriC*¸ positioned at the 0°/360° chromosome position that initiates replication. At these sites DnaA forms a highly ordered nucleoprotein complex, the DNA-unwinding element (DUE) (Fernandez-Fernandez et al, 2011; Katayama et al, 2010), effectively melting and unwinding the local double stranded DNA to allow the recruitment of the replication machinery (Duderstadt et al, 2010; Fernandez-Fernandez et al, 2011).

Working together with *oriC*-bound DnaA, in *B. subtilis*¸ the helicase loader (DnaI) and co-loader proteins (DnaD and DnaB) that are also recruited to this site actively load the helicase (DnaC) to establish the replication fork (Bruand et al, 1995; Smits et al, 2010; Velten et al, 2003). DNA primase (DnaG), DNA polymerase III holoenzyme (PolC) and the accessory polymerase (DnaE) then bind to the *oriC* region and, together with the other replication proteins, form the replisome thus completing the initiation stage (Smits et al, 2010). A similar process, although with differing proteins, occurs in *E. coli,* as reviewed recently (Beattie & Reyes-Lamothe, 2015). [Note, particularly that the DNA helicase in *E. coli* is named DnaB, not DnaC as it is in *B. subtilis* and that there is no homolog of the *B. subtilis* DnaB in *E. coli*.]

Starting at *oriC,* DNA synthesis occurs bi-directionally around the circular chromosome (Daniel & Errington, 2003; Lemon & Grossman, 2000; Pomerantz & O'Donnell, 2007). The two replication forks continue bi-directionally until they encounter the terminus region (Ter), at which point the replisome disassembles allowing the decatenation and subsequent complete separation of the newly replicated sister chromosomes (Bussiere & Bastia, 1999; Lewis, 2001). Resolution of the chromosomes, when required, is then completed by the combined action of TopoIV recombinases located at the terminus (XerCD in *E. coli*, and RipX and CodV in *B. subtilis*) and DNA translocases (FtsK in *E. coli*, and SpoIIIE in *B. subtilis*) (Duggin et al, 2008; Grainge et al, 2007; Grainge et al, 2011; Kaimer et al, 2011; Lemon et al, 2001; Sivanathan et al, 2009).

1.4 Chromosome segregation

In *B. subtilis* and *E. coli*, DNA replication and chromosome segregation occur concomitantly. Soon after the origin regions are replicated, they migrate in opposite directions to locate at the future division sites, located at the cell quarter positions (Berkmen & Grossman, 2007). Most research on chromosome segregation in bacteria has focussed on how these newly-replicated origin regions separate. Separation involves the ParABS system and SMC (Structural Maintenance of Chromosome) condensin complex in *B. subtilis*, and the MukBEF complex in *E. coli*.

Although it is now known to be required for chromosome separation in a number of bacteria, including *B. subtilis*, the ParABS system was first identified by the discovery of two proteins, ParA and ParB, required for effective plasmid partitioning on the P1 plasmid hosted in *E. coli* (Abeles et al, 1985). ParB was found to bind co-operatively to the *parS* cis-acting site along with ParA, a Walker-type ATPase, to form a large nucleoprotein complex resulting in replicated plasmids segregating bidirectionally to the cell poles (Funnell, 1988). Since its discovery, *par* loci have been subsequently found on the chromosome of over 65% of all sequenced bacterial genomes (Livny et al, 2007), including *B. subtilis.* In *B. subtilis* however, the components of the ParABS system are known as Soj (ParA) and Spo0J (ParB) because they had been previously observed in *B. subtilis* having an effect on sporulation (Ireton et al, 1994). Cells lacking Spo0J mislocalise sister origin positions (Lee & Grossman, 2006), suggesting a role for this protein in separating the newly duplicated chromosome origins in *B. subtilis*. Subsequently it was shown that Spo0J binds to several *parS* sites located within the *oriC* region (Autret et al, 2001; Lin & Grossman, 1998), and in cells labelled with Spo0J-GFP, Spo0J co-localizes with *oriC* and appears as distinct compact foci positioned at the cell quarters (Glaser et al, 1997; Marston & Errington, 1999).

Several elegant studies in recent years have revealed significant insight into the roles of the ParABS system and the SMC condensin complex in chromosome segregation in *B. subtilis.* Following binding to *parS,* Spo0J spreads onto non-specific neighbouring DNA, drawing them together to form a nucleoprotein complex (see Figure 1B) (Broedersz et al, 2014; Glaser et al, 1997; Murray et al, 2006). The method

by which Spo0J spreads has been recently proposed by Graham *et al.*, such that Spo0J forms clusters on neighbouring DNA bridging them together, forming DNA loops (Graham et al, 2014). The formation of these long-distance DNA loops is suggested to facilitate the condensation and compaction of the origin-proximal region of the chromosome as well as the recruitment and loading of the SMC constituents (Figure 1.1B) (Graham et al, 2014). The SMC condensin complex (from now on referred to as simply SMC), made up of proteins SMC, ScpA and ScpB, and supplemented by the ParABS system, is then suggested to draw the sister origins away from each other (Wang et al, 2014a). Essentially, SMC resolves the origins enabling ParABS to actively segregate origins towards opposite poles.

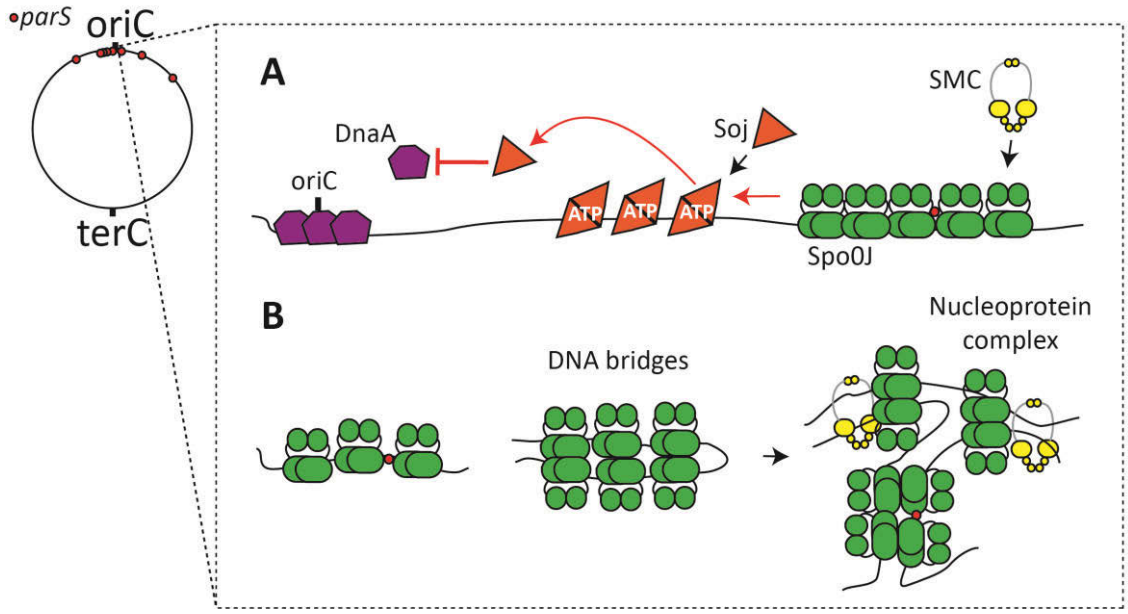

Figure 1.1: Roles for *Spo0J* in chromosome replication and segregation. (A) Role of Spo0J in chromosome replication. DNA-bound Spo0J not only recruits SMC but also regulates the ability of Soj to inhibit DNA replication through DnaA. Spo0J inhibits Soj dimerization by stimulating its ATPase activity, triggering its monomer form and dissociation from the DNA (red arrows). The Soj monomer is now free to inhibit DnaA by preventing its oligomerization (red arrows). In its ATP-bound state, Soj binds DNA, thereby relieving the inhibition on DnaA, allowing replication initiation. (B) Model for the role of Spo0J in chromosome segregation by mediating the formation of DNA bridges and large nucleoprotein complexes. Spo0J binds at *parS* sites and spreads on the surrounding DNA forming DNA bridges and trapping DNA loops. Spo0J-mediated recruitment of SMC allows efficient chromosome segregation.

The extent to which Soj actually plays a role in the active segregation of chromosomes is unknown. Interestingly it was shown that the primary role of Soj is likely to be in regulating the initiation of DNA replication (Figure 1.1A). It does this by directly interacting with the initiation protein, DnaA (Murray & Errington, 2008), inhibiting or promoting DnaA activity. As a monomer, Soj inhibits DnaA activity by preventing formation of its helical oligomer, whereas the Soj dimer relieves this inhibition by allowing DnaA to form oligomers. This ability to switch however is mediated by its interaction with DNA-bound Spo0J (Figure 1.1A) (Scholefield et al, 2011). So it is now clear that Spo0J has two separate roles, one in the regulation of DnaA via its effect on Soj self-association, and another in chromosome segregation. These functions have been shown to reside in different domains (Gruber & Errington, 2009).

The mechanism of chromosome segregation in *E. coli* is more elusive. While the ParABS system is absent in this organism it does possess a distant relative of the SMC complex, MukBEF, a protein complex existing in enterobacteria and some γ-proteobacteria (Hiraga, 2000; Niki et al, 1991). This complex plays a key role in separating newly replicated *oriC* regions (Danilova et al, 2007) and, together with topoisomerase IV (TopoIV), in promoting DNA decatenation (Nicolas et al, 2014). Although it doesn't share any homology with Spo0J, MukB is thought to have a similar bridging function, in that it binds DNA forming a cluster, creating bridges with randomly colliding protein-free DNA. Rybenkov *et al.* postulates that the formation of these bridges stabilises DNA compaction, potentially assisting in pulling apart the sister chromosomes (Rybenkov et al, 2014). It is unlikely these proteins are the sole players in chromosome segregation and there are several hypotheses as to how *E. coli* and other bacteria segregate their chromosomes (Bates & Kleckner, 2005; Lemon & Grossman, 2000; Woldringh, 2002). In fact, biophysical models in *E. coli* suggest that chromosome segregation is generated via entropic forces (Jun & Mulder, 2006). Application of polymer physics concepts to the bacterial chromosome by Jun and Mulder, resulted in a passive segregation model where the replicated sister chromosomes themselves possess internal forces leading to entropic repulsion or exclusion (Jun & Mulder, 2006). However, recent evidence suggests that these

entropic forces are insufficient to complete whole chromosome segregation (Di Ventura et al, 2013; Junier et al, 2014), highlighting the high complexity of chromosome segregation which requires several different components or modes of action for successful execution.

1.5 Cell division and regulation of division-site placement

Cell division is dependent on the localisation of numerous specific division proteins to the right place (midcell) at the right time within the cell cycle. The first and foremost of these proteins to localize to midcell is the tubulin-like protein, FtsZ which assembles at the inner face of the cytoplasmic membrane into a ring structure known as the Z ring (Szwedziak et al, 2015). The Z ring then facilitates the recruitment of all the other division proteins, together called the divisome (Adams & Errington, 2009; de Boer, 2010; Lutkenhaus et al, 2012), and provides the contractile force required for the invagination of the envelope layers. Thus, precise recruitment of FtsZ to midcell is central to the regulation of cell division and FtsZ has, over the last 20 years, become one of the most studied bacterial proteins. Much has been elucidated about FtsZ and most, if not all, of the divisome proteins (Lutkenhaus et al, 2012), but what yet escapes us is how the assembly of this crucial machinery, not only precisely finds the midcell, but how it does so in concert with the replication and segregation of the chromosome? This question is of utmost importance as the correct timing and positioning of the Z ring between the DNA at midcell is quintessential to the competitive long-term survival of bacteria.

1.5.1 Negative regulators of Z ring placement

For the past two decades, the positioning of Z ring formation has been described as regulated by the combined action of the Min system and nucleoid occlusion. The Min system prevents the Z ring from forming at the cell poles and nucleoid occlusion prevents the Z ring from forming within the vicinity of the chromosome (Bernhardt & de Boer, 2005; Pichoff & Lutkenhaus, 2001; Wu & Errington, 2004). The overall result is that the two systems prevent the Z ring from forming anywhere other than the cell centre (Figure 1.2A).

Since the discovery of the Min system over 30 years ago (de Boer et al, 1989; Reeve et al, 1973; Teather et al, 1974), extensive research has revealed several components of this system that function in a co-operative manner to inhibit polar Z ring assembly and division at the poles. In *E. coli* and *B. subtilis* the Min system consists of two main proteins, MinC and MinD, that function to prevent FtsZ assembly and cell division at the cell poles, and additional Min proteins unique to each organism, that assist in different modes of action. For a complete review of the Min system and its mode of action, the reader is encouraged to read recent reviews (Kretschmer & Schwille, 2014; Margolin & Rowlett, 2015; Shih & Zheng, 2013).

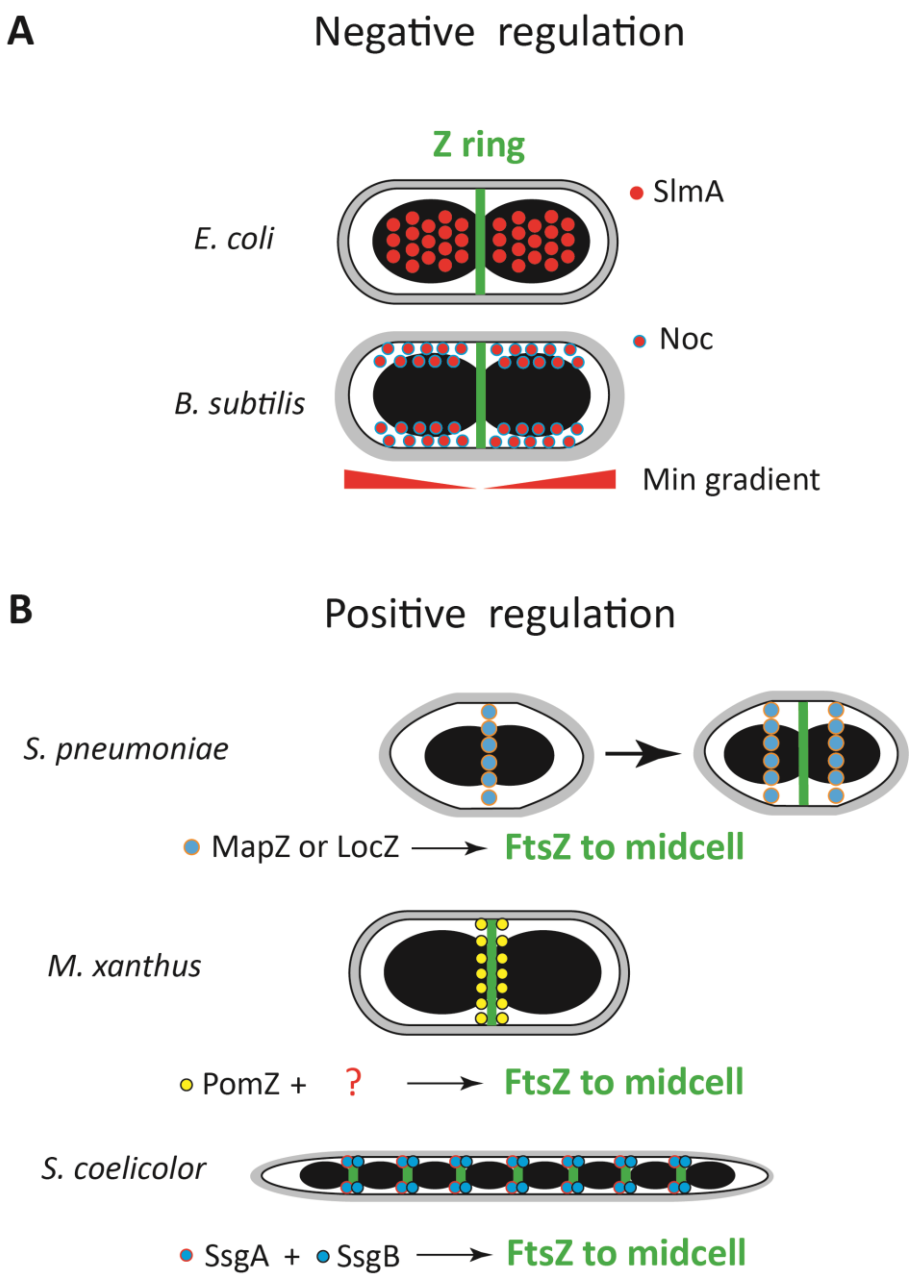

Figure 1.2: Regulation of Z ring positioning. (A) Negative regulation of Z ring position by the combined activity of nucleoid occlusion proteins and the Min system gradient. These two systems act by preventing non-productive accumulations of FtsZ at non-medial locations, thereby enhancing efficient and timely Z ring assembly solely at midcell. (B) Positive regulation of Z ring position in diverse bacteria. In all cases a midcell marking protein assembles at midcell prior to FtsZ, thereby defining the midcell accumulation site for Z ring assembly.

Nucleoid occlusion on the other hand, inhibits Z ring formation over the DNA, and is mediated by proteins SlmA (in *E. coli*) and Noc (in *B. subtilis*) (Bernhardt & de Boer, 2005; Wu & Errington, 2004). Although no sequence homology exists between the two, both SlmA and Noc possess similar characteristics: both proteins bind to specific regions scattered around the chromosome, except for the terminus region, which is largely devoid of these binding sites (Wu et al, 2009). This pattern of binding supports the proposal that as chromosome replication nears completion and the terminus region occupies the central position in the cell, SlmA and Noc are no longer present in this region, relieving this area of nucleoid occlusion, thus allowing a Z ring to form there (Wu & Errington, 2004). SlmA and Noc however, have differing modes of action. Recent studies into the activity of SlmA have elucidated two potential mechanisms as to how it inhibits Z ring formation. In the first, SlmA promotes FtsZ depolymerisation (Cho & Bernhardt, 2013; Cho et al, 2011; Du & Lutkenhaus, 2014). When bound to its specific DNA binding sites (SBS), SlmA attaches to the highly conserved C-terminal tail of FtsZ where it competes for binding with other interacting or regulatory partners of FtsZ, including ZipA, FtsZ, ZapD, MinC and ClpX (Du & Lutkenhaus, 2014). This promotes further interactions between SlmA and FtsZ, leading to FtsZ protofilament breakage independent of the GTPase activity of FtsZ (Cabre et al, 2015; Du & Lutkenhaus, 2014). In a second, alternative hypothesis, Tonthat *et al.* have suggested that SlmA binds to DNA as a dimer of dimers and spreads along nascent DNA where it forms higher-order nucleoprotein complexes that capture and inhibit FtsZ from coalescing into functional Z rings (Tonthat et al, 2013). Continuing studies into the activity of SlmA are required to elucidate which hypothesis is correct, and, further, to understand how SlmA is able to carry out these membrane-localised functions when tethered to the DNA.

In contrast, Noc in *B. subtilis* mediates its nucleoid occlusion effect by recruiting DNA to the membrane periphery via its newly discovered ability to bind the membrane (Adams et al, 2015). Adams *et al.* propose a model in which Noc mediates its Z ring inhibitory function by physically crowding the available space between the DNA and the membrane periphery such that Z rings are unable to form there (Adams et al, 2015). The model raises several questions. Is Noc abundant enough within the cell to

mediate this crowding effect on its own or are there other protein players involved? Is this Noc activity coupled with the transertion effect (a theory postulated over 20 years ago, which couples transcription, translation and insertion of membrane proteins)? Additionally, what effect does this recruitment of the DNA to the cell periphery have on chromosome organisation and what happens to this organisation in the absence of Noc? Noc could potentially impact chromosome organisation or segregation in a way not previously considered. Noc belongs to the ParB family and shares ~40% sequence homology with the known chromosome segregation protein, Spo0J (Sievers et al, 2002). Furthermore, unlike in *B. subtilis*, *Staphylococcus aureus* cells with a *noc* deletion form a significant number of anucleate cells, even during normal, unperturbed growth (Veiga et al, 2011), thus suggesting a role for Noc in chromosome segregation in this organism. This raises the possibility that Noc could also be impacting chromosome organisation or segregation in *B. subtilis* to influence cell division.

Continued study of the Min system and nucleoid occlusion regulatory systems has shown that they cannot be the sole regulators of correct placement of the Z ring at midcell. Under normal growth conditions, when either the Min system or Noc/SlmA in *B. subtilis* or *E. coli* are deleted, cell growth and division continues to occur normally. However, although division is significantly perturbed in *B. subtilis* and *E. coli* cells devoid of both the Min system and their respective nucleoid occlusion proteins, Z rings nonetheless preferentially form at midcell in internucleoid positions with high precision (Bailey et al, 2014; Bernhardt & de Boer, 2005; Rodrigues & Harry, 2012). Thus, it appears that the role of the Min system and Noc/SlmA is to ensure there is sufficient FtsZ for Z ring assembly at the desired division site in *B. subtilis* and *E. coli* by limiting the regions in which FtsZ can accumulate. Additionally, a number of bacteria possess only one system, or do not possess either the nucleoid occlusion or the Min protein homologues. Instead, positive mechanisms regulating Z ring positioning have recently been revealed by studies on several of these bacteria, including *Streptococcus pneumoniae, Myxococcus xanthus* and *Streptomyces coelicolor*. These are illustrated in Figure 1.2B.

1.5.2 Positive regulators of Z ring placement

A novel protein in *S. pneumoniae,* recently described by two independent studies, is named MapZ (Mid-cell Anchored Protein Z) or LocZ (Localising at midcell of FtsZ) (Fleurie et al, 2014; Holečková et al, 2015). MapZ localises to the midcell division site prior to any division proteins, including FtsZ and FtsA. This localisation of MapZ drives the recruitment of FtsZ to its midcell position. Following Z ring assembly, MapZ splits into two rings, which migrate bidirectionally, in tandem with the equatorial rings, to the future division sites (Fleurie et al, 2014; Holečková et al, 2015).

Similarly, the ParA-like protein, PomZ (Positioning at Midcell of Fts*Z*), discovered by Treuner-Lange *et al.* in *M. xanthus,* localises at the cell centre prior to, and independently of, FtsZ (Treuner-Lange et al, 2013). However, PomZ appears to have a positive spatial and temporal regulatory role. In newborn cells, PomZ is seen to co-localise with the nucleoid. Only once the nucleoid replicates does PomZ migrate to midcell to promote FtsZ recruitment. How it does so is not yet understood. The lack of *in vitro* interaction between purified FtsZ and PomZ, led Treuner-Lange *et al.* to postulate the existence of interacting partners to mediate PomZ regulatory activity on FtsZ (Treuner-Lange et al, 2013).

Interacting proteins positively regulating Z ring placement have also been observed in *S. coelicolor. S. coelicolor* possesses a novel set of proteins unique to Actinobacteria which promote FtsZ recruitment and polymerisation at the correct site. In sporulating *S. coelicolor* cells, the membrane-associated SsgB is localised at midcell by its interaction with SsgA; SsgB then recruits and tethers FtsZ to the division site (Traag & van Wezel, 2008; Willemse et al, 2011).

An outstanding question in these organisms is how do these proteins recognise the future division site? Is there a signal or unidentified marker? And do such positive systems exist in bacteria that possess the Min system and/or nucleoid occlusion proteins? Given that neither the Min system nor nucleoid occlusion are essential in positioning the Z ring correctly in either *E. coli* or *B. subtilis*, it would suggest some other regulatory system exists in these bacteria. A recent positive regulation link has

been found between cell division and glycolysis in *B. subtilis.* Monahan *et al.* describe a model in which PDH E1α (the E1α subunit of pyruvate dehydrogenase, required for the metabolism of pyruvate at the final stage of glycolysis) positively regulates Z ring assembly by co-localizing with the chromosome in a pyruvate-dependent manner (Monahan et al, 2014). This system may help to coordinate bacterial division with nutritional conditions to ensure the survival of newborn cells. Indeed, increasing evidence is pointing towards aspects of DNA replication and chromosome organisation/segregation influencing cell division in *B. subtilis* and *E. coli*.

1.6 Coordinating cell division with DNA replication

The first suggestion of a coordinated link between DNA replication and cell division in bacteria came from studies in *B. subtilis. B. subtilis* cells are able to begin septation when only 70% of the chromosome has been replicated (Wu et al, 1995). Given that Z ring formation precedes septation, this means mechanisms must be at play to trigger this first stage of cell division earlier on in DNA replication. Moreover, blocking the initiation of DNA replication in *B. subtilis* significantly affects Z ring positioning, suggesting a link between these two processes (Harry et al, 1999; Regamey et al, 2000). Examining this more closely Moriya *et al.* examined the effect of different blocks at the initiation stage of DNA replication and found that, the earlier the block in initiation, the less likely a Z ring would form at midcell, with completion of the initiation stage allowing midcell Z rings to form at wild-type levels. Moriya *et al.* proposed a model, called the Ready-Set-Go model, linking the progression of initiation of DNA replication to midcell Z ring assembly, such that as the initiation phase progresses, midcell becomes increasingly available or "potentiated" for Z ring assembly (Figure 1.3). This coincides nicely with the finding that the initiation phase of DNA replication in *B. subtilis* involves several proteins that assemble at *oriC* in a step-wise manner (Smits et al, 2010). Most significantly, the "Ready-Set-Go" phenomenon is independent of Noc (Moriya et al, 2010), and has a positive influence on Z ring placement. What this Z ring potential at midcell actually is, is currently unclear. It is possible that the build-up of the replisome proteins at the medially located *oriC* acts as a beacon for progressive FtsZ

accumulation there. Importantly, this study highlighted that Noc activity is insufficient in inhibiting cell division during initiation of DNA replication, suggesting other Noc-independent inhibition strategies must be in place within cells for proper cell division, an idea also supported by studies of Bernard *et al* (Bernard et al, 2010).

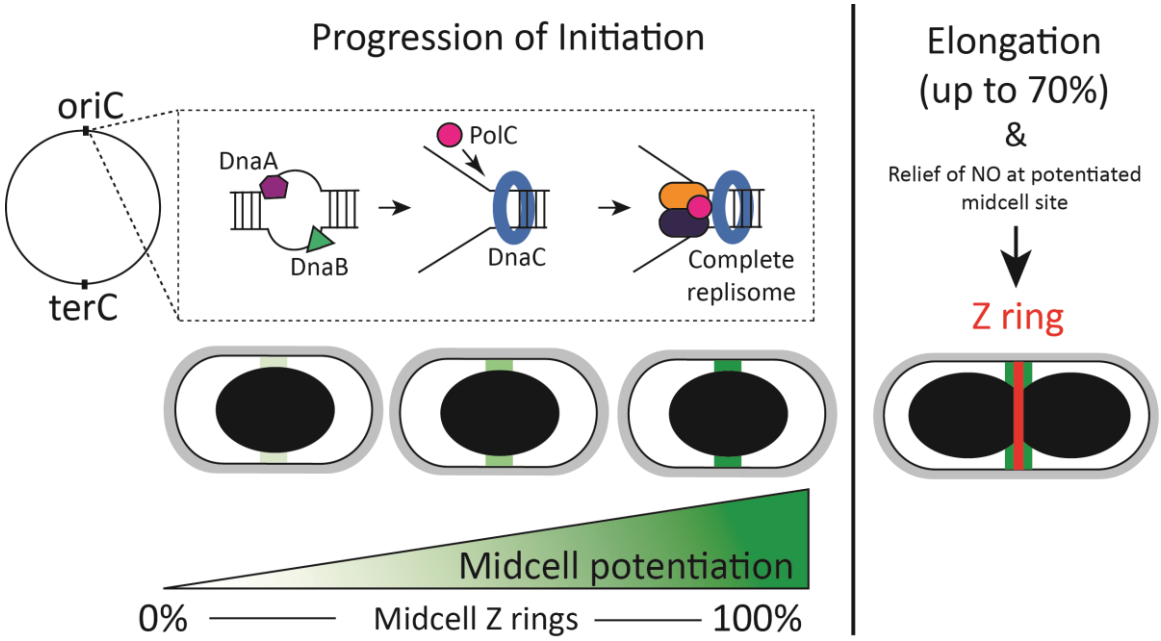

Figure 1.3: The Ready-Set-Go model linking DNA replication initiation to midcell Z ring assembly. On the left panel, early in the cell cycle the progression of DNA replication initiation is dependent on the ordered assembly of initiation proteins and replisome components. The midcell position is potentiated for Z ring assembly there as the initiation stage progresses towards complete replisome assembly. Complete replisome assembly allows for 100% midcell Z ring assembly. On the right panel, upon 70% completion of chromosome replication, relief of nucleoid occlusion allows the Z ring to assemble at the midcell potentiated site that was established earlier in the DNA replication cycle.

Linkage between initiation of DNA replication and cell division in *B. subtilis* is further demonstrated in studies by Arjes *et al.* The authors show that extended inhibition of DNA replication initiation results in an irreversible block to cell division and vice versa. This phenomenon was adequately termed the point of no return (PONR) (Arjes et al, 2014). What the trigger for the PONR is and why bacteria are unable to resume growth remain outstanding questions. The phenomenon is however independent of the SOS-response and cellular levels of DnaA and FtsZ; and microarray data suggest that the trigger for the PONR may be post-transcriptional (Arjes et al, 2014).

More recently, midcell Z ring assembly has also been linked to DNA replication in *E. coli*. Cambridge *et al.* found midcell Z ring assembly was inhibited when DNA replication elongation was blocked (Cambridge et al, 2014). Importantly, this occurred in a SlmA-, MinC- and SOS-independent manner. Overall, this finding suggests that DNA replication playing a positive role in Z ring positioning is not exclusive to *B. subtilis*, but is likely to occur in a number of organisms.

1.7 Coordinating cell division with chromosome organisation and segregation

While the nucleoid occlusion proteins Noc and SlmA are typically associated with coordinating cell division and chromosome segregation, a variety of mutations in chromosome segregation proteins have long been known to lead to incorrect Z ring positioning in both *E. coli* and *B. subtilis* (Ireton et al, 1994; Niki et al, 1991), providing clear evidence that the two processes are connected. The absence of any of the constituents of the *E. coli* MukBEF complex results in temperature sensitivity, loss of chromosome organisation and condensation, and generation of ~5% anucleate cells at the permissive temperature due to Z ring misplacement (Niki et al, 1991). Similarly, *B. subtilis* cells lacking *smc* (under slow growth conditions) or *spo0J* exhibit aberrant positioning, or level of condensation of the nucleoid, and also result in formation of anucleate cells (Britton et al, 1998; Ireton et al, 1994; Lee & Grossman, 2006; Ogura et al, 2003). In minimal media, deletion of both *smc* and *spo0J* enhances this effect whereby the frequency of anucleate cells increases to

19%, and 12% of cells with nucleoids guillotined by the septum (Lee & Grossman, 2006). While these cell division phenotypes of chromosome segregation mutants have been known for a long time, it remains unclear if chromosome segregation and division site positioning are coupled by the chromosome segregation proteins themselves. At the heart of this question is the fact that misplacement of Z rings in chromosome segregation mutants can occur indirectly through nucleoid occlusion: chromosome segregation mutants alter chromosome architecture, thus resulting in improper Noc/SlmA-DNA localization within the cell and misplaced Z rings. However, it still remains possible that chromosome segregation proteins may actually directly contribute to Z ring placement, independently of their indirect consequences on nucleoid occlusion. One hypothesis is that they may participate directly in establishing the Z ring site; however no direct interaction between chromosome segregation proteins and FtsZ has ever been reported in the literature. A second hypothesis is that through their chromosome-organising activities, they contribute with an unknown aspect of chromosome organisation that is directly linked to cell division. In favour of this hypothesis is the recent observation that the organisation of a specific region of the *E. coli* chromosome contributes to establishing the Z ring position at midcell. Bailey *et al.* found that the Ter macrodomain of the chromosome in *E. coli* becomes important for midcell Z ring positioning in the absence of SlmA and the Min system (Bailey et al, 2014). Specifically, combining the *slmA min* double mutant with a mutant in MatP (the protein that organises the Ter macrodomain) affected midcell Z ring precision. The authors also demonstrated that this effect is mediated through interactions between MatP and the divisome proteins ZapB and ZapA. Thus, these results suggest that the organisation of the Ter macrodomain plays a positive role in Z ring positioning. Intriguingly, in the absence of this link to the Ter macrodomain, SlmA and the Min system, there is still a slight midcell bias for Z ring placement. Thus, these modest effects to Z ring positioning suggest that there many levels of control are required for bacteria to coordinate division with chromosome organisation.

In analogy to MatP, and as mentioned above, Spo0J, SMC and MukBEF are suggested to be involved in the overall organisation of the origin region following its

replication (Graham et al, 2014; Rybenkov et al, 2014; Wang et al, 2014c). Marbouty *et al.* and Wang *et al.* have very recently utilised Hi-C techniques in *B. subtilis* to elucidate the structure of the chromosome in this organism (Marbouty et al, 2015; Wang et al, 2015). As well as identifying both short- and long-range chromosomal DNA interactions within the *B. subtilis* chromosome, both these studies directly demonstrate the requirement of the ParABS system and SMC complex in origin-region resolution, reformation and segregation following its duplication. In doing so, these studies make it intriguing to see which chromosome interaction domains are lost in chromosome organisation mutants resulting in abnormal Z ring formation such as those in the absence of *spo0J, smc* or *mukB*. It is possible that changes to chromosome architecture as a result of the action of chromosome segregation proteins is vital for large scale compaction of the origin region to bring together sequence-distal operons to allow for important interactions, for example to form a signal or to localise protein-protein interactions required for proper Z ring formation.

1.8 Concluding remarks

Critical to a greater understanding of the spatial and temporal dynamics of cell division and chromosome segregation proteins and chromosomal loci is a greater appreciation of the architecture of the chromosome under various conditions, and the important role this plays in cell cycle regulation. For example, it is not yet clear exactly how or in what way cellular processes such as DNA replication, chromosome segregation or transcription affect chromosome architecture. Isolating the influence of each of these processes on chromosome architecture, and pinpointing cause and effect, will be challenging. Recent advances in technologies to look more closely at how the chromosome is compacted and organised will be of great value in this endeavour. Genome-wide conformation capture techniques such as Hi-C and super-resolution microscopy allow us to detect chromosome interaction domains and infer information on the spatial organisation of the chromosome (Le et al, 2013; Le & Laub, 2014). Examining chromosome architecture on a more global scale using these technologies and in different environmental or growth conditions will give us insight into how bacteria coordinate chromosome replication, segregation and Z ring formation under various situations to allow proper daughter cell propagation.

1.9 Thesis aims

The primary objective of the work presented in this thesis was to gain insight into whether chromosome organisation plays into the link between initiation of DNA replication and midcell Z ring assembly in the model organism *B. subtilis*.The Ready-Set-Go model proposes that the link between the early stages of DNA replication and Z ring positioning relies on the progress of the initiation phase of DNA replication which increases the potential for a Z ring to form at midcell. Importantly this is observed only when the nucleoid occlusion protein, Noc, is absent. Interestingly, the four DNA replication inhibition treatments used to support this model were shown to result in different nucleoid morphologies (including single-lobed and bilobed nucleoids) which correlated with their ability to form Z rings at midcell. That is, only when the nucleoid formed a bilobed morphology was a Z ring able to form at midcell over the nucleoid. However, one of the replication blocks applied (the temperature-sensitive *dnaB-1* mutant) never results in Z rings at midcell irrespective of the nucleoid morphology. It was this observation, changes to nucleoid morphology correlating with Z ring positioning, that provided evidence that proteins required for chromosome organisation and/or segregation may play a role in this link between DNA replication initiation and Z ring positioning. One possible scenario is that inactivation of a specific replication protein causes changes to chromosome segregation and therefore midcell Z ring potential. Two key players shown to have both an effect on chromosome segregation and DNA replication initiation are Soj and Spo0J.

Chapter 3 addresses whether Soj and Spo0J do play a role in Z ring positioning during initiation of DNA replication. Z ring positioning is examined in the absence of *soj* and *spo0J* (both together and separately) during an early and late block to initiation of DNA replication (via the inactivation of DnaB and addition of HPUra to inhibit DNA polymerase III, respectively). The gross morphology of the nucleoid is also explored to examine whether there is a correlation between changes in Z ring positioning and nucleoid morphology (single-lobed, bilobed or spread morphology).

Chapter 4 examines how Spo0J regulates Z ring positioning by determining whether the increase in midcell Z ring assembly observed in the absence of Spo0J is a direct result of this absence, or an indirect effect on Noc activity. Therefore Chapter 4 examines whether changes to Z ring positioning in the absence of *spo0J* is due to changes to Noc localisation and activity.

Chapter 5 also explores how Spo0J regulates Z ring positioning but from a different perspective. Evidence presented in Chapters 3 and 4 show changes to Z ring positioning attributed to changes in nucleoid morphology due to Spo0J. Through its interaction partners, Spo0J has been shown to play a dual role during the cell cycle via influences on both initiation of DNA replication and chromosome segregation. It is the latter relationship that becomes the focus of Chapter 5. Spo0J is required for the recruitment of SMC (structural maintenance of the chromosome) condensin complex to its location at the origin region (Gruber & Errington, 2009; Sullivan et al, 2009; Wang et al, 2015). However, it is SMC that is seen to be the key driver for changes in nucleoid morphology (Sullivan et al, 2009; Wang et al, 2014c). Therefore, it is possible that the changes in Z ring positioning and nucleoid morphology observed in the absence of *spo0J* when initiation of DNA replication is blocked can be attributed to SMC, and it is this idea that is explored in Chapter 5.

Chapter 2.
Materials and Methods

2.1 Chemicals, reagents and solutions

The chemicals and reagents used throughout this work were typically analytical reagent grade and were obtained from Amresco, BDH Chemicals or Sigma unless otherwise specified. Commonly used aqueous buffers and solutions are listed in Table 2.1.

Table 2.1: Commonly used aqueous buffers and solutions

Buffer/Solution	Constituents[a]
GTE	50 mM glucose, 20 mM Tris-Cl, 10 mM EDTA, pH 7.5
PBS	137 mM NaCl, 2.7 mM KCl, 10.1 mM Na_2HPO_4, 1.8 mM KH_2PO_4; pH 7
MSA	8 mM K_2HPO_4, 4.4 mM KH_2PO_4, 1.5 mM $(NH_4)_2SO_4$, 340 mM tri-sodium citrate dihydrate ($Na_3C_6H_5O_7 \cdot 2H_2O$)
PC Buffer (10X)	0.63 mM trisodium citrate ($Na_3C_6H_5O_7 \cdot 2H_2O$), 6.1 mM K_2HPO_4, 4.4 mM KH_2PO_4; pH 7
SDS-PAGE loading buffer	62.5 mM Tris-HCl, 10% glycerol (v/v), 5% 2-mercaptoethanol (v/v), 2% SDS (sodium dodecyl sulfate) (v/v), 0.1% bromophenol blue (v/v), pH 6.8
SDS running buffer (10X)	0.2 M Tris base, 1.5 M Glycine, 35 mM SDS
TBE	89 mM Tris-HCl, 89 mM boric acid, 2.5 mM EDTA, pH 8.3
TE	10 mM Tris-HCl, 1 mM EDTA, pH 8.0
TES	200 mM Tris-HCl, 5 mM EDTA, 100 mM NaCl, pH 7.5
Trace metals	50 mM $CaCl_2$, 5 mM $MnCl_2$, 0.005 mM $FeCl_3 \cdot 6H_2O$, 2.5mM $CuCl_2.2H_2O$, 1.25 mM $ZnCl_2$, 0.25 mM $CoCl_2.6H_2O$, 0.29 mM $Na_2MoO_4 \cdot 2H_2O$
Western lysis buffer	10 mM $MgCl_2$, 500 µg/ml lysozyme, 300 µg/ml phenylmethylsulfonylfluoride, 100 µg/ml DNase I, 1X TE
Western transfer buffer	20 mM tris base, 0.15 M glycine, 3.5 mM SDS, 20% MeOH (v/v)
XS Buffer (2X)	2% potassium ethyl xanthogenate, 1600 mM ammonium acetate, 200 mM Tris-HCl, 36 mM EDTA, 2% SDS, pH 7.42% potassium ethyl xanthogenate, 1600 mM ammonium acetate, 200 mM Tris-HCl, 36 mM EDTA, 2% SDS, pH 7.4
TKE flow buffer	10 mM Tris–HCl, 15 mM NaCl, 1 mM EDTA

[a] All buffers and solutions were made up in Milli-Q® purified water (MQW; Millipore) and are listed at the normal working concentration (1×) or stated otherwise. All percentages are given as weight per volume (w/v) unless otherwise noted.

2.2 *Bacillus subtilis* strains and growth conditions

All strains used in this thesis are listed below in Table 2.2. For those strains that were produced in this work, experimental details on construction methods are detailed in the Results (Chapters 3 to 5) where relevant. The *B. subtilis* 168 background strain used in this work was SU5 (*trpC2*). The *trpC2* genotype is an auxotrophic requirement for tryptophan. In regards to the strains displaying a *trpC2*$^{+}$ *dna-1* genotype, since the *dna-1* gene in strain SU661 is not tagged with an antibiotic marker for selection, and it is not possible to select for temperature sensitivity, this strain was created by congression, whereby two markers were inserted into the recipient strain simultaneously. Thus a two-step selection of transformants was performed to create SU661. Firstly *trpC2*$^{+}$ transformants were selected by their ability to grow in the absence of tryptophan and then subsequently those transformants that also contain the *dna-1* mutation were selected by their inability to grow at the high temperature of 48°C.

Table 2.2: *Bacillus subtilis* strains

Strain	Genotype	Source/Reference
SU5	168 *trpC2*	E. Nester
SU492	168 *trpC2 amyE::(spc* P_{xyl}*-ftsZ-yfp)*	Lab stock
SU533	168 *trpC2 Δnoc::cat*	Lab stock
SU629	168 *trpC2 Δnoc::tet amyE::(spc* P_{xyl}*-noc-yfp)*	Lab stock
SU656	168 *trpC2 Δnoc::tet*	Lab stock
SU661	168 *trpC2*$^{+}$ *dna-1*	Lab stock
SU746	168 *trpC2*$^{+}$ *dna-1 amyE::(spc* P_{xyl}*-ftsZ-yfp)*	This work
SU747	*trpC2 Δsoj ::neo*	(Scholefield et al, 2011)
SU748	*trpC2 Δspo0J::neo, amyE::spo0J (cat)*	(Gruber & Errington, 2009)
SU750	*trpC2, Δspo0J::neo, amyE::spo0J*^{L12S} *(cat)*	(Gruber &

		Errington, 2009)
SU751	*trpC2, Δspo0J::neo, amyE::spo0J$^{L5H, S68P}$ (cat)*	(Gruber & Errington, 2009)
SU752	*trpC2, Δspo0J::neo, amyE::spo0J$^{L12S, D73G, V198A}$ (cat)*	(Gruber & Errington, 2009)
SU753	*trpC2, Δspo0J::neo, amyE::spo0J^{N112S}(cat)*	(Gruber & Errington, 2009)
SU754	*trpC2, Δspo0J::neo, amyE::spo0J^{R149G} (cat)*	(Gruber & Errington, 2009)
SU755	*trpC2, Δspo0J::neo, amyE::spo0J^{N112S} (cat)*	(Gruber & Errington, 2009)
SU717	*hutM(345°)::lacO (cat), thrC(283°)::lacI-cfp (erm), spo0J-mCherry (kan), cgeD(181°)::Ppen*(TATG->TAGG)-tetR-yfp (tet)*	(Lee & Grossman, 2006)
SU765	168 *trpC2 Δsoj-spo0J::tet*	This work
SU766	168 *trpC2^{+} dna-1 Δsoj-spo0J::tet*	This work
SU767	168 *trpC2 amyE::(spc P_{xyl}-ftsZ-yfp) Δsoj-spo0J::tet*	This work
SU768	168 *trpC2^{+} dna-1 amyE::(spc P_{xyl}-ftsZ-yfp) Δsoj-spo0J::tet*	This work
SU769	168 *trpC2 Δspo0J::kan*	This work
SU770	168 *trpC2^{+} dna-1 Δspo0J::kan*	This work
SU771	168 *trpC2 Δsoj::kan*	This work
SU772	168 *trpC2^{+} dna-1 Δsoj::kan*	This work
SU783	168 *trpC2 hutM(345°)::lacO(cat), thrC (283°)::lacI-cfp(erm) amyE::(spc P_{xyl}-ftsZ-yfp)*	This work
SU784	168 *trpC2^{+} dna-1 hutM(345°)::lacO(cat), thrC (283°)::lacI-cfp(erm) amyE::(spc P_{xyl}-ftsZ-yfp)*	This work
SU802	168 *trpC2^{+} dna-1 Δnoc::cat*	This work
SU803	168 *trpC2 Δnoc::cat Δsoj-spo0J::tet*	This work
SU804	168 *trpC2^{+} dna-1 Δnoc::cat Δsoj-spo0J::tet*	This work
SU823	168 *trpC2 Δsoj-spo0J::tet hutM(345°)::lacO(cat), thrC (283°)::lacI-cfp(erm) amyE::(spc P_{xyl}-ftsZ-yfp)*	This work
SU824	168 *trpC2^{+} dna-1 Δsoj-spo0J::tet hutM(345°)::lacO(cat), thrC (283°)::lacI-cfp(erm) amyE::(spc P_{xyl}-ftsZ-yfp)*	This work
SU827	168 *trpC2 Δnoc::cat Δsoj::kan*	This work
SU828	168 *trpC2^{+} dna-1 Δnoc::cat Δsoj::kan*	This work

SU829	168 *trpC2 Δnoc::cat Δspo0J::kan*	This work
SU830	168 *trpC2^{+} dna-1 Δnoc::cat Δspo0J::kan*	This work
SU831	168 *trpC2 Δnoc::cat amyE::(spc P$_{xyl}$-ftsZ-yfp)*	This work
SU832	168 *trpC2^{+} dna-1 Δnoc::cat amyE::(spc P$_{xyl}$-ftsZ-yfp)*	This work
SU833	168 *trpC2 Δnoc::cat Δspo0J::kan amyE::(spc P$_{xyl}$-noc-yfp)*	This work
SU834	168 *trpC2^{+} dna-1 Δnoc::cat Δspo0J::kan amyE::(spc P$_{xyl}$-noc-yfp)*	This work
SU835	168 *trpC2 Δnoc::cat Δsoj-spo0J::tet amyE::(spc P$_{xyl}$-ftsZ-yfp)*	This work
SU836	168 *trpC2^{+} dna-1 Δnoc::cat Δsoj-spo0J::tet amyE::(spc P$_{xyl}$-ftsZ-yfp)*	This work
SU837*	168 *trpC2 Δspo0J::neo, amyE::spo0J^{L12S} (cat)*	This work
SU838*	168 *trpC2 Δspo0J::neo, amyE::spo0J$^{L5H, S68P}$ (cat)*	This work
SU839*	168 *trpC2 Δspo0J::neo, amyE::spo0J$^{L12S, D73G, V198A}$ (cat)*	This work
SU840*	168 *trpC2 Δspo0J::neo, amyE::spo0J^{N112S} (cat)*	This work
SU841*	168 *trpC2 Δspo0J::neo, amyE::spo0J^{R149G} (cat)*	This work
SU842*	168 *trpC2 Δspo0J::neo, amyE::spo0J^{N112S} (cat)*	This work
SU843*	168 *trpC2^{+} dna-1 Δspo0J::neo, amyE::spo0J^{L12S} (cat)*	This work
SU844*	168 *trpC2^{+} dna-1 Δspo0J::neo, amyE::spo0J$^{L5H, S68P}$ (cat)*	This work
SU845*	168 *trpC2^{+} dna-1 Δspo0J::neo, amyE::spo0J$^{L12S, D73G, V198A}$ (cat)*	This work
SU846*	168 *trpC2^{+} dna-1 Δspo0J::neo, amyE::spo0J^{N112S} (cat)*	This work
SU847*	168 *trpC2^{+} dna-1 Δspo0J::neo, amyE::spo0J^{R149G} (cat)*	This work
SU848*	168 *trpC2^{+} dna-1 Δspo0J::neo, amyE::spo0J^{N112S} (cat)*	This work
SU849	*smc-ssrA loxP (kan), lacA::P$_{xyl}$A Ec sspB loxP(erm)*	(Wang et al, 2014c)
SU850	168 *trpC2 smc-ssrA loxP (kan), lacA::PxylA Ec sspB loxP (erm)*	This work
SU851	168 *trpC2^{+} dna-1 smc-ssrA loxP (kan), lacA::PxylA Ec sspB loxP (erm)*	This work
SU852	*scpB-yfp (spc)*	(Sullivan et al, 2009)
SU853	*yhdG::scpAB (phleo)*	(Sullivan et al, 2009)
SU862	168 *trpC2* yhdG::scpAB *(phleo)*, scpB-yfp *(spc)*	This work
SU863	168 *trpC2^{+} dna-1 yhdG::scpAB (phleo), scpB-yfp (spc)*	This work
SU864	168 *trpC2 Δspo0J::neo, yhdG::scpAB (phleo), scpB-yfp (spc)*	This work
SU865	168 *trpC2^{+} dna-1 Δspo0J::neo, yhdG::scpAB (phleo), scpB-yfp*	This work

	(spc)	
SU866	168 *trpC2 Δspo0J::neo, amyE::spo0J^{L12S} (cat), yhdG::scpAB (phleo), scpB-yfp (spc)*	This work
SU867	168 *trpC2^{+} dna-1 Δspo0J::neo, amyE::spo0J^{L12S} (cat), yhdG::scpAB (phleo), scpB-yfp (spc)*	This work
SU868	168 *trpC2 Δspo0J::neo, amyE::spo0J^{R149G} (cat), yhdG::scpAB (phleo), scpB-yfp (spc)*	This work
SU869	168 *trpC2^{+} dna-1 Δspo0J::neo, amyE::spo0J^{R149G} (cat), yhdG::scpAB (phleo), scpB-yfp (spc)*	This work
SU870	168 *trpC2 Δnoc::tet Δspo0J::neo, amyE::spo0J^{L12S} (cat)*	This work
SU871	168 *trpC2 Δnoc::tet Δspo0J::neo, amyE::spo0J^{R149G} (cat)*	This work
SU872	168 *trpC2^{+} dna-1 Δnoc::tet Δspo0J::neo, amyE::spo0J^{L12S} (cat)*	This work
SU873	168 *trpC2^{+} dna-1 Δnoc::tet Δspo0J::neo, amyE::spo0J^{R149G} (cat)*	This work

* Strains have been renamed in Chapter 5 for simplicity. Please refer to Chapter 5, section 5.2.1.1 for change in nomenclature.

Growth media used to cultivate *B. subtilis* cells are listed in Table 2.3. Unless otherwise specified, all cells were grown in liquid Antibiotic medium 3 (also referred to as Penassay Broth; PAB) or on tryptose blood agar base (TBAB). Spores were germinated and outgrown in germination medium defined (GMD). Liquid cell cultures were incubated with vigorous shaking in a gyratory water-bath (OLS200; Grant), and growth was monitored by recording the optical density at 600 nm (OD_{600}) using a spectrophotometer (UV-1601 Shimadzu). GMD was supplemented with L-tryptophan (50 mg/mL), and when required, GMD was also supplemented with xylose as specified in the text. Antibiotics used for selection are listed below in Table 2.4. Bacterial strains cultures were stored in 16% (v/v) glycerol at -80°C.

Table 2.3: *Bacillus subtilis* growth media

Medium	Constituents [a]
Penassay Broth (PAB)	1.75% Bacto antibiotic medium 3
Tryptose blood agar base (TBAB)	3.3% TBAB
Germination media defined (GMD)	80 mM K_2HPO_4, 44 mM KH_2PO_4, 15 mM $(NH_4)_2SO_4$, 3.4 mM sodium citrate, 0.5% glucose, 0.3% monosodium glutamate, 0.3% asparagine, 0.05% Bacto casamino acids, 0.02% $MgSO_4.7H_2O$
MD Medium	10% (v/v) 10X PC buffer, 2% glucose, 2.5 µg/mL tryptophan, 0.5% ammonium ferric citrate $[Fe(NH_4)_3(C_6H_5O_7)_2]$, 2.5 µg/mL aspartate, 0.3% $MgSO_4$
Sporulation agar	0.8% Bacto nutrient broth, 13.4 mM KCl, 1 mM $Ca(NO_3)_2$, 0.5 mM NaOH, 0.01 mM $MnCl_2$, 0.001mM $FeSO_4$, 0.001 mM $MgSO_4.7H_2O$, 1.5% Bacto agar

[a] All media was made using purified and deionised water (Mill-Q water, MQW), and sterilised by either autoclaving or 0.2 µm filtration. TBAB, Bacto Agar, Bacto antibiotic medium 3, Bacto casamino acids and Bacto nutrient broth were from Difco. All percentages are given as w/v, unless otherwise stated.

Table 2.4: Antibiotics used for selection in *Bacillus subtilis*

Drug/Antibiotic[a]	Working concentration (µg/ml)
Chloramphenicol	5
Erythromycin	0.5-1
Kanamycin[b]	2-10
Phleomycin	0.4
Spectinomycin	60
Tetracycline	10

[a] Stock solutions were prepared by dissolving antibiotics either in ethanol or ROW and filter sterilizing (0.2 µm filter). Erythromycin, kanamycin, phleomycin and spectinomycin were stored at 4°C, and chloramphenicol and tetracycline at -20°C. [b] Kanamycin was used in place of neomycin for the relevant strains listed in Table 2.2 per the recommendation of the strain donator.

2.2.1 Testing for the disruption of the *amyE* locus in *Bacillus subtilis* cells

This work involved the insertion of the *ftsZ-yfp* gene cassette into the *amyE* locus of the *Bacillus subtilis* chromosome. The *amyE* locus encodes for the synthesis of a starch degrading enzyme, amylase, which breaks down starch into simple sugars (Feucht and Lewis, 2001). To test that the *amyE* gene has been disrupted (i.e. does not produce amylase), and therefore indicating a gene insertion, *Bacillus subtilis* cells were streaked out onto TBAB agar plates containing 1% (w/v) starch and incubated overnight at 30°C. Culture plates were then stained by liquid iodine. Agar in the vicinity of colonies with a disrupted *amyE* gene was stained purple, whilst agar surrounding colonies still possessing a functional *amyE* gene remained colourless.

2.2.2 Testing for the temperature sensitive DNA replication mutation

A temperature sensitive DNA replication mutant (*dna-1*) of *B. subtilis* was used in this work to block DNA replication initiation. To test whether all strains created and used in this work possessed the temperature sensitive mutant, strains were streaked out onto TBAB agar plates and incubated overnight at 30°C (permissive temperature) or 48°C (non-permissive temperature). Strains that grew at 30°C but were unable to at 48°C were considered to be temperature sensitive, whilst cells that were not temperature sensitive grew at both temperatures.

2.3 Preparation, germination and outgrowth of *B. subtilis* spores

Spores were prepared following a similar method as outlined in Harry *et al.*, (1999). An overnight culture was prepared by inoculating 10 mL PAB with a single colony of *B. subtilis* and incubated at 30°C overnight with low agitation. The overnight culture was subsequently used to inoculate 10 mL of fresh PAB to an OD_{600} of 0.05. The culture was then grown with vigorous shaking to early stationary phase (OD_{600} ~1). 400 µL of the culture was spread out onto a sporulation agar plate (18 cm petri dish) and incubated in a 30°C oven for approximately 7 day until majority of the cells (~80%) had developed bright-phase mature spore, as seen by phase-contrast

microscopy. When the spores were ready to be harvested, the spores were resuspended in sterile reverse osmosis water (ROW) and centrifuged for 10 minutes at 10,000 *g* at 4°C. Spores were then washed twice in ROW, resuspended in 25 mL TE buffer supplemented with lysozyme (1 mg/mL; Sigma) to lyse any vegetative cells (spores are resistant to lysozyme) and incubated at 30°C for 1.5 hours with vigorous shaking. SDS (2% (v/v)) was added to the culture to dissolve the cell membrane of the vegetative cells and incubated at 30°C for a further 30 minutes. Together, lysozyme and SDS remove the vegetative cells from the suspension. The suspension was then centrifuged for 10 minutes at 10,000 *g* at 4°C, and the resulting pellet was washed up to 8 times in sterile ROW until only bright-phase spores remained. The final pellet was resuspended and stored at 4°C in sterile ROW. Spore concentration was determined by absorbance given that 10^{10} spores/mL results in an OD_{625} of 50. Spores were germinated at a concentration of 2 x 10^8 spores/mL in GMD at 34°C with vigorous shaking and were continued at either 34°C or 48°C depending on the experiment performed. Spores were grown out to a point where cell lengths were similar to allow for comparison at a similar cell cycle stage. Therefore, outgrowth times varied amongst strains. Refer to text for specific spore outgrowth times and conditions for each strain described.

2.4 Preparation and transformation of competent *Bacillus subtilis* cells

2.4.1 Preparation of competent *Bacillus subtilis* cells

Bacillus subtilis cells were made competent as follows. A single colony of the strain to be made competent was cultivated at 30°C in PAB overnight with the addition of auxotrophic requirements specific to the strain. The overnight culture was used to inoculate 10 mL fresh MD medium (See Table 2.3) supplemented with 100 µL 10% casamino acids (CAA, Difco) to an OD_{600} of 0.05. The MD medium culture was incubated at 30°C with vigorous shaking until the culture reached an OD_{600} of 1 - 1.5. An equal volume of MD medium was added to the culture and incubated for a further 1 hour at 30°C. Glycerol was added to the culture to a final concentration of

16% (v/v) and 1mL aliquots of the competent cell culture were stored at -80°C until required.

2.4.2 Transformation of competent *Bacillus subtilis* cells

The donor chromosomal DNA (5-10 µL; approximately 100 µg) was added to an 800 µL aliquot of competent cell culture, along with a no DNA control. The culture was incubated at 30°C with vigorous shaking for 30 minutes. The culture was supplemented with 50 µL 10% CAA and incubated for a further 1.5 hours at the same temperature. Culture was then spun down at 10,000 *g* for 2 minutes. Supernatant was removed and the resulting pellet was resuspended in 200 µL MSA. 100 µL of the culture was spread out onto TBAB agar plates supplemented with required antibiotics. The plates were incubated at 30°C for 24 hours for potential transformants to appear.

2.5 General DNA methods

2.5.1 *Bacillus subtilis* chromosomal DNA extraction

Chromosomal DNA was extracted and purified from *Bacillus subtilis* cells as follows. 3 mL of overnight culture of the required strain was centrifuged for 2 minutes at 10,000 *g*. The supernatant was removed and the pellet was resuspended in 500 µL TES. 25 µL of 10 mg/mL lysozyme, made up fresh in TES, was supplement to the culture and incubated at 37°C for 30 minutes. An equal volume (525 µL) of XS Buffer (2X; See Table 2.1) was added to the culture and incubated at 65°C for a further 1-2 hours. Next, the cell culture was vortexed for 10 seconds, and then kept on ice for 30 minutes. The cell suspension was then centrifuged for 10 minutes at 14,000 *g* in a microcentrifuge. The supernatant was removed and placed into fresh eppendorf tubes and an equal volume of isopropanol was added to the supernatant. This was then incubated at room temperature for 5 minutes followed by gentle inversion until the DNA was precipitated. The DNA was then plated by centrifugation for 2 minutes at 10,000 *g*, and supernatant was removed. The DNA pellet was resuspended in 500 µL ice cold 70% ethanol, and then centrifuged for 2 minutes at 10,000 *g* once again. The supernatant was removed and the DNA pellet was left to air-dry for 20-30

minutes at room temperature to evaporate any remaining ethanol. The DNA pellet was then resuspended in 200 µL TE (1X) supplemented with RNAse (100 µg/mL). The chromosomal DNA was stored at 4°C and used for transformation and PCR.

2.5.2 Polymerase Chain Reaction (PCR)

PCR was used in this study to validate the deletion of genes from the *Bacillus subtilis* strains created. For all PCR reactions used to check gene deletions, *Taq* polymerase (New England Biolabs) and 1X Thermo Pol buffer (New England Biolabs) was used. Single-stranded oligonucleotide primers for PCR were generated by IDT and supplied in a lyophilised form. Primers were dissolved in MQW to a final concentration of 100 µM and stored at –20°C. Primers used are listed below in Table 2.5. The PCR reaction mixtures consisted of template DNA (100 ng for chromosomal DNA), 500 nM of each primer (see Table 2.5), 1X amplification buffer, 200 µM of dNTP mix (Fermentas) and 1.25 U of DNA polymerase (*Taq* polymerase), made up to 50 µL in MQW. PCR mixtures were subjected to the following temperature cycle using a thermo cycler (Mastercycler; Eppendorf): 10 minutes at 95°C (for initial denaturation of the template), 30 cycles consisting of 95°C for 1 minutes, (template denaturation), X °C for 1 minutes (primer annealing) and 72°C for Y sec (extension), followed by a further 5 minutes at 72°C for final extension (where X = predicted oligonucleotide annealing temperature minus ~3 °C, and Y = 1 minutes per kb to be amplified). The PCR reaction products were analysed via agarose gel electrophoresis (See Section 2.5.4).

Table 2.5: Primers used for PCR reaction

Sequence 5' to 3'	Description
GCTGTTTCATTTGGTTCTGG	Forward primer upstream of *amyE*
CTTTTGCGTTGGTTGTATCC	Reverse primer downstream of *amyE*
GACGCTTGGAGGAGAACTTGAG	Forward primer upstream of *noc*
GGGACATGCAGTAATTTCACC	Reverse primer downstream of *noc*
CCATCCTGTTTCCACGTTCTG	Forward primer upstream of *soj-spo0J*
GGCAAATGTTCTAGCGGAAGG	Reverse primer downstream of *soj-spo0J*

2.5.3 Determination of DNA concentration

DNA concentrations were determined using a spectrophotometer as described by Sambrook *et al.* (Sambrook et al, 1989).

2.5.4 Agarose gel electrophoresis

Agarose gels were prepared on a horizontal slab gel apparatus (Bio-rad). Agarose (type 1: low electroendosmosis; Sigma) at 0.7-2% (w/v) was dissolved in electrophoresis buffer (TBE) and gels were cast with a well-forming comb in place. Gels contained 60 ng/mL of GelRed® (Biotium) to visualise the DNA. The PCR amplified DNA was prepared in 1X gel loading dye blue (New England Biolabs) and loaded into the pre-cast wells. Bacteriophage λ DNA pre-cut with *Hind*III (New England Biolabs) was used for size standards, enabling the size estimation of DNA fragments greater than 1 kb. Agarose gels were run submerged under a volume of 1X TBE electrophoresis buffer that lay above the surface of the gel at 80 V for approximately 1 hour. The gels were visualised via exposure to short-wavelength UV light (254 nm) using a transilluminator (Ingenius3; Syngene) and recorded as a digital image using a charge-coupled device (CCD) camera (Synoptics CAM-FLXCM; Syngene) linked to GeneSys molecular imaging software, version 1.5.0.0 (Syngene).

2.5.5 DNA sequencing

Specific regions of the *B. subtilis* chromosome were amplified and sequenced during this study to confirm the correct construction of strains and/or the presence of particular mutations (Table 2.2). PCR was employed to amplify the regions of interest, as described in Section 2.5.2. Purified PCR products, along with appropriate primers, were then sent to the Australian Genome Research Facility (AGRF; University of Queensland, Australia), where sequencing reactions were performed. Sequencing data was analysed using the Lasergene® (DNASTAR) software.

2.6 Microscopy Methods

2.6.1 Immunofluorescence microscopy (IFM)

IFM was used for the detection of the FtsZ protein in various strains of *B. subtilis* under various conditions as specified in the text. The IFM method used in this study is based on the method previously described in Harry *et al.* (1995), with the exception that methanol was used as a fixative agent in the cell fixation process (Harry et al, 1995). Mid-exponential vegetative cells or outgrown spores (1 mL) were concentrated by centrifugation at 10,000 *g* for 2 minutes and resuspended in 500 µL PBS. This suspension was then added to 10 mL ice-cold methanol (-20°C), mixed by inversion and then fixed at -20°C for 1 - 2 hours. Fixed cells were pelleted by centrifugation for 5 minutes at 4400 *g*, and then resuspended in 500 µL PBS. Fixed cells were once again pelleted and resuspended in 90 µL GTE. Meanwhile, multi-well microscope slides (ICN Biochemicals) were prepared for cell adhesion by treating the wells with 0.1% poly-L-lysine solution (Sigma) for 2 minutes at room temperature, followed by aspirating the wells dry and washing them twice with MQW. Slides were allowed to dry before applying the cell samples. Cell samples were then permeabilized with the addition of 10 µL of lysozyme (10 mg/mL made up in GTE) and then immediately added to the wells onto the multi-well slide. Cells were incubated on the slides for 3 minutes and the remaining liquid was aspirated off until wells were dry. Blocking solution (2% BSA (w/v), 0.05% (v/v) Tween 20 in PBS) was added to the wells and incubated for 15 minutes. From this point onwards, wells were not allowed to dry out. The wells were washed once with PBS. Primary antibodies specific to FtsZ (See Table 2.6) was made up to a 1:10,000 dilution and added in 10 µL volumes to each well and the slide was incubated overnight at 4°C in a humidified chamber (a closed petri dish with a damp tissue).

The primary antibody solution was aspirated off the next morning and the slide was washed with PBS ten times without allowing the wells to dry out completely. The wells were then blocked with 5% goat serum (diluted in PBS) for 30 minutes. The goat serum was aspirated off and wells were washed once with PBS. A secondary antibody with a fluorescent conjugate (i.e. goat anti-rabbit secondary antibody

conjugated to Alexa 488; see Table 2.6) was diluted in PBS containing 2% BSA and added to the wells and incubated at room temperature for 1 hour in the dark. Wells were then washed with PBS ten times. The slide was mounted with PBS containing glycerol (50%) and a fluorescent DNA stain 4′6-diamidino-2-phenylindole (DAPI; 0.4 µg/mL), and then covered with a coverslip. The edges of the coverslip were sealed with nail polish. Images were obtained as described in Section 2.6.4 and slides were stored at -20°C.

Table 2.6: Antibodies used for primary and secondary detection for both IFM and Western blot analysis

Antibody raised against	Source	Origin	Dilution used	Antibody type/conjugate
FtsZ (primary)	S. Moriya	Rabbit	1:10,000 (IFM) 1:1,000 (Western blot)	Whole serum
SMC (primary)	S. Moriya	Rabbit	1:10,000 (IFM) 1:1,000 (Western blot)	Whole serum
Rabbit Ig (secondary)	Molecular Probes	Goat	1:10,000 (IFM)	Alexa 488
Rabbit Ig (secondary)	Promega	Goat	1:1,000 (Western Blot)	Horseradish peroxidase

2.6.2 Ethanol fixation for nucleoid visualisation

Cells were fixed for nucleoid visualisation using an ethanol-fixation method. Vegetative cell or outgrown spore cultures (1 mL) were collected and pelleted for 2 minutes at 10,000 *g* in a microcentrifuge. The supernatant was removed and the pellet was resuspended in 300 µL PBS. 700 µL of cold ethanol (95% (v/v)) was then added to fix the cells. Cells were fixed for 1 – 5 days at 4°C. The fixed cell suspension (400 µL) was pelleted for 3 minutes at 10,000 *g* in a microcentrifuge, and the pellet was washed twice in 200 µL PBS by resuspension and centrifugation. Cells were resuspended in 200 µL PBS supplemented with DAPI (0.4 µg/mL). The fixed cells, in 10 µL volumes, were then transferred to poly-L-lysine treated multi-well slides (ICN Biochemicals; as described in Section 2.6.1), and incubated at room temperature for

up to 30 minutes in the dark. The excess liquid was aspirated off and wells were washed once with MQW. The slide was mounted in PBS containing glycerol (50%) and the edges of the coverslip were sealed with nail polish. Images were obtained as described in Section 2.6.4 and slides were stored at -20°C.

2.6.3 Preparation of cells for live cell fluorescence microscopy

To examine the localisation of YFP fusion proteins, live cells expressing the fusion were collected and immobilised on agarose-coated microscope slides as follows. First, Gene frame (AB Gene) was used to create a small square well on the surface of a glass slide. Agarose (type1; Sigma) was dissolved at 2% (w/v) in MQW using a microwave oven and 70 µL of this agarose solution was added to centre of the well. A coverslip was immediately placed on top to produce a flat surface, and the agarose was allowed to cool within the well for a minimum of 5 minutes. Vegetative cell or outgrown spore culture (up to 1 mL) supplemented with DAPI (0.4 µg/mL) for nucleoid visualisation was pelleted by centrifugation for 2 minutes at 10,000 *g* using a microcentrifuge. The coverslip on the agarose was removed while the samples were centrifuged to allow for the agarose to partially dry. The majority of the supernatant was removed from the centrifuged samples, with approximately 10µL remaining to resuspend the pellet. To mount the cells for fluorescence microscopy, the coverslip from the agarose pad was gently removed and 3 µL of the concentrated cell culture was spread along the flat agarose surface. A new coverslip was then gently applied and the cells were visualised immediately.

2.6.4 Phase-contrast and fluorescence microscopy

Cells were visualised using phase-contrast and fluorescence on a Zeiss Axioplan 2 fluorescence microscope at 100x magnification using a Plan ApoChromat (100× NA 1.4; Zeiss) objective lens. The light source was a 100 W high pressure mercury lamp passed through the following filter blocks: with exposure times of 50 – 700 ms: for visualising Alexa 488 (Filter set 09, Zeiss; 450 - 490 nm BP excitation filter, 515 nm long pass (LP) barrier filter), for visualising DAPI (Filter set 02, Zeiss; 365 nm excitation filter, 420 nm long pass (LP) barrier filter), for visualising CFP (Filter Set

31044 v2, Chroma Technology; 426-446 nm excitation filter, 455 nm beamsplitter, 460-500 nm barrier filter), and for visualizing YFP (Filter set 41029, Chroma Technology). AxioCam MRm camera was used for image collection. Images were processed and analysed using AxioVision software, version 4.8 (Zeiss).

2.6.5 Cell scoring and statistics

Cell length values were scored directly from digital micrographs using AxioVision software, version 4.8 (Zeiss), with the appropriate scaling. The positioning analysis of fluorescent signals of interest (including the Z ring seen as a band and *oriC* seen as a focus within the cell) was determined by measuring the distance from the fluorescence signal to the nearest cell pole and by dividing this value by the cell length, with 0.5 being exactly midcell. Numerical values derived for each cell length and position was exported from the AxioVision software as a text file, and imported into Excel (Microsoft) for data processing and statistical analysis. Excel was used to calculate the mean, standard deviation, standard error of the mean (SEM), the 95% confidence interval for the mean, the number of cells counted (n) for each data set. Excel and SigmaPlot (Systat Software Inc) was used to generate the graphs presented in this study.

Statistical analysis of the data obtained was carried out using the "Kolmogorov - Smirnov" test via an online calculator (http://www.physics.csbsju.edu/stats/KS-test.n.plot_form.html). The "Kolmogorov - Smirnov" test was used to compare the precision of midcell Z ring or *oriC* positioning between wild-type and mutant strains. This test was performed using a 95% confidence interval, where $P < 0.05$ was indicative of a statistically significant difference between the data sets compared. Statistical tests were performed following personal communication with Dr. Fraser Torpy.

2.7 DNA content quantification via flow cytometry

To examine DNA content per cell, flow cytometry was used as described by Okumura *et al.* (Okumura et al, 2012). 10 mL of spore or vegetative cells were grown to the desired stage of growth (in the context of this thesis, this was the stage at which Z

rings were examined for each relevant strain or condiition), before chloramphenicol was added to a final concentration of 200 µg/ml. Cells were then incubated for a further 5 hours to allow for completion of any ongoing rounds of replication, without allowing any new rounds of replication or division to occur (outgrown spores were not subjected to the chloramphenicol treatment, instead were grown to strain specifications as described in text before being collected and fixed as follows). Cells were then pelleted for 3 minutes at 6,000 *g* in a microcentrifuge. The supernatant was removed and the pellet was resuspended in 2 mL TKE flow buffer. Cells were again pelleted for 3 minutes at 6,000 *g* and resuspended in 100 µL TKE flow buffer. 1 mL cold ethanol (77% (v/v)) was then added to fix the cells. Cells were incubated overnight at 4°C. Cells were then subjected to 3X washing with TKE flow buffer before being resuspended in 1 mL TKE buffer containing 250 µg/mL RNaseA and incubated at 37°C for 1 hour. Cells were again washed 3X with TKE flow buffer. Cell concentration was then adjusted by spectrophotometry to OD_{600} 0.01 with TKE flow buffer. SYTO16 (1 µM; Molecular Probes) was then added to the cell suspension at RT in the dark for 1 hour. The DNA content of the cell suspensions was then measured using an LSRII (Becton Dickinson), and data was analysed using FACSDiva software (version 8.0.1; Becton Dickinson).

2.8 Western blot analysis

2.8.1 Whole cell protein extraction for Western blotting

Cell lysates for Western blot analysis were prepared in the following way. *B. subtilis* cells (10 mL of exponentially-growing vegetative cells; OD_{600} 0.4-0.6, or outgrown spores to specified time) were centrifuged (12 000 *g*, 3 minutes) and the supernatant removed. The pellets were resuspended in adjusted amounts of lysis buffer (Table 2.1) so that each sample would contain an equal OD_{600} once resuspended (as a reference, the sample with the highest OD_{600} was always resuspended in 250 µL of lysis buffer, and the other samples were adjusted relative to this sample). This would ensure an equal loading of total protein onto the SDS-PAGE gels. The samples were then incubated at 37°C for 5 minutes and snap frozen in liquid nitrogen. SDS-PAGE loading buffer was added to a 1X final concentration (see Table 2.1) to the samples,

and the samples were then heated at 95°C for 5 minutes and stored at -20°C until required. Thawed samples were heated at 100°C for 2 minutes prior to loading onto a denaturing polyacrylamide gel (Section 2.8.2).

2.8.2 SDS-polyacrylamide gel

Resolving gels were prepared using the components in Table 2.7 APS and TEMED were added immediately before pouring. The components were mixed gently, so as not to introduce air bubbles, and loaded into the gel casting apparatus (BioRad Mini-Protean 3 gel slabs). A layer of isopropanol was pipetted onto the top of the gel to isolate it from the air. Once the gel had solidified, the stacking gel was made up as listed in Table 2.7.

Table 2.7 Constituents used to make the SDS-polyacrylamide gel

Polyacrylamide Gel constituents	Volume added	
	7.5% Resolving gel	Stacking gel
MQW	5 mL	3.6 mL
1.5 M Tris-HCl (pH8.8)	2.5 mL	N/A
0.5 M Tris-HCl (pH6.8)	N/A	750 µL
10% (w/v) SDS	100 µL	50 µL
30% (w/v) Acrylamide/Bis (37:5:1, BioRad)	2.5 mL	650 µL
10% (w/v) Ammonium persulphate (APS)	100 µL	50 µL
TEMED (N,N,N'N'-tetramethyl-ethylenediamine; BioRad)	10 µL	25 µL

The stacking gel was applied to the top of the resolving gel and a plastic comb was immediately inserted into the gel to create wells. After the gel had solidified, it was transferred to a Protean 3 (BioRad) gel-running tank and submerged in 1x SDS PAGE running buffer. The comb was removed and appropriate volumes of samples (5-20 µl) were loaded. 10 µl of Novex Prestained Protein Standards (Invitrogen) were also loaded. Protein samples were prepared as described in Section 2.8.1. Proteins were separated by electrophoresis at 90 V for 10 minutes, followed by 175 V until the blue dye front of the sample buffer was at the base of the gel plate (approximately 40 minutes). Following electrophoresis, the gel was either prepared for Western

blotting (Section 2.8.3 and 2.8.4) or stained in a staining solution [0.125% (w/v) Coomassie Brilliant Blue R250, 30% (v/v) methanol, 10% (v/v) acetic acid] for 2-4 hours before finally destaining with 2 or 3 changes of destain solution [30% (v/v) methanol, 10% (v/v) acetic acid] over 3-4 hours.

2.8.3 Western transfer

Immunoblot polyvinylidene difluoride (PVDF) membrane (BioRad) was cut to the same size as the SDS PAGE gel. The membrane was submerged briefly in 100% (v/v) methanol before being rinsed in sterile MQW and then equilibrated in Western transfer buffer for 10 minutes. Protein was transferred from the gel to the PVDF membrane by electroblotting in Western transfer buffer using Mini Trans-Blot apparatus (BioRad) at 30 V for 2 hours. The PVDF membrane was allowed to dry on blotting paper for 5 minutes before being blocked in blocking buffer overnight at 4°C with gentle shaking.

2.8.4 Immunodetection and quantification

After Western transfer, the blot was incubated in blocking solution [PBS + 5% (w/v) skim milk] for 2 hours at RT with rocking. The blot was then incubated with primary antibody (see Table 2.6 for antibody types and concentrations) diluted in blocking solution for 2 h at room temperature with rocking. The blot was rinsed three times, 5 minutes each, in PBS + 0.05% (v/v) Tween 20 + 5% (w/v) skim milk), then incubated in HRP-conjugated secondary antibody (see Table 2.6) diluted in blocking solution for 1 hour at RT. The blot was rinsed three times in PBS for 5 minutes each. Following this, the blot was incubated with the ECL (enhanced chemiluminescence; GE Healthcare) kit reagents and prepared for chemiluminescent detection according to the manufacturer's instructions. The membrane was then scanned for chemiluminescent reaction between the ECL reagents and the horseradish secondary antibody, using the ChemiDoc XRS+ imaging system (Bio-Rad). The ECL reaction peaks after a couple of minutes and for this reason the chemiluminescent reaction was acquired 6 times over 300 seconds to ensure that at least one of the images acquired would represent the peak-point of the reaction (i.e. generally the

image with highest intensity that is not saturated). Band intensities were analysed by ImageJ (version 1.49; NIH).

UTS
UNIVERSITY OF TECHNOLOGY SYDNEY

Chapter 3.
Spo0J influences Z ring positioning when the early stages of DNA replication are blocked

i3 ithreeinstitute

3.1 Introduction

Correct positioning of the division site at midcell in *B. subtilis* is linked to the initiation stage of DNA replication (Harry et al, 1999; Moriya et al, 2010; Regamey et al, 2000). The four treatments to inhibit the initiation of DNA replication used previously (*dna-1*, *polC133*, +HPUra and –thymine treatment) were shown to result in different frequencies of Z rings forming at the cell centre (Moriya et al, 2010). For example, very few midcell Z rings form when initiation of DNA replication is blocked early on via inactivation of the initiation helicase co-loader protein, DnaB, via the *dna-1* allele. In contrast, a higher frequency of midcell Z rings is observed when the initiation of DNA replication is blocked at a later stage, just prior to DNA elongation. These observations led to the proposed Ready-Set-Go model, which suggests that as initiation of DNA replication progresses, the ability of FtsZ to accumulate into a Z ring at midcell increases (Moriya et al, 2010). Importantly, this positive correlation between progression of the initiation phase of replication and the ability of the cell to form a Z ring at midcell is only seen in the absence of the nucleoid occlusion protein Noc.

One question that arises from the Ready-Set-Go model is, how does this link between initiation of DNA replication and midcell Z ring assembly come about? Is it a direct link such that the replisome proteins, already positioned at the midcell site, are directly controlling Z ring assembly at this site in some way? Or could there be an indirect link such that the replisome proteins affect chromosome organisation in a way that subsequently affects Z ring assembly at midcell. This second idea is supported by the observation that the ability to form Z rings at midcell in the aforementioned four treatments correlates with different nucleoid morphologies; with an increase in midcell Z rings during an initiation block frequently accompanied by a more ‘spread’ (bilobed) nucleoid morphology across the cell centre. Intriguingly, Z rings would not form over the nucleoid in the *dna-1* cells at the non-permissive temperature, irrespective of its morphology. These observations suggest common pathways and proteins for chromosome replication and organisation and or/ segregation, such that inactivation of a specific replication protein directly causes

changes to chromosome organisation, thus enabling bacterial cells to find their middle.

The well conserved proteins, Soj and Spo0J, remain two of the most studied proteins involved in chromosome organisation and segregation in a number of organisms (Badrinarayanan et al, 2015; Hajduk et al, 2016; Mierzejewska & Jagura-Burdzy, 2012; Wang & Rudner, 2014). Studies into the functions of Soj and Spo0J uncovered their effects on chromosome segregation. It was first observed that in vegetative cells, the absence of *spo0J* leads to a 100-fold increase (1-2%) in the formation of anucleate cells (Ireton et al, 1994) highlighting abnormal Z ring positioning. Further studies revealed lengthening in, or decondensation of, nucleoids in about 20% of cells in the absence of both Soj and Spo0J, or just Spo0J alone (Britton et al, 1998; Ireton et al, 1994; Lee & Grossman, 2006; Ogura et al, 2003). Additionally, cells lacking Spo0J show a loss in the quarter positioning of the origin of DNA replication (a sign of origin resolution) such that sister chromosome origins were positioned closer to midcell, suggesting Spo0J assists in the resolution and separation of newly replicated origins (Lee & Grossman, 2006). These observations highlight a defect in chromosome segregation and a subsequent effect on cell division by mispositioning of the division site.

Although the roles of Soj and Spo0J in *B. subtilis* have been extensively studied over the last few decades, the exact means by which these proteins mediate chromosome segregation remains unclear. Their known roles in both DNA initiation of replication and chromosome segregation ((Ireton et al, 1994; Lee & Grossman, 2006; Ogura et al, 2003; Scholefield et al, 2011), see Chapter 1 for further detail), along with the observed difference in chromosome morphologies when initiation of replication is inhibited at different stages mentioned earlier, make them likely candidates for playing a role in the initiation of DNA replication/Z ring positioning link. It is this idea that is explored in this chapter and throughout the thesis. One possibility is that Spo0J and Soj organise the chromosome differently in each of the four treatments (*dna-1* and *polC* temperature-sensitive mutants, +HPUra and –thymine) as a

consequence of the stage of initiation that is blocked, which in turn affects Z rings from forming at the cell centre.

Therefore, the primary aim of the work presented in this chapter was to investigate whether Soj and/or Spo0J play a role in the link between the initiation phase of DNA replication and division site placement in *B. subtilis*. To address this, Z ring positioning was examined in the absence of Soj and Spo0J (together and separately) when initiation of DNA replication was blocked via the inactivation of DnaB. Morphological changes to the nucleoid were also examined in these experiments. Similarly, Z ring positioning and nucleoid morphology were examined in the absence of Soj and Spo0J at a later stage of initiation, just prior to DNA elongation, via the addition of HPUra. Chromosome organisation changes were examined in more detail in the absence of *soj* and *spo0J* during the two tested DNA initiation replication blocks (inactivation of DnaB and addition of HPUra) by labelling an origin-proximal region. Finally, the level of DNA replication occurring within each of these experiments was examined by measuring DNA content via flow cytometry, to ensure that any changes to Z ring positioning observed were not a result of active DNA replication (i.e. the suppression of the initiation of DNA replication blocks).

3.2 Results

3.2.1 The absence of both *soj* and *spo0J* partially restores midcell Z ring formation in cells with an early block to initiation of replication

Disclaimer: Section 3.2.1 was completed just prior to the commencement of this PhD project. It has been included as part of the results to address the chapter aim holistically, and to allow adequate and clear interpretation and comparison of the data.

3.2.1.1 *Z ring positioning in the absence of soj-spo0J when DnaB is inactive*

When initiation of DNA replication is blocked at the early stage in the *dnaB* mutant (*dna-1*) at the non-permissive temperature, very few Z rings form at the cell centre (~10%). To determine whether Soj and Spo0J have an effect on Z ring positioning during initiation of DNA replication, Z ring positioning was examined in live outgrown spores. A deletion of both genes was initially explored to be able to utilise the spore outgrowth system, as only strains with a deletion of both *soj* and *spo0J* can produce spores (Ireton et al, 1994). FtsZ was tagged using a second xylose-inducible copy of FtsZ tagged with yellow fluorescent protein (FtsZ-YFP). Spores of the wild-type strain, *dna-1* mutation, *Δsoj-spo0J* and *dna-1 Δsoj-spo0J* (SU492, SU746, SU767 and SU768, respectively; see Materials and Methods Table 2.3) were germinated at 34°C in GMD supplemented with 0.02% xylose for 20 minutes before being shifted to the non-permissive temperature (48°C; prior to any initiation of DNA replication (Harry, 2001; White & Sueoka, 1973)) for 70 minutes. Z ring positioning results are shown in Figure 3.1 and Table 3.1. As a control, Z ring positioning was also examined at the permissive temperature here and in later experiments. Z ring positioning was found to be predominantly at midcell in all conditions and therefore has not been included in the results (data not shown). Consistent with published results (Harry et al, 1999; Moriya et al, 2010), wild-type (SU5) and *dna-1* (SU661) formed midcell Z rings with frequencies of 93% and 9%, respectively (note: midcell is considered to be the central 10% of a cell, as this is where majority, ~85%, in the wild-type strain. This classification of midcell is maintained throughout the thesis; see Materials and

Methods 2.6.5 for more detail; (Moriya et al, 2010)). A near-wild-type midcell Z ring frequency was observed in *Δsoj-spo0J* (85%). Interestingly, midcell Z ring frequency increased from 9 to 40% in *dnaB* mutant cells when both *soj* and *spo0J* are deleted (essentially the same results were obtained for vegetative cells, as well as when using IFM instead of live cell microscopy with FtsZ-YFP (data not shown)). In other words there is a partial increase in midcell Z rings. Furthermore, this level of increase in midcell Z ring formation was similar to that observed in this *dnaB* mutant in the absence of *noc* (see Chapter 1, section 1.6; (Moriya et al, 2010)).

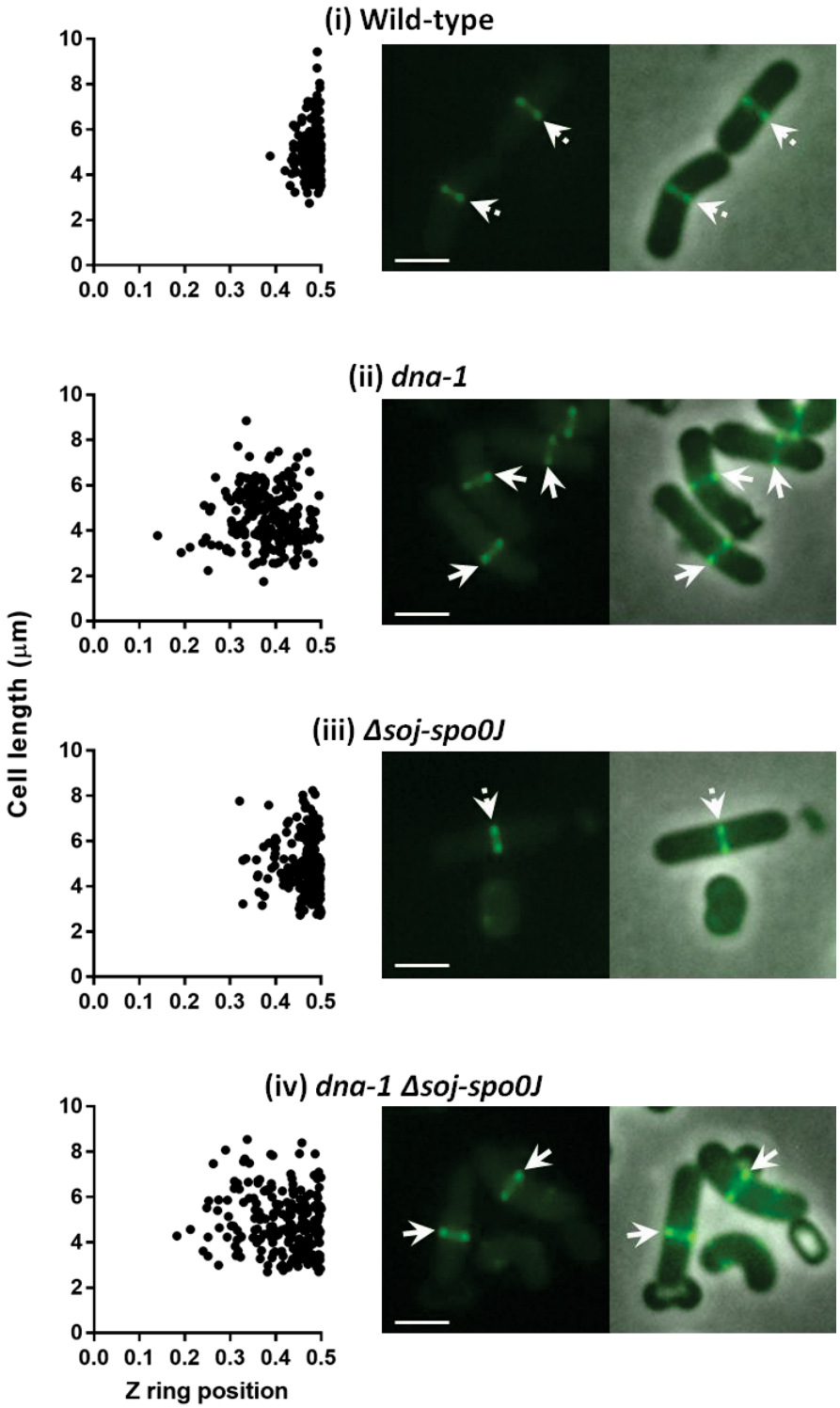

Figure 3.1: Z ring positioning when initiation of DNA replication is blocked during spore outgrowth in the *dna-1* temperature-sensitive mutant. Spores were germinated in GMD containing 0.02% xylose (v/v) for 20 minutes at the permissive temperature (34°C), then shifted to the non-permissive temperature (48°C) for a further 90 minutes (wild-type; SU492, *dna-1*; SU746, *Δsoj-spo0J*; SU767 and *dna-1 Δsoj-spo0J*; SU768). Figure shows scatter plots of Z ring positioning (left) and representative images of Z rings observed in live cells

(right) in (i) wild-type, (ii) *dna-1*, (iii) *Δsoj-spo0J* and (iv) *dna-1 Δsoj-spo0J*. Representative microscope images show falsely coloured green (left), and an overlay of FtsZ-YFP and phase-contrast (right). Broken arrows show centrally positioned Z rings, and full arrows show acentral Z rings. Scale bars represent 2 μm. Z ring position is determined by measuring the distance from the Z ring to the nearest cell pole and dividing this value by the cell length, with 0.5 being exactly midcell. A Z ring is considered to be at midcell if it was positioned within the range of 0.45-0.50, as this is where most Z rings form in the wild-type strain. n > 200. See subsequent Table 3.1 for midcell Z ring frequencies and average cell lengths (±SD) for each strain.

Table 3.1: Analysis of Z ring positioning in the *dna-1* temperature-sensitive mutant in the absence of *soj-spo0J* at 48°C.

Strain	Average cell length (±SD) [a]	% Midcell Z rings [b]
Wild-type	3.95 ± 0.61	93%
dna-1	4.23 ± 0.57	9%
Δsoj-spo0J	4.19 ± 0.71	85%
dna-1 Δsoj-spo0J	4.21 ±0.59	40%

[a] Table shows average cell length (±SD) and [b] percent of Z rings in the midcell range (0.45-0.5). Midcell is considered to be between 0.45 and 0.50 as this is where majority of Z rings form in wild-type cells. Scatter plots of Z ring positioning are depicted in Figure 3.1. See Figure 3.1 for strain growth conditions and midcell Z ring characterisation.

3.2.1.2 *Co-visualisation of the nucleoid and Z ring in dna-1 Δsoj-spo0J outgrown spores*

Following the same conditions above, the DNA was co-visualised with Z rings in the four strains using DAPI. This revealed different nucleoid morphologies in all the strains which were grouped into 3 categories (see Figure 3.2): cells with a single region of DNA were denoted as "single-lobed" (Figure 3.2i); cells with two adjacent regions of DNA were termed "bilobed" (Figure 3.2ii); and cells with DNA that had a spread appearance through part or the entire cell were denoted "spread" (Figure 3.2iii). No cells of the *dna-1* or *dna-1 soj-spo0J* strains were seen to have a wild-type-like nucleoid morphology shown in Figure 3.2 iv.

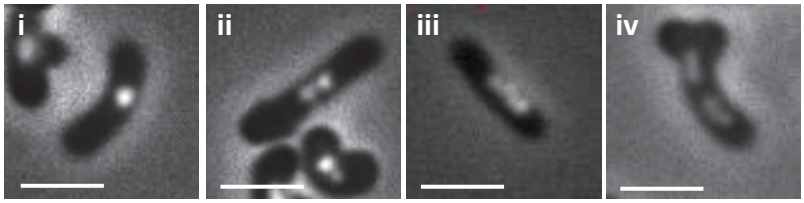

Figure 3.2: Different nucleoid morphologies observed in Δsoj-spo0J cells when initiation of DNA replication is inhibited by the *dna-1* mutation. (i) single-lobed, (ii) bilobed, and (iii) spread nucleoid; and (iv) a wild-type cell with replication occurring normally. Scale bar represents 2μm.

Consistent with previous reports (Moriya et al, 2010), in the *dna-1* strain (SU746) at the non-permissive temperature, the predominant nucleoid morphology was single-lobed (Figure 3.3 and Table 3.2). This occurred at a frequency of 78%, followed by bilobed nucleoids at a frequency of 16%, and 6% spread morphology was observed. In only 2% of the cells did a Z ring occur at the cell centre over the unreplicated nucleoid. The *dna-1 soj-spo0J* mutant had a very different frequency pattern of nucleoid morphologies compared to the *dna-1* mutant (Figure 3.3 and Table 3.2), with only half of the frequency of single-lobed nucleoids as that observed in the *dnaB* mutant, and more than a two-fold higher frequency of bilobed nucleoids than the *dna-1* strain (37% versus 16%, respectively). Furthermore, a significant increase

in spread nucleoids was observed in the *dna-1 soj-spo0J* mutant at 48°C. Of the 40% Z rings that formed at the cell centre, there was an equal number of Z rings forming over the unreplicated nucleoid (21%; 1% single-lobed, 8% bilobed and 12% spread), or adjacent to an unreplicated nucleoid that had moved off-centre (20%; 10% single-lobed, 9% bilobed and 1% spread). Therefore when DNA initiation replication is blocked in the *dna-1* mutation in the absence of both *soj* and *spo0J*, Z rings form more readily at the cell centre. This appears to correlate with a change to nucleoid morphology, highlighted by a decrease in single-lobed nucleoids and instead an increase in both bilobed and spread nucleoids. Given this correlation between increase in midcell Z rings and increase in bilobed or spread nucleoid morphologies, it was important to consider the possibility that this increase in midcell Z ring frequency seen in the *dna-1 soj-spo0J* mutant at the non-permissive temperature was attributed to a relief in the block to initiation of DNA replication such that some active replication was occurring and Z rings could more readily form at the centre. This however was shown not to be the case, with the block to initiation of DNA replication being maintained. This result is presented in section 3.2.5.

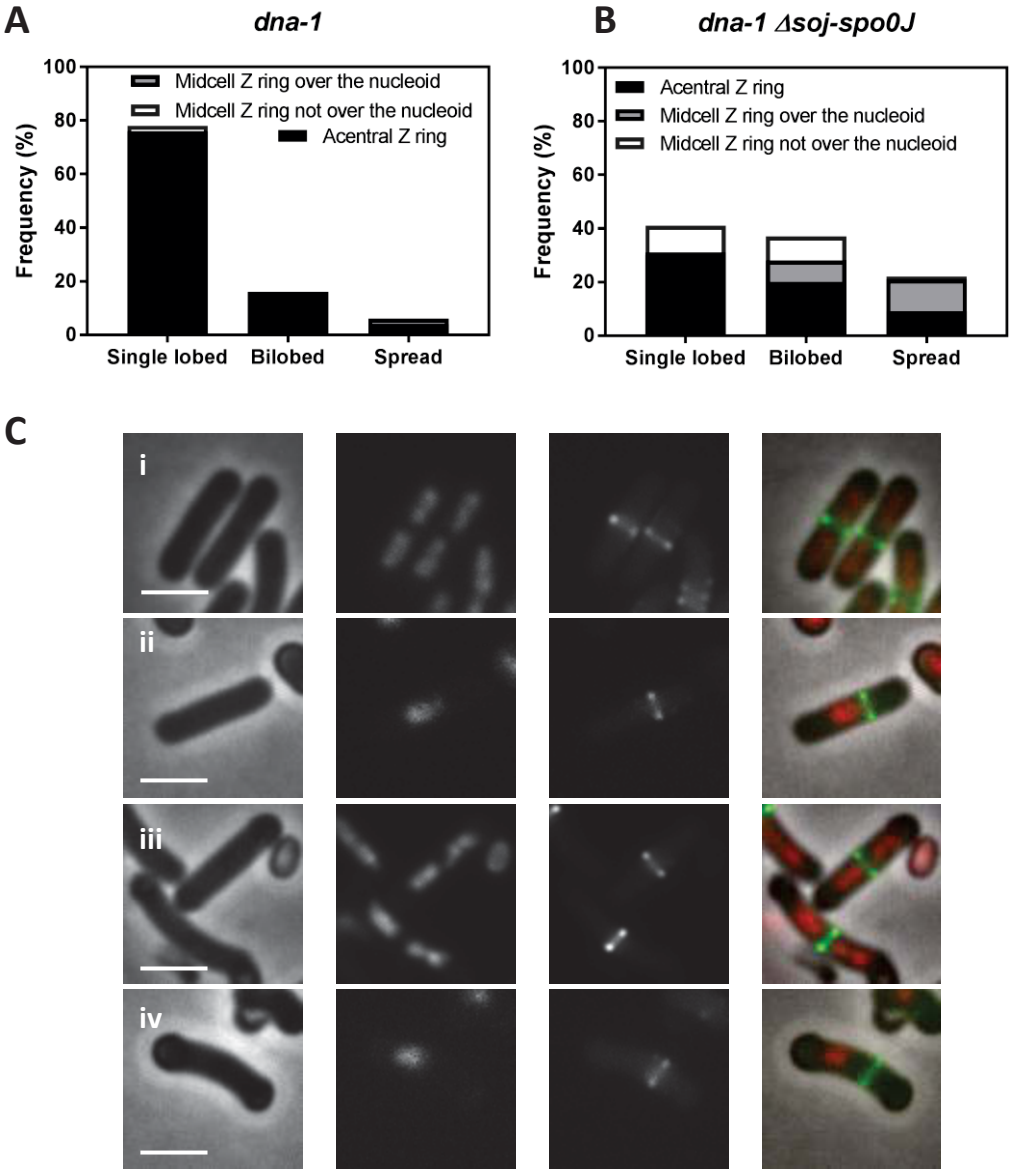

Figure 3.3: Z ring and nucleoid co-visualisation in live *ftsZ-yfp*-containing *B. subtilis* outgrown spore cells at 48°C. Spores were germinated at 34°C for 20 minutes in GMD supplemented with 0.02% xylose, and then shifted to 48°C for 65 minutes. (A and B) Histogram representation of Z ring position relative to different nucleoid type in (A) *dna-1 ftsZ-yfp* and (B) *dna-1 Δsoj-spo0J ftsZ-yfp.* The height of each bar represents the frequency of each nucleoid type, showing the proportion of acentral Z rings (black), midcell Z rings over the nucleoid (grey) and midcell Z rings not over the nucleoid (white). See Table 3.2 for numerical values of the data. (C) Representative images of the predominant Z ring position in each strain with (i) midcell in wild-type cells; (ii) acentral, to one side of the nucleoid in *dna-1*; (iii) midcell in *Δsoj-spo0J* cells when replication is occurring; and (iv) an acentral Z ring seen in *dna-1 Δsoj-spo0J* cells. Representative images above show in each column: phase-

contrast; DAPI (0.4 μg/mL); FtsZ-YFP; and an overlay of the three preceding images. Scale bar represents 2 μm. n > 200.

Table 3.2: Frequency of different nucleoid morphologies and midcell Z rings when initiation of DNA replication is blocked.

	Nucleoid morphology					
Z ring position	**Single-lobed**		**Bilobed**		**Spread**	
	dna-1	*dna-1 Δsoj-spo0J*	*dna-1*	*dna-1 Δsoj-spo0J*	*dna-1*	*dna-1 Δsoj-spo0J*
Acentral Z ring (%)	76	30	16	20	4	9
Midcell Z ring over the nucleoid (%)	0	1	0	8	2	12
Midcell Z ring not over the nucleoid (%)	2	10	0	9	0	1

3.2.2 Z rings form at the cell centre only in the absence of *spo0J*

Disclaimer: The data presented henceforth was completed during the PhD project.

The leading question from the previous section was whether it is the absence of both *soj* and *spo0J* together that causes an increase in the frequency of midcell Z rings in the *dnaB* mutant at the non-permissive temperature or whether the absence of just one of them causes it. To test this, individual deletion mutants of *soj* and *spo0J* were created and tested in the temperature-sensitive *dna-1* mutation. To examine which of the two proteins was responsible for the effect on Z ring positioning when initiation is blocked by inactivating DnaB, vegetatively growing cells, rather than the spore outgrowth system, were used. This is because the absence of *soj* or *spo0J* inhibits spore formation, whilst a deletion of both *soj* and *spo0J* overcomes this inhibition and allows spore formation (Ireton et al, 1994).

3.2.2.1 *Z ring positioning in the absence of soj or spo0J*

To obtain strains for visualisation of Z rings in the absence of *soj* or *spo0J* in the DNA initiation mutant *dna-1*, strains SU5 (wild-type) and SU661 (*dna-1*) were transformed with SU747 (donated by H. Murray) or SU748 (donated by S. Gruber) chromosomal DNA to obtain SU771 (*Δsoj*) and SU772 (*dna-1 Δsoj*), or SU769 (*Δspo0J*) and SU770 (*dna-1 Δspo0J*), respectively (see Materials and Methods Table 2.2). Kanamycin-resistant transformants were checked for temperature sensitivity for the *dna-1* mutation strain, and gene deletion was checked via PCR (data not shown).

To visualise Z rings, vegetative cells of the six strains; wild-type (SU5), *dna-1* (SU661), *Δsoj* (SU771), *dna-1 Δsoj* (SU772), SU769 (*Δspo0J*) and SU770 (*dna-1 Δspo0J*) were grown to mid-exponential phase, then shifted to the non-permissive temperature for 1 hour before being collected for IFM. Z ring positioning results are shown in Figure 3.4. Consistent with previous results, wild-type (SU5) and *dna-1* (SU661) formed midcell Z rings with frequencies of 92% and 10%, respectively (Figure 3.4 and Table 3.3). The absence of *soj* in the wild-type background (SU771) had no effect on Z ring positioning at the non-permissive temperature, with 90% Z rings forming at the cell centre (0.45-0.5 range, Figure 3.4 iii). Interestingly, little restoration of Z ring positioning was observed in the *dna-1 Δsoj* cells (12%) in comparison with the block to initiation (*dna-1*) alone. This suggests that Soj alone is not responsible for the increase in midcell Z ring positioning when DnaB is inactive as that seen in *dna-1 Δsoj-spo0J*.

The deletion of *spo0J* in the wild-type background on the other hand, as expected from a previous report, resulted in a slight decrease in midcell Z ring frequency (77%; (Ireton et al, 1994). Additionally, this frequency was consistent with the midcell Z ring frequency at the permissive temperature, suggesting that this is not an effect of the inactivation of *dna-1*. Unlike *Δsoj*, a deletion of *spo0J* when DNA initiation of replication is blocked via the *dna-1* mutant caused a significant increase in midcell Z rings (39%). This is essentially the same frequency of Z rings observed at midcell in the absence of both *soj* and *spo0J* (41%) in the *dna-1* mutant in the spore outgrowth experiments in the previous section. Overall these results demonstrate that the

increase of midcell Z ring formation in the absence of *soj-spo0J* operon can be attributed solely to the absence of *spo0J.*

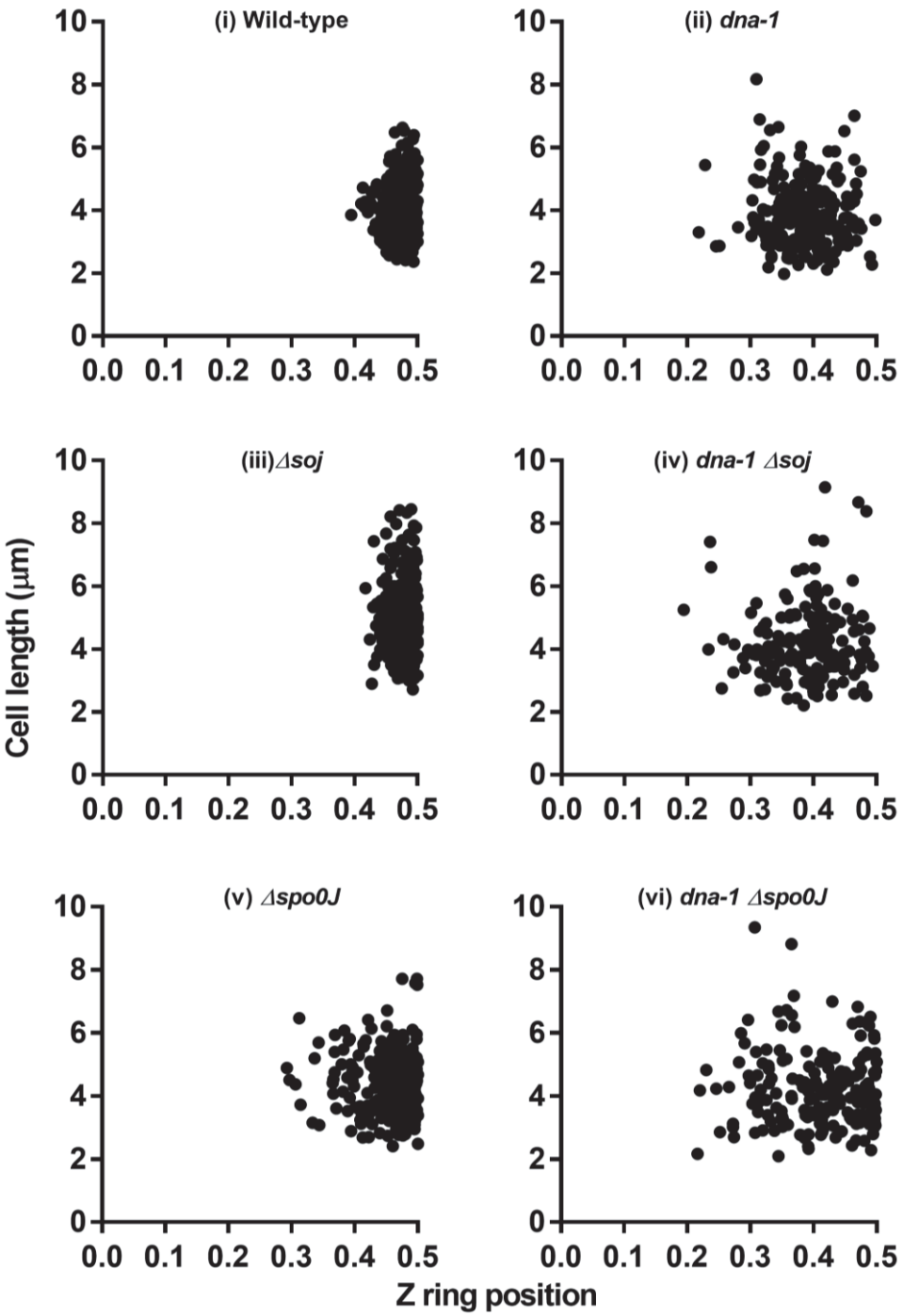

Figure 3.4: Z ring positioning when either *Soj* or *Spo0J* are absent and initiation of DNA replication is blocked early on in the *dnaB* mutant. Strains were grown in PAB at the permissive temperature (30°C) to mid-exponential phase of growth and then shifted to the non-permissive temperature (48°C) for 60 minutes. Scatter plots showing Z ring positioning in vegetatively grown fixed cells of (i) Wild-type (SU492), (ii) *dna-1* (SU746), (iii) *Δsoj* (SU771), (iv) *dna-1 Δsoj* (SU772) (v) *Δspo0J* (SU769) and (vi) *dna-1 Δspo0J* (SU770). Z ring position is determined by measuring the distance from the Z ring to the nearest cell pole and dividing this value by the cell length, with 0.5 being exactly midcell. A Z ring is considered to be at

midcell if it was positioned within the range of 0.45-0.50, as this is where most Z rings form in the wild-type strain. n > 200. See Table 3.3 for midcell Z ring frequencies and average cell lengths (±SD) for each strain.

Table 3.3: Analysis of Z ring positioning in the *dna-1* temperature-sensitive in the absence of *soj-spo0J* at 48°C.

Strain	Average cell length (±SD) [a]	% Midcell Z rings [b]
Wild-type	3.89 ± 0.70	92%
dna-1	4.54 ± 0.99	10%
Δsoj	4.47 ± 0.82	90%
dna-1 Δsoj	4.47 ± 0.87	12%
Δspo0J	4.08 ± 1.20	77%
dna-1 Δspo0J	4.19 ± 1.04	39%

[a] Table shows average cell length (±SD) and [b] percent of Z rings in the midcell range (0.45-0.5). Midcell is considered to be between 0.45 and 0.50 as this is where majority of Z rings form in wild-type cells. Scatter plots of Z ring positioning are depicted in Figure 3.4. See Figure 3.4 for strain growth conditions and midcell Z ring characterisation.

3.2.2.2 *Changes to nucleoid morphology observed in the absence of soj or spo0J*

The absence of *soj* and *spo0J*, or just *spo0J*, in otherwise wild-type cells has been shown to give rise to spread nucleoids in 20% of the cell population (Britton et al, 1998; Ireton et al, 1994; Lee & Grossman, 2006; Ogura et al, 2003). Given the significant difference in midcell Z ring formation between *Δsoj* and *Δspo0J* cells when initiation of DNA replication is blocked via DnaB inactivation, it was plausible that, much like the double knockout (*Δsoj-spo0J* in the *dna-1* mutant), there is a change in the nucleoid morphology populations to one that may be more favourable to midcell Z ring formation in the *spo0J* single mutant when DnaB is inactive. If this were true, then for the *dna-1 Δspo0J* strain, we would expect to see a decrease in the predominant single-lobed nucleoids seen in just the *dna-1* mutant, toward a more

bilobed or spread nucleoid morphology population, reminiscent of that of the double knockout (*dna-1 soj-spo0J*).

To visualise nucleoid morphology, vegetative samples were grown to mid-exponential phase, shifted to the non-permissive temperature for 1 hour to inactivate DnaB, and fixed via ethanol fixation (see Materials and Methods section 2.6.2). Nucleoid morphologies in these cells were observed separately to Z ring positioning as nucleoid staining during IFM is of limited quality and not possible to accurately score. Visualisation using DAPI revealed different nucleoid morphologies in all the strains which were grouped into 3 categories as defined previously (see Section 3.2.1.2) Examples of each nucleoid morphology and their frequency in each sample can be seen in Figure 3.5A.

The deletion of *soj* when initiation is blocked via *dna-1* (SU772) did not have significant impacts to the nucleoid morphology distribution in comparison to *dna-1* (SU661), with the majority of cells possessing a single-lobed nucleoid (83% in *dna-1* in comparison to 88% in *dna-1 Δsoj;* Figure 3.5B). However a significant decrease in single-lobed nucleoids was observed in the *dnaB* mutant when *spo0J* was absent (from 83% to 51%). This is consistent with the frequencies of the three nucleoid morphologies seen in the absence of both *soj* and *spo0J* in outgrowing spores. In summary, the lack of *spo0J* when initiation of DNA replication is blocked allows for more midcell Z rings to form at the cell centre, and this correlates with significant changes to nucleoid morphology such that there was an increase in bilobed and spread nucleoids.

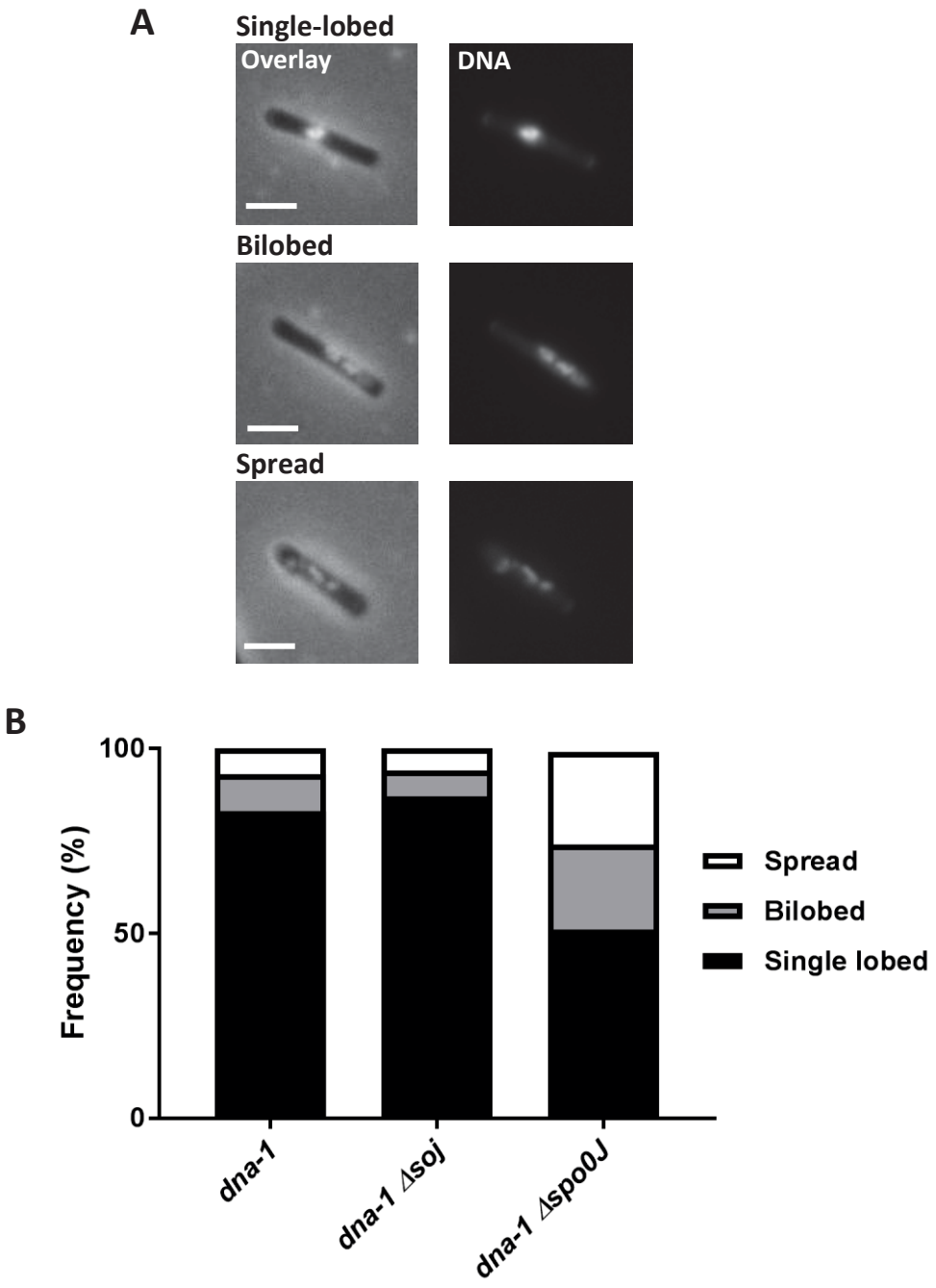

Figure 3.5: Nucleoid morphology in ethanol-fixed DAPI stained vegetative cells of *dna-1*, *dna-1 Δsoj* and *dna-1 Δspo0J*. Strains were grown in PAB to mid-exponential stage of growth at the permissive temperature (30°C) and then shifted to the non-permissive temperature (48°C) for 60 minutes. (A) Representative images of the three nucleoid morphologies observed; overlay of DAPI and phase-contrast (left) and DAPI only (right). (B) Bar graph showing the ratio of the three morphology types in each strain. Scale bar represents 2 µm; n > 200.

3.2.3 Investigating Z ring positioning and nucleoid morphology when entry to DNA chain elongation is blocked in the absence of *soj* and *spo0J*.

3.2.3.1 *Z ring positioning in the absence of soj and spo0J in the presence of HPUra*

Previously, it had been shown that an increase midcell Z ring positioning correlated with the progression into the round of replication (Moriya et al, 2010). In other words, blocking an early stage of initiation of DNA replication results in fewer midcell Z rings than blocking a later stage. Like *Δnoc*, *Δspo0J* allows an increase in midcell Z ring formation when DNA replication initiation is blocked i.e. via a mutation in *dnaB.* Does the absence of *spo0J* also restore midcell Z ring formation in the HPUra condition?

To test this, Z ring positioning was examined in the absence of *spo0J* at a much later stage of initiation of DNA replication. We used the addition of HPUra [6-para-hydroxyphenylazo)-uracil], a known DNA polymerase III inhibitor, to test this. When HPUra is added to germinating spore cells, initiation of DNA replication can complete but DNA synthesis is inhibited (Bazill & Gross, 1972; Cozzarelli, 1977; Regamey et al, 2000). These experiments had to be done in germinating cells since addition of HPUra to vegetatively growing cells would result in an immediate halt to DNA synthesis rather than just inhibiting the initiation phase of replication. Also since strains with individual deletions of either *soj* or *spo0J* are unable to sporulate, a double deletion had to be used to test what effect Spo0J has on Z ring positioning when initiation is blocked just prior to DNA elongation. Furthermore, since Z ring positioning in the absence of *soj-spo0J* is no different than that observed for the absence of *spo0J,* examining Z ring positioning with HPUra treatment in the absence of both *soj* and *spo0J* would still be informative of the role of Spo0J in Z ring placement during initiation of DNA replication.

To test this, a live cell approach was used to visualize Z rings more readily than with IFM. Both live visualisation and IFM techniques to observe Z ring positioning have been used in the previous experiments, with consistent results regardless of the technique used. Therefore, we deemed it reasonable to use live visualisation here and to make adequate comparisons and conclusions between all results. Spores of the wild type strain (SU492; *trpC2 amyE::(spc Pxyl-ftsZ-yfp)*) and *Δsoj-spo0J* strain (SU767; *trpC2 amyE::(spc Pxyl-ftsZ-yfp) Δsoj-spo0J::tet*) were germinated and outgrown at 34°C in GMD in the presence and absence of HPUra (100 μM). GMD was also supplemented with xylose (0.02%) for Z ring visualisation. Wild-type (SU492) cells readily formed Z rings at the central position with a frequency of 93% (Figure 3.6 and Table 3.4). Similarly, *Δsoj-spo0J* cells formed Z rings at midcell with a frequency of 88%. The addition of HPUra to wild-type cells (SU492) on the other hand, decreased the midcell Z ring frequency to 20%, consistent with previously published results (Moriya et al, 2010). Interestingly, Z ring formation at midcell increased significantly in the *Δsoj-spo0J* strain (SU767) with the addition of HPUra, with a midcell Z ring frequency of 57%. This reveals that the absence of *soj-spo0J* restores midcell Z ring formation also when DNA replication is blocked just prior to the elongation stage, and to a greater extent than that seen in the earlier block to initiation (*dna-1 Δsoj-spo0J*; 41% midcell Z rings). Thus the effect of deleting *soj-spo0J* is similar to that observed in the absence of Noc (Moriya et al, 2010); more midcell Z rings are seen at the later block (+HPUra) than that in the earlier block to initiation of DNA replication (DnaB inactivation).

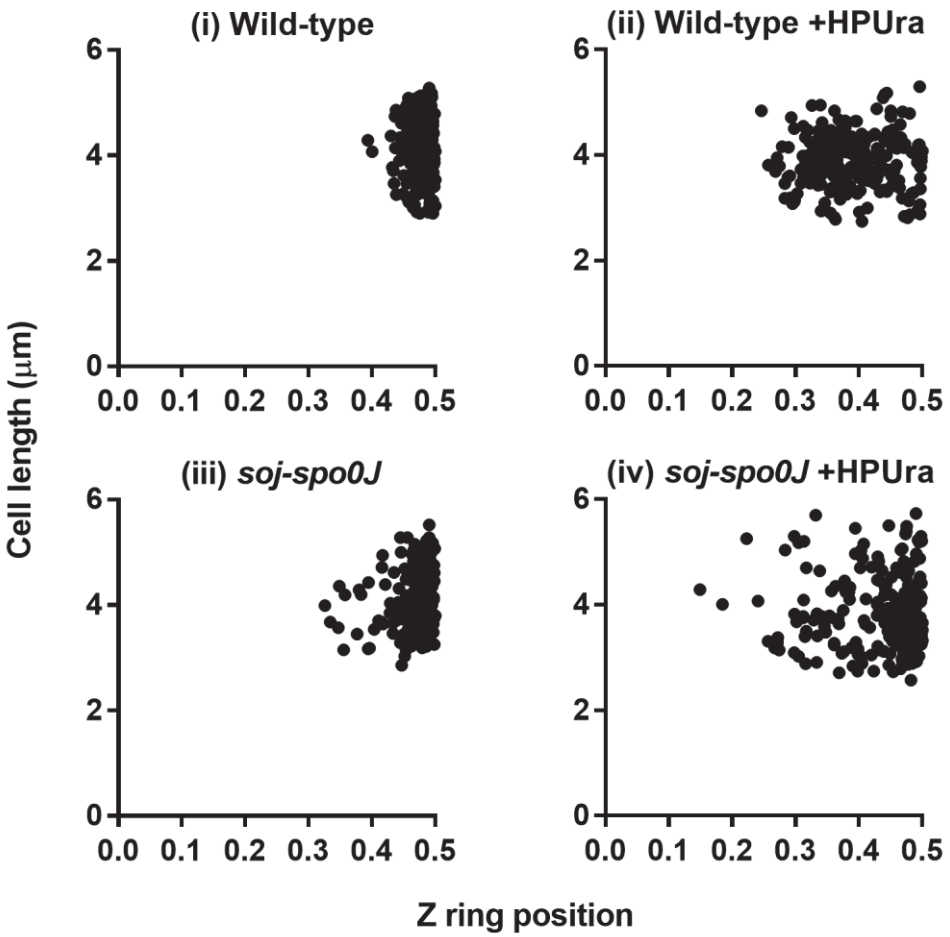

Figure 3.6: Z ring positioning when entry into DNA chain elongation is blocked during spore outgrowth in the presence of HPUra. Wild-type (SU492) and *Δsoj-spo0J* (SU767) spores were germinated in GMD containing 0.02% xylose (v/v), in the absence or presence of HPUra (100 μM) for 125 minutes and 135 minutes at 34°C, respectively. Figure shows scatter plots of Z ring positioning in: (i) wild-type, (ii) wild-type +HPUra, (ii) *Δsoj-spo0J* and (iv) *Δsoj-spo0J* +HPUra. Scale bars are 2 μm. Z ring position is determined by measuring the distance from the Z ring to the nearest cell pole and dividing this value by the cell length, with 0.5 being exactly midcell. A Z ring is considered to be at midcell if it was positioned within the range of 0.45-0.50, as this is where most Z rings form in the wild-type strain. n > 200. See subsequent Table 3.4 for midcell Z ring frequencies and average cell lengths (±SD) for each strain.

Table 3.4: Analysis of Z ring positioning in the absence of *soj-spo0J* with the addition of HPUra.

Strain	Average cell length (±SD) [a]	% Midcell Z rings [b]
Wild-type	3.98 ± 0.61	93%
Δsoj-spo0J	4.05 ± 0.50	88%
Wild-type +HPUra	4.18 ± 0.52	20%
Δsoj-spo0J +HPUra	3.93 ± 0.63	57%

[a] Table shows average cell length (±SD) and [b] percent of Z rings in the midcell range (0.45-0.5). Midcell is considered to be between 0.45 and 0.50 as this is where majority of Z rings form in wild-type cells. Scatter plots of Z ring positioning are depicted in Figure 3.6. See Figure 3.6 for strain growth conditions and midcell Z ring characterisation.

3.2.3.2 *Characterization of nucleoid morphologies when early DNA elongation is blocked in Δsoj-spo0J*

In the previous section (see section 3.2.1.2) it was shown that when initiation of DNA replication is blocked via DnaB inactivation in the absence of *spo0J* (or both *spo0J* and *soj*) an increase in midcell Z ring frequencies correlated with an increase in bilobed or spread nucleoid morphologies. To test whether this is the case for a later block in initiation of DNA replication via HPUra addition, nucleoids were examined in live cells with the addition of HPUra when both *soj* and *spo0J* were either present or absent. Again three types of nucleoid morphologies were observed when HPUra was added to both populations: single-lobed, bilobed and spread. Examples of each type of morphology are shown in Figure 3.7A, and their frequencies in both the samples in Figure 3.7B. The nucleoid morphologies seen and described here are consistent with the individual mutants in *dna-1* (*dna-1 Δsoj* and *dna-1 Δspo0J*).

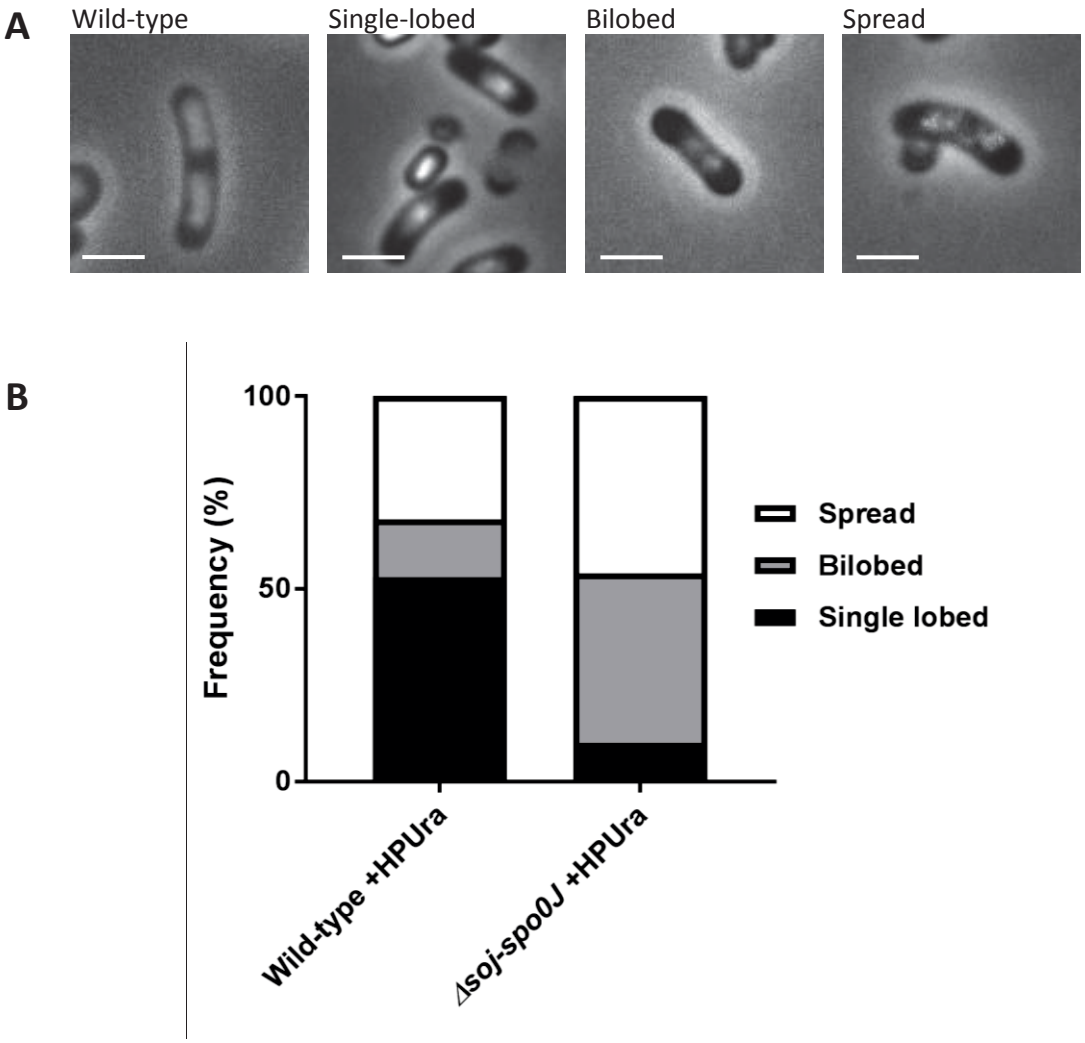

Figure 3.7: Nucleoid morphology in live DAPI-stained outgrown spores of wild-type and *Δsoj-spo0J* outgrown spores in the presence of HPUra. Spores were germinated in GMD with the addition of HPUra (100 µM) for 125 minutes and 135 minutes at 34°C, respectively. (A) Representative overlay images (phase contrast and DAPI) of the three morphologies observed, and a wild-type cell for comparison. (B) Bar graph showing the frequency of the three morphology types in each strain. Scale bar represents 2µm; n > 200.

Consistent with previous results (Moriya et al, 2010), the predominant nucleoid morphology seen in SU492 (*ftsZ-yfp*) cells grown in the presence of HPUra was a single-lobed morphology (61%), followed by spread (28%) and then bilobed (11%). The deletion of *soj-spo0J* (SU767, *ftsZ-yfp*) on the other hand shows a clear change in the frequency of nucleoid types. Only 16% of the cell population contained a single-lobed nucleoid, in contrast to the wild-type population where more than half the

cells contained a single-lobed nucleoid (61%). Instead, a spread nucleoid morphology was predominant in the *Δsoj-spo0J* cell population when DNA elongation is blocked, with a frequency of 59%. This was followed by 25% of cells possessing bilobed nucleoid morphology. Overall, similar to that in the temperature sensitive *dnaA-1* strain, the absence of *soj* and *spo0J* results in increase bilobed or spread nucleoid morphologies when entry to DNA chain elongation is blocked via the addition of HPUra.

3.2.3.3 *Co-visualisation of Z rings and nucleoids when entry to DNA elongation is blocked in Δsoj-spo0J*

A significant increase (20% to 57%) in the frequency of midcell Z rings resulted when DNA chain elongation was blocked (HPUra addition) in the absence of both *soj* and *spo0J*. Considering this increase in midcell Z ring frequency with the higher frequency of bilobed or spread nucleoid morphology, it was important to consider that the absence of *soj-spo0J* may allow for a change in nucleoid morphology to one that might be expected to allow for more midcell Z rings, due to a lower concentration of DNA (absence of condensation) at the cell centre. Therefore nucleoids and Z rings were co-visualised in live outgrown spores of wild-type and *Δsoj-spo0J* cells expressing *ftsZ-yfp* (SU492 and SU767, respectively). Table 3.4 shows the frequency distribution of Z ring position amongst the different nucleoid morphologies with HPUra addition, both in the presence or absence of *soj-spo0J*. Figure 3.7 shows representative images of the most common types of cells observed.

Consistent with results shown in the previous section, the predominant phenotype observed with HPUra addition in the wild-type background (SU492) was an acentral Z ring, positioned to the side of a centrally positioned single-lobed nucleoid (43% of all phenotypes observed (Table 3.5; Figure 3.8i). Of the few Z rings that did form centrally over the DNA in this strain, nucleoids were of a bilobed or spread morphology (6% and 7%). Most interestingly, almost all Z rings that formed at midcell in the absence of *soj-spo0J* formed over either a spread or bilobed nucleoid (40% and 12%, respectively; Figure 3.8ii). These results show that addition of HPUra in the absence of *soj-spo0J* allows Z rings to readily form at the cell centre over spread or bilobed nucleoids. Furthermore, the increase in bilobed or spread

morphology appears to correlate with the restoration of midcell Z ring formation. Although occurring to a greater extent, this decrease in single-lobed nucleoids when *soj-spo0J* is absent is reminiscent of that observed in the *dna-1* mutant. This increase in bilobed or spread nucleoids together with the significant increase in midcell Z ring assembly supports the idea that there are changes to the nucleoid (such as a decrease in local DNA concentration) when *soj-spo0J* are absent that allow for Z rings to form more readily at the cell centre.

Table 3.5: Frequency of different nucleoid morphologies and midcell Z rings when entry to DNA elongation is blocked.

	Nucleoid morphology					
	Single-lobed		**Bilobed**		**Spread**	
Z ring position	Wild-type +HPUra	*Δsoj-spo0J* +HPUra	Wild-type +HPUra	*Δsoj-spo0J* +HPUra	Wild-type +HPUra	*Δsoj-spo0J* +HPUra
Acentral Z ring (%)	43	3	9	14	25	25
Midcell Z ring over the nucleoid (%)	2	0	6	12	7	40
Midcell Z ring not over the nucleoid (%)	3	5	1	0	4	1

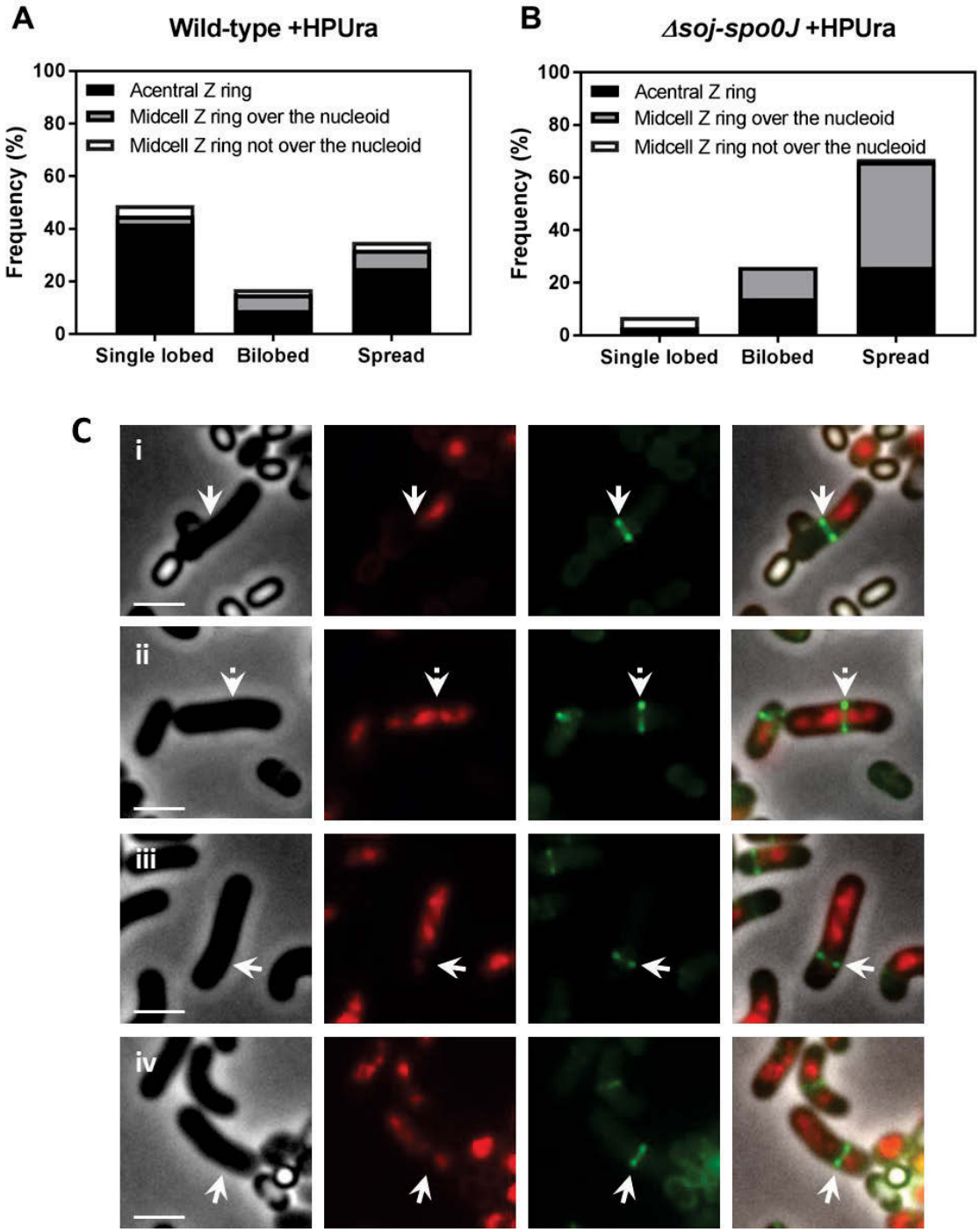

Figure 3.8: Co-visualization of the Z ring and nucleoids in wild-type and *Δsoj-spo0J* live outgrown spores when early elongation is blocked by addition of HPURa. Wild-type (SU492) and *Δsoj-spo0J* (SU767) spores were germinated in GMD containing 0.02% xylose (v/v), in the absence or addition of HPURa (100 µM) for 125 minutes and 135 minutes at 34°C, respectively. (A and B) Histogram representation of Z ring position relative to different nucleoid types in (A) Wild-type +HPURa and (B) *Δsoj-spo0J* +HPURa. The height of each bar represents the frequency of each nucleoid type, showing the proportion of acentral Z rings

(black), midcell Z rings over the nucleoid (grey) and midcell Z rings not over the nucleoid (white). n > 200. See Table 3.5 for numerical values of the data. (C) Representative images of predominant combinations Z ring positions and nucleoid types quantified in A and B: (i) acentral Z ring adjacent to a single-lobed nucleoid from wild-type +HPUra, and (ii) central Z ring forming over a spread nucleoid, (iii) acentral Z ring adjacent to spread nucleoid and (iv) acentral Z ring forming over a spread nucleoid, from *soj-spo0J* +HPUra. Images are DAPI pseudo-coloured in red (right), FtsZ-YFP pseudo-coloured in green (middle) and overlay (left). Scale bars are 2 µm.

3.2.4 Investigating changes to chromosome organisation via *oriC*-labelling when initiation of DNA replication is blocked in the absence of *soj* and *spo0J*

It is clear that the different blocks to initiation of DNA replication give rise to different midcell Z ring frequencies (for example, 10% in *dna-1* in comparison to 22% in wild-type cells grown in the presence of HPUra; (Moriya et al, 2010)). Midcell Z ring frequencies are further increased with the deletion of *soj* and *spo0J* (or just *spo0J*). To add to this, nucleoid morphologies change variably with these treatments, with a tendency to spread more in the absence of *spo0J* and this correlates with increased midcell Z ring frequency (at least when the spread DNA occurs across the cell centre). It is however unknown how the chromosome is organised during these different situations. It has been suggested that the nucleoid takes up a structured organisation within the cells, with different regions taking up certain positions within the cell at different points of replication (Wang et al, 2014a). One such region is the origin of replication (*oriC*). The on-going consensus on chromosome organisation at the on-set of initiation of DNA replication is that the chromosome is organised with the origin and terminus regions positioned at the cell centre, flanked by the left and right arms of the circular chromosome on their respective sides of the cell. Once DNA synthesis commences, the origin is duplicated, and one copy of each moves toward their respective cells quarter positions (Berkmen & Grossman, 2007; Wang et al, 2014b). It is possible that the replication initiation proteins (for example, DnaB) are affecting the nucleoid organisation during initiation of DNA replication in some

way, such that chromosomal loci are kept in distinct positions that inhibit Z ring formation. Furthermore, a deletion of *spo0J* during the two different blocks to replication initiation (at the early and late stage, via the inactivation of DnaB and addition of HPUra, respectively) results in a change to the nucleoid morphology (from predominantly single-lobed nucleoids to bilobed or spread nucleoids in both the *dna-1* mutant and the addition of HPUra), which correlates with more Z rings readily forming at midcell. While there is a change in nucleoid morphology that correlates with an increase in midcell Z ring frequency, could it be that there is a change in chromosome loci positioning? For example, the data presented above shows an increase in bilobed or spread nucleoid in the absence of *soj-spo0J* which correlates with an increase in midcell Z ring formation. However, despite this change in gross morphology, not all Z rings form over these nucleoids suggesting that there must be further differences. One such difference may be the positioning of chromosomal loci, such as the origin, within these bilobed or spread nucleoids that prevents the Z ring from forming at midcell. Therefore, to examine this, an origin-proximal region was localised within the cell and determined whether these changes, if any, correlate with the different midcell Z ring frequencies.

To examine whether positioning of the origin region has been altered and whether this correlates with changes to the frequency of Z ring position in the presence or absence of *soj* and *spo0J* when initiation of DNA replication is blocked via either DnaB inactivation or addition of HPUra, an origin-proximal region was visualised in live outgrown spores. A fluorescent lac operator (lacO)/lac repressor (LacI) system was used to visualise the origin-proximal region at location 345° on the chromosome (Lee & Grossman, 2006; Lemon & Grossman, 2000; Veening et al, 2009). Recipient strains wild-type (SU492; *ftsZ-yfp*), *dna-1* (SU746), *Δsoj-spo0J* (SU767) and *dna-1 Δsoj-spo0J* (SU768) were transformed via a two-step process with donor DNA SU717 (*hutM(345°)::lacO, thrC (283°)::lacI-cfp*) to create the *lacO lacI ftsZ-yfp* equivalent strains of wild-type (SU783), *dna-1* (SU784), *Δsoj-spo0J* (SU823) and *dna-1 Δsoj-spo0J* (SU824), respectively (See Materials and Methods Table 2.2). This two-step transformation first introduced a cyan fluorescent protein fusion to *lacI* (LacI-CFP) into the genome at the non-essential *thrC* gene. A 256-copy tandem *lacO* repeat, to

which LacI-CFP binds, was then inserted at *hutM* within the genome. Chloramphenicol- and erythromycin-resistant transformants were confirmed for temperature sensitivity (where relevant) and chromosome *oriC* foci visualisation, and spores were subsequently prepared.

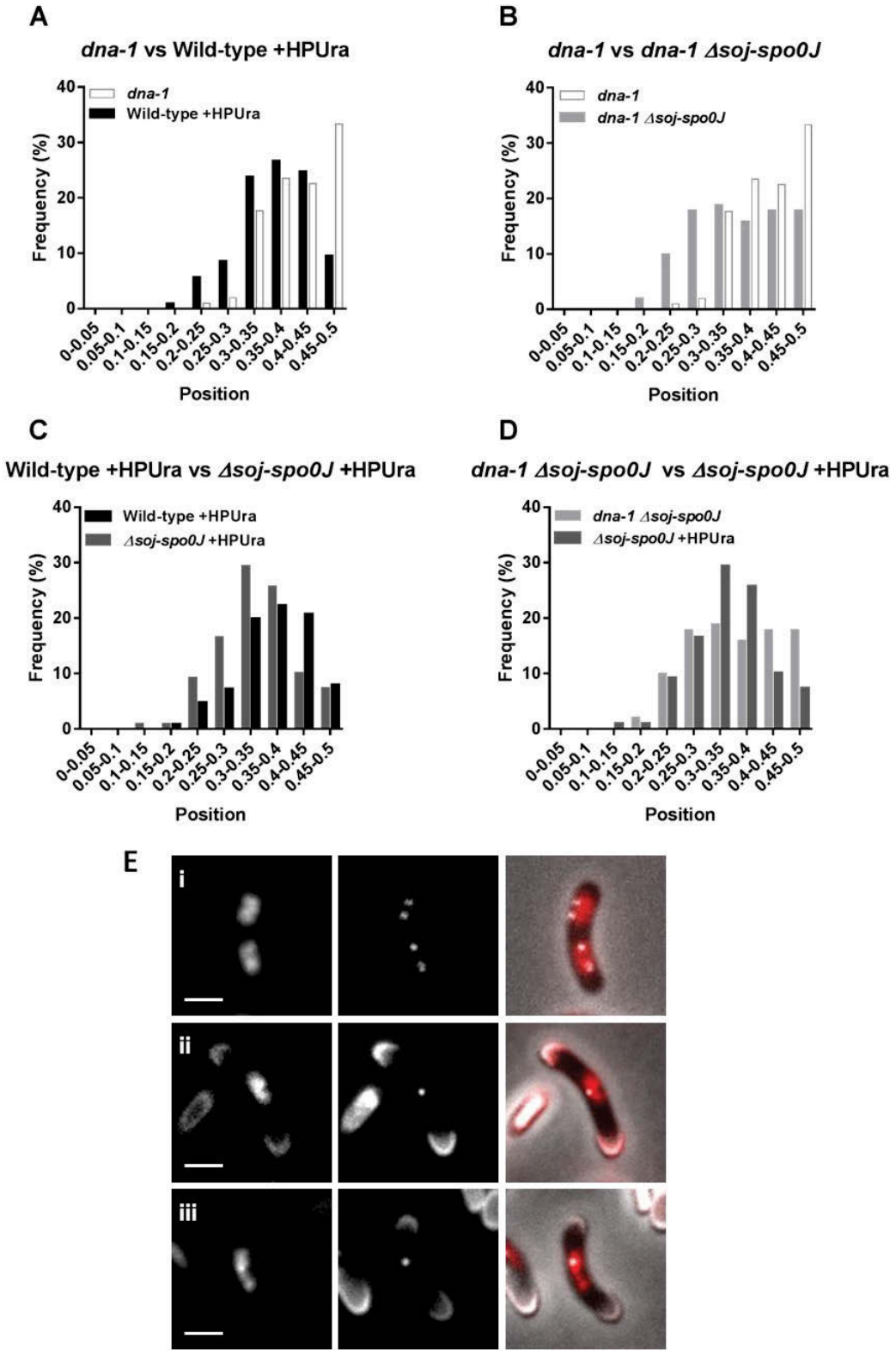

Figure 3.9: Origin-proximal focus localisation when initiation of DNA replication is blocked at different stages in the absence of *soj-spo0J*. Spores were germinated in GMD with the addition of xylose and with the addition (where relevant) of HPUra at 34°C for 20 minutes

before being shifted to the non-permissive temperature for 90 minutes to block initiation of DNA replication. Cells were collected and DAPI was added for DNA visualisation. Figure shows histogram of origin positioning in: (A) *dnaA-1* (SU784) vs, wild-type (SU783), (B) *dnaA-1* (SU784) vs. *dnaA-1 Δsoj-spo0J* (SU824), (C) wild-type +HPUra (SU783) vs *Δsoj-spo0J* +HPUra (SU823); and (D) *dnaA-1 Δsoj-spo0J* (SU824) vs *Δsoj-spo0J* +HPUra (SU823). Origin positioning has been plotted in ratio to cell length with 0 (on the x-axis) marking the cell pole and 0.5 signifying midcell. n > 200. (E) Example images of origin-proximal foci: (i) multiple origin foci in replicating wild-type cells; and single origin foci, either positioned (ii) at the cell centre or (iii) acentrally in non-replicating cells. Images are DAPI (left), origin-localised LacI-CFP (middle) and an overlay of the two with phase-contrast (right; DAPI shown in red). Scale bars are 2 μm.

Initial investigations found different origin focus positioning between all strains (Figure 3.9). Consistent with a previous finding, origin focus localisation occurred predominantly at the cell centre in the *dnaB* mutant (Figure 3.9A; (Regamey et al, 2000)). A shift of the origin region off-centre was observed in the later block to initiation (via addition of HPUra, Figure 3.9A), highlighting that when initiation of DNA replication is halted later on, *oriC* positioning is altered. Similarly, the absence of *soj* and *spo0J* when DnaB is inactive also indicates an altered positioning of origin focus away from midcell compared to the *dnaB* mutant alone (Figure 3.9B). Likewise, the later block to initiation of DNA replication (+HPUra) demonstrates a shift of the focus away from the cell centre when *soj* and *spo0J* are absent (Figure 3.9C). Making direct comparison between the two different blocks to initiation of DNA replication when *soj* and *spo0J* are absent, a clear shift of the focus can be observed in the later block (+HPUra) away from the cell centre, more so than that observed for the earlier block (Figure 3.9D). A shift in origin positioning was observed, therefore suggesting a possibility that moving the origin away for the cell centre could allow for midcell Z ring assembly.

3.2.5 Synthesis of DNA does not account for the increase in midcell Z rings in the absence of *soj-spo0J* when initiation of DNA replication is blocked.

When initiation of DNA replication is blocked, either by DnaB inactivation or addition of HPUra, in the absence of *soj* and *spo0J,* a large portion of the cells possess bilobed or spread nucleoids. This change to the nucleoid morphology was found to correlate with an increase in midcell Z rings. Although not likely, it is possible that the increase in midcell Z rings observed in *dna-1 Δsoj-spo0J* or *Δsoj-spo0J* +HPUra is due to DNA synthesis occurring. In other words, could the deletion of *spo0J* partially relieve or overcome the inhibition of DNA replication, giving rise to an increase in midcell Z rings? The nucleoid morphologies discussed in the sections above do not seem to suggest rescue of DNA replication, as it would be expected to see nucleoids separate into two clear entities like that in wild-type cells, and this is not observed (Figure 3.10).

To test whether the increase in frequency in midcell Z rings could be attributed to DNA replication occurring, flow cytometry was used to measure DNA content in germinated spores. Flow cytometry is an ideal method for this as it provides a high-throughput and unbiased analysis of a large population of cells. To quantify DNA content bacterial cells are stained with certain dyes which when passed through the flow cytometer, emit a level of fluorescence which is proportional to the amount of dye bound to DNA. Here, a DNA-specific fluorescent dye (SYTO16; Molecular Probes) was utilised, which when passed through the flow cytometer, quantifies DNA fluorescence within single cells and therefore the DNA initiation replication frequency. This method was complemented by the use of the origin-labelled strains from the above section (section 3.2.4) to quantify the number of origin foci per cell. Both the *dna-1* and *dna-1 Δsoj-spo0J* strains showed less than 1% of the cell population with more than one focus per cell (data not shown).

For simplicity, one example of the results obtained will be shown in this section; however this method was applied for all experiments throughout this thesis to

determine whether DNA replication was actually occurring in samples where it was blocked (including the *dna-1* temperature sensitive mutant and the addition of HPUra). All samples were grown as described previously in this chapter before chloramphenicol was added. Samples were then collected, washed, stained with the fluorescent dye and flow cytometry was used to quantify DNA content of each cell (see Materials and Methods section 2.7 for protocol). The output data shows the fluorescence intensity (x-axis) plotted against cell count (y-axis). If no replication is occurring, then data should show a sharp peak to the far left of the x-axis, signifying a single copy of the chromosome within the cells. If DNA replication If occurring, on the other hand, then the data should show two peaks further to the right of the x-axis (i.e. greater fluorescent signal), signifying either 2 or 4 copies of DNA per cell, depending on the stage of replication at which the cells were fixed.

In Figure 3.10, SYTO16 fluorescence, and thus DNA content is translated into intensity peaks (Figure 3.10). As expected, wild-type and *Δsoj-spo0J* cells showed normal replication; two peaks representing 2 and 4 chromosomes per cell. The *dnaB* mutant and wild-type cells with the addition of HPUra were used as the non-replicative control, and as expected, showed a single peak signifying one chromosome per cell. Similarly, one chromosome per cell was also observed in both the *dna-1 Δsoj-spo0J* cells and *Δsoj-spo0J* cells grown with HPUra confirming a complete block to DNA synthesis. These results show that the increases to the frequency of midcell Z rings as a result of DnaB inactivation or the block prior to DNA elongation via the addition of HPUra are not due to the initiation block being overcome and subsequent DNA synthesis.

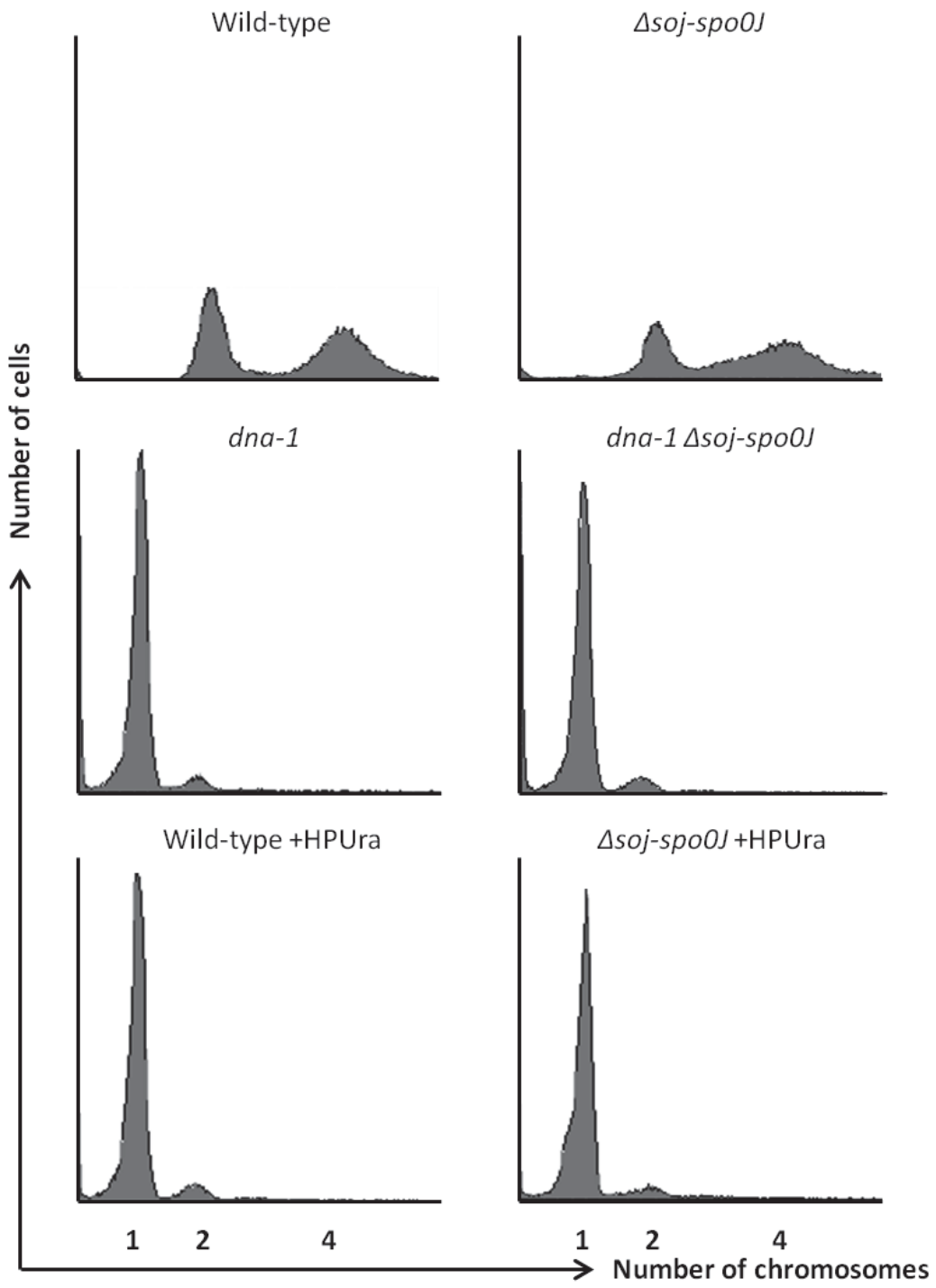

Figure 3.10: Flow cytometry profiles of *Δsoj-spo0J* strains when initiation of DNA replication is blocked via *dna-1* mutation or addition of HPUra. Flow cytometry profiles in controls where initiation of DNA replication is progressing normally (wild-type and *Δsoj-spo0J*) or blocked (controls: *dna-1* and wild-type +HPUra; and test strains: *dna-1 Δsoj-spo0J* and *Δsoj-spo0J* +HPUra). Profiles shown are based on outgrown spores, grown and fixed for flow cytometry analysis as per the protocol detailed in Materials and Methods (see Materials and Methods section 2.7). n = 10,000.

3.3 Discussion

Fundamental to the successful propagation of bacteria is the correct positioning and assembly of the Z ring to allow the production of two viable daughter cells. How this occurs is yet to be fully understood. However, some insight into how this occurs, at least in *B. subtilis*, comes from the study leading to the Ready-Set-Go model which identified a relationship between the progression of initiation of DNA replication and the increasing potential at midcell for Z ring formation (Moriya et al, 2010). The starting point for this chapter was to investigate whether the chromosome segregation protein Spo0J plays a role in the effect observed as described in the Ready-Set-Go model. Spo0J is a candidate player here because of the different changes to nucleoid morphology observed in the Ready-Set-Go model data. Therefore, Z ring positioning was examined in the absence of *spo0J* when initiation of DNA replication was blocked. Intriguingly, it was found that the absence of *spo0J* allows for an increase in midcell Z ring assembly. Furthermore, a change in nucleoid morphology was also observed, which correlated with the increased midcell Z rings. The implications of these results are discussed below.

In the data that led to the Ready-Set-Go model, when *Δnoc* cells are blocked via inactivation of DnaB, 45% of Z rings form at the cell centre. Then, when *Δnoc* cells are grown in the presence of HPUra to block initiation of DNA replication later on, 75% of cells form Z rings at midcell (Moriya et al, 2010). Exploring Z ring positioning at the earliest block to initiation of DNA replication (via the *dna-1* mutation) when *spo0J* is absent found a significant increase in frequency of midcell Z rings. This provided the first evidence that the chromosome organisation protein Spo0J does play a role in positioning the division site during initiation of DNA replication. In other words, like Noc (Moriya et al, 2010), Spo0J prevents midcell Z ring formation when initiation of DNA replication is blocked. Testing a later block to initiation of DNA replication (just prior to DNA elongation via the addition of +HPUra) also resulted in an increase in midcell Z ring frequency in the absence of *soj* and *spo0J*. These results highlight the potential involvement of Spo0J in inhibiting midcell Z ring assembly too early on in the cell cycle. Additionally, like that in the absence of Noc as

revealed by the Ready-Set-Go model, a progressive link between initiation of DNA replication and Z ring positioning is apparent in the absence of Spo0J.

3.3.1 Spo0J impacts Z ring positioning by affecting nucleoid morphology

The way in which Spo0J regulates midcell Z ring assembly during initiation of DNA replication appears to relate with changes to nucleoid morphology. This is in direct contrast to Noc which has no effect on nucleoid morphology. Both the early and late blocks to initiation of DNA replication (*dna-1* and addition of HPUra) in the absence of *spo0J* result in a significant decrease from the predominantly single-lobed nucleoid morphology seen in each block alone, to a higher frequency of bilobed and spread nucleoids when *spo0J* is absent. Further, a significant increase in midcell Z rings occurs over these nucleoid morphologies (bilobed and spread) in the absence of *soj* and *spo0J* in comparison to the block to initiation of DNA replication alone. This is in significant contrast to the absence of *noc* where nucleoid morphologies remain unchanged when the initiation of DNA replication is blocked at various stages. In the absence of Noc, the nucleoid remains in a predominantly single-lobed morphology and the Z ring is able to form over it at midcell (Moriya et al, 2010). This highlights that although Spo0J is having a similar effect on Z ring positioning during initiation of DNA replication, it does not appear to be doing so in the same manner as Noc.

Indeed these changes to nucleoid morphology are not unexpected, as it has been shown previously that Spo0J is required for chromosome maintenance, including condensing the DNA and holding the origins of replication together until segregation is ready to proceed (Graham et al, 2014; Lee & Grossman, 2006; Sullivan et al, 2009; Wang et al, 2014c). So how does Spo0J impact Z ring positioning by affecting nucleoid morphology? The data seems to suggest this and there are two ways in which Spo0J could do this: firstly via the nucleoid occlusion protein Noc, and secondly through changes to chromosomal arm interactions.

3.3.1.1 *Noc-mediated nucleoid occlusion*

The simplest possibility for the increase in midcell Z ring assembly when initiation of DNA replication is blocked is that in the absence of *spo0J*, the changes to nucleoid morphology observed actually changes Noc localisation and therefore Noc activity. Noc binds to numerous specific locations along the chromosome with the exception of the terminus region (74 Noc DNA-binding sites (Wu et al, 2009)), and prevents Z ring assembly over the unreplicated nucleoid with no observed effect to nucleoid morphology. It is possible that the absence of *spo0J* could be causing changes to chromosome conformation such that Noc no longer localises with the DNA, disabling the function of Noc. This would in turn allow Z rings to form more readily over the unreplicated DNA. Thus, this would suggest that during initiation of DNA replication, Spo0J is indirectly affecting midcell Z ring assembly by affecting the localisation and, hence, activity of Noc. Furthermore, it would suggest that Spo0J is required to maintain the nucleoid in a morphology that allows for proper Noc activity. This idea is explored further in Chapter 4.

3.3.1.2 *Chromosomal inter-arm interactions*

Alternatively, Spo0J is required to keep the chromosome in a specific conformation during the progression of initiation of DNA replication to negatively regulate central Z ring formation. Spo0J binds specifically to several origin-proximal *parS* sites, from which Spo0J coalesces non-specifically with neighbouring DNA to form distinct nucleoprotein complexes (Chen et al, 2015), an event seen to be important for origin resolution (Marbouty et al, 2015; Wang et al, 2015). Movement of the leading *parS* site (*pars*^{359}) to ectopic locations on the chromosome leads to a delay in chromosome segregation (Lee & Grossman, 2006). Furthermore, loss of Spo0J leads to a loss of origin localisation during DNA elongation (Lee & Grossman, 2006). These studies highlight the need for proper Spo0J binding to ensure proper chromosome organisation during DNA replication.

More specifically, recent Hi-C data investigating chromosome conformation and how the ParABS system plays into this has identified a significant role for Spo0J. For example, research by Marbouty *et al.* and Wang *et al.* found that in *B. subtilis*, the

bilobed nucleoid morphology seen when initiation of DNA replication is blocked in the *dna-1* mutation is composed of the left and right arm (Marbouty et al, 2015; Wang et al, 2015). Furthermore, Wang *et al.* found that loss of ParB (Spo0J) leads to loss of chromosomal inter-arm interactions (Wang et al, 2017). The authors thus speculated that ParAB recruitment of SMC is what drives this orientation. Hence, the nucleoid morphology data presented in this chapter is consistent with these observations and supports the idea that when initiation of DNA replication is blocked in the absence of *spo0J,* the two arms resolve. This in turn allows for the assembly of the Z ring at midcell.

Specific chromosome organisation has also been shown to be important for cell cycle regulation in other organisms. For example, although playing a more significant role closer to the time of DNA replication termination, MatP, ZapA and ZapB in *E. coli* form a direct link with the Ter region of the chromosome and regulate Z ring positioning, in turn coupling cell division and chromosome segregation (Bailey et al, 2014; Buss et al, 2013; Buss et al, 2015; Buss et al, 2017) . However, what this specific chromosome conformation in *B. subtilis* actually is will require further investigation.

Continuing on with this idea, it is possible that there is a further aspect of nucleoid morphology that is linked to inhibiting midcell Z ring assembly. More specifically, could changing the nucleoid morphology under these conditions be impacting transertion? The transertion theory describes the coupling of transcription, translation and insertion of membrane proteins which is hypothesised to tether networks of nascent proteins, mRNAs and genes to the inner membrane, thus coupling DNA dynamically to the bacterial cell envelope (Norris, 1995; Norris & Madsen, 1995; Woldringh, 2002). As such, transertion is suggested to be involved in DNA compaction or expansion, and tethering DNA to the membrane (Bakshi et al, 2014; Bakshi et al, 2015; Jin et al, 2013). This accumulation of activity between the DNA and the membrane would generate molecular crowding in areas of increased transertion, and in turn would pose well to regulate Z ring assembly and subsequent septum formation (Sun & Margolin, 1998; Sun & Margolin, 2004). Could the results presented here suggest a role for Spo0J in transertion? The chromosome inter-arm

interactions mentioned above are characterised as being areas of high transcription (Le et al, 2013; Le & Laub, 2014; Marbouty et al, 2015; Wang et al, 2015). The loss of these interactions in the absence of *parB* (*spo0J*) in *B. subtilis* could suggest a change in the transcription activity, and thus transertion activity, in the midcell region of the cell leading to changes in midcell Z ring assembly.

As mentioned above, transertion aids in the tethering of the DNA to the membrane. Interestingly, in the results presented in this chapter, a significant number of cells form Z rings at the cell centre because the nucleoid has moved off centre. This is consistent with the idea that Spo0J is required to organise the chromosome in a specific manner to facilitate transertion, thus tethering the unreplicated nucleoid to the midcell. Additionally, tethering of the DNA to the cell centre might also aid Noc in its transertion-like Z ring inhibitory role at midcell.

3.3.2 Does the origin of replication affect Z ring positioning?

Blocking initiation of DNA replication in the absence of *spo0J* resulted in a change in nucleoid morphology, which correlated with an increase in midcell Z ring assembly. A question that arose from these data was whether chromosomal loci, such as the origin of replication (*oriC*), were positioned differently in these cells and whether this impacted Z ring positioning. Therefore a fluorescent lac operator (lacO)/lac repressor (LacI) system was used to visualise the origin-proximal region at location 345° on the chromosome. It has been previously shown that *oriC* takes on a centralised position in the *dna-1* mutation (Regamey et al, 2000). Interestingly however, it was found that the origin was more centrally localised during the earliest stages of initiation of DNA replication (DnaB inactivation) than that at the later stage (addition of HPUra). Furthermore, *oriC* localisation was further perturbed in both blocks to initiation of DNA replication such that *oriC* moved off centre when *spo0J* was removed, consistent with recent findings (Wang et al, 2014b). This suggests that *oriC* localisation does impact Z ring positioning during initiation of DNA replication and that Spo0J is required to localise *oriC* to midcell.

So how could the origin region impact Z ring positioning? The origin region is the most active site within the cell with regard to gene transcription and translation of mRNA. Thus, if the origin region does impact Z ring formation at midcell, then the data is consistent with the idea of transertion presented above. More specifically, the data supports the idea that during initiation of DNA replication, Spo0J is required to keep the DNA in a conformation that allows the DNA to tether to the membrane at the future midcell division site in a transertion-like effect (Gruber et al, 2014; Wang et al, 2014c). Loss of Spo0J on the other hand leads to a loss of this tethering at midcell resulting in origin movement away from the cell centre, relieving the midcell site of origin-associated transertion and allowing midcell Z ring assembly.

Although in the context of the research question asked, the localisation approach was appropriate to gain an idea of *oriC* localisation. There are however caveats to the technique used. The fluorescent lac operator (lacO)/lac repressor (LacI) system, or more specifically the lac operator, introduces a large tandem array into the genome which has been suggested to potentially perturb chromosome architecture (Le & Laub, 2014). Indeed, a small change to the nucleoid morphology profile was observed in the data presented in this study where a greater fraction of the DNA was of spread morphology or was moved off centre. Therefore, it would be beneficial to repeat these experiments with a significantly smaller number of arrays (a tenth of the original array number) and super-resolution microscopy, a technique that has now been used in other localisation studies (Hensel et al, 2013; Wang et al, 2011). This would also allow for further in-depth investigations into how the origin is positioned in relation to Z ring positioning and different nucleoid conformations.

3.3.3 Testing Spo0J further in the HPUra condition

The similar Z ring positioning and nucleoid morphology results observed between vegetatively grown *Δspo0J* cells and the outgrown *Δsoj-spo0J* spore cells, suggests that Spo0J is the protein required to prevent midcell Z ring formation, and not Soj, at least when DnaB is inactivated. However, a caveat remains in the HPUra experiments, as these experiments require the use of *Δsoj-spo0J* spores to ensure

that initiation of DNA replication is blocked just prior to DNA synthesis. It is assumed, based on the DnaB inactivation results that it is likely Spo0J to be responsible for the increase to midcell Z ring frequency. However, it cannot be definitely ruled out that Soj is not having some effect at this specific block to DNA replication initiation via the addition of HPUra. It would thus be ideal to explore this further in the future. One way this could be achieved is by examining alternative blocks to initiation of DNA replication that is not dictated by the use of the spore outgrowth system (for example, the *polC* mutation; (Moriya et al, 2010)). Alternatively, the spore germination system could be used to test the HPUra condition, by tagging either Soj or Spo0J with an inducible degradable allele to be deactivated separately following spore germination (Griffith & Grossman, 2008; Wang et al, 2014c).

UTS
UNIVERSITY OF TECHNOLOGY SYDNEY

Chapter 4. Investigating the role of Spo0J and Noc in division site placement

ithreeinstitute

4.1 Introduction

In the study leading up to the Ready-Set-Go model, different treatments to inhibit the initiation phase of DNA replication gave rise to different midcell Z ring frequencies. It was not until Noc was removed that the frequency of midcell Z rings was observed to increase with the progress of the initiation phase of replication (Moriya et al, 2010). Similarly, in the previous chapter it was discovered that deletion of *soj-spo0J* (or just *spo0J*) in the *dna-1* mutant, results in a similar increase in the frequency of midcell Z rings to that of the *noc* deletion. Why does the absence of *spo0J* promote Z rings to form at midcell to a similar extent as observed in the absence of *noc*? One possible explanation for this is that the absence of *spo0J* is affecting Noc function in some way which in turn increases midcell Z ring frequency under these conditions. In Chapter 3, it was shown that Spo0J impacts nucleoid morphology, and Z ring positioning appears to correlate with this. For example, in the *dna-1* mutant, midcell Z rings were observed to form more readily over bilobed nucleoids. The same observation was made in the +HPUra condition. Hence, Spo0J impacts nucleoid morphology, and this could be having a direct effect on the way Noc is distributed around the chromosome. To elaborate further, it has been shown that Noc binds to specific sequences along the DNA, with a preference towards the origin region, and a general absence from the terminus region. Perhaps if you change the nucleoid morphology, this orientation changes and Noc is no longer capable of binding to the DNA as needed to invoke its nucleoid occlusion effect.

Therefore, the overall aim of this chapter is to examine if the effect Spo0J has on Z ring positioning during initiation of DNA replication is an indirect effect on Noc activity. To do this, two approaches are used. Firstly, to examine whether Noc DNA-binding is abolished with the loss of *spo0J*, Noc localisation was examined in the absence of *spo0J* when initiation of DNA replication is blocked. If Noc binding to DNA is abolished in the absence of *spo0J*, this would support the idea that Spo0J reduces Z ring positioning via affecting Noc localization during the initiation phase of DNA replication. A second test to determine whether Spo0J is acting indirectly through Noc to affect Z ring assembly was to investigate Z ring positioning in the absence of

both *spo0J* and *noc* when initiation of DNA replication is blocked. If the combined absence of *spo0J* and *noc* does not invoke an increase in midcell Z ring assembly compared to that of the single mutants, then this again would support the idea that the restoration of midcell Z ring assembly in the absence of *spo0J* when initiation of DNA replication is blocked is not attributed to Spo0J. Instead, it would suggest that it is an indirect effect on the activity of the nucleoid occlusion protein, Noc. Alternatively, if an increase in midcell Z ring frequency is observed with the combined absence of *spo0J* and *noc*, then it would suggest that the two proteins affect Z ring positioning separately and Noc is still active in the *spo0J* mutant.

4.2 Results

4.2.1 Examining Noc localization in the absence of *spo0J* when initiation of DNA replication is blocked at the earliest stage

A key question arising from the previous chapter is whether the effects on Z ring positioning seen in the absence of *spo0J* during initiation of DNA replication are due to changes in the Z ring-inhibitory nucleoid occlusion effect of Noc. This could occur through the loss of Noc binding to DNA in a *Δspo0J* strain. Noc is known to localise with the nucleoid in growing cells and is proposed to invoke its nucleoid occlusion function through this binding to the DNA (Adams et al, 2015; Wu & Errington, 2004; Wu et al, 2009). It is possible that significant changes to nucleoid morphology (increase in bilobed or spread nucleoids; see Chapter 3, section 3.2.2.2) observed in the absence of *spo0J* in the *dna-1* mutation leads to loss of Noc co-localisation with the nucleoid, suggesting loss of Noc binding and activity.

To examine Noc localization, live cells were used. A yellow-fluorescent-protein fusion to the C-terminal end of Noc (Noc-YFP; SU629, Table 2.2) was introduced into the relevant strains lacking the native copy of Noc, such that the Noc-YFP copy was the only copy of Noc present in the cells. This *noc-yfp* expression cassette is under the control of the P_{xyl} promoter (xylose inducible) and is integrated into the chromosome at the non-essential *amyE* locus. This expression cassette has been successfully used

to localize Noc in the Harry lab and was found to have an optimum inducible range of 0.2-0.5% xylose (Wu et al, 2009).

To obtain strains for the live visualisation of Noc in the *dna-1* DNA replication mutant background, strains SU533 (*Δnoc*), SU802 (*dna-1 Δnoc*), SU829 (*Δspo0J Δnoc*) and SU830 (*dna-1 Δspo0J Δnoc*) were transformed with SU657 (*noc-yfp*) chromosomal DNA to create SU831 (*Δnoc, noc-yfp*; wild-type), SU832 (*dna-1*, *Δnoc, noc-yfp*), SU833 (*Δspo0J Δnoc noc-yfp*) and SU834 (*dna-1 Δspo0J Δnoc noc-yfp*), respectively. Spectinomycin-resistant transformants were checked for temperature sensitivity and disruption of the *amyE* locus. As a control, Z ring positioning was examined in these Noc-YFP strains and it was seen that Noc-YFP does not affect Z ring positioning in either the wild-type or *dna-1* mutant background at both the permissive and non-permissive temperature (data not shown). To visualise Noc localisation, the constructed strains were grown vegetatively in PAB with 0.3% xylose at the permissive temperature (30°C) to the mid-exponential point, before being diluted with PAB to OD_{600} 0.05, and shifted to the non-permissive temperature of 48°C for 1 hour. Cells were then collected, mixed with DAPI and prepared for live visualisation (see Materials and Methods 2.6.3).

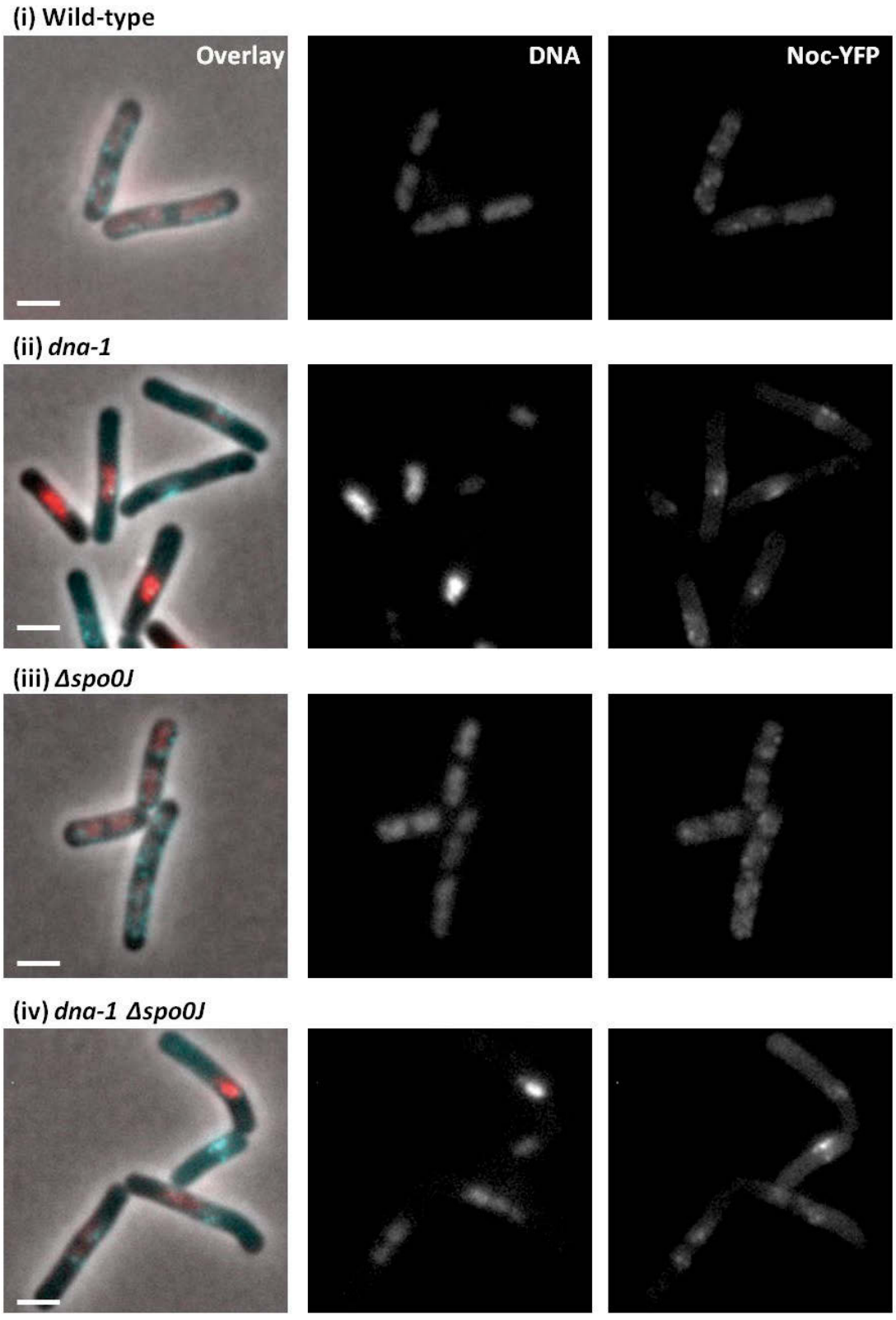

Figure 4.1: Noc localisation in the absence of s*po0J* when initiation of DNA replication is blocked. Strains (i) wild type (SU831), (ii) *dna-1* (SU832), (iii) *Δspo0J Δnoc* (SU833), and (iv) *dna-1 Δspo0J Δnoc* (SU834), possessing Noc tagged with a yellow fluorescent protein (*noc-yfp*; falsely coloured cyan) were grown vegetatively in PAB supplemented with 0.3% xylose.

Cells were grown at the permissive temperature (30°C) to the mid-exponential point then shifted to the non-permissive temperature (48°C) before being collected for live visualisation. DNA was also stained with DAPI (falsely coloured red) to allow co-visualisation of Noc and the nucleoid. Scale bar = 2 μm.

Noc co-localised with the nucleoid in both wild-type and *Δspo0J* backgrounds (Figure 4.1 i and iii, respectively). Blocking initiation of DNA replication in the *dnaB* mutant did not alter Noc co-localisation with the nucleoid (Figure 4.1 ii), with Noc-YFP localising with the unreplicated nucleoid in the form of faint uniform localisation or distinct foci. Likewise, Noc appears to maintain a preference for localisation with the nucleoid in the absence of *spo0J* when initiation of DNA replication is blocked (Figure 4.1 iv). Some variability in Noc localisation can at times be seen in *dna-1 Δspo0J* where it does not localize in between bilobed nucleoids (Figure 4.1 iv). However whether this is due to a change in the nucleoid morphology or due to the limitations of visualisation of the protein is not clear. It is unlikely that this small decrease in Noc co-localisation accounts for the change in midcell Z ring frequency as this localisation pattern with the bilobed nucleoid is also seen in the *dnaB* mutant (Spo0J^{+}), and Z rings rarely form over the bilobed nucleoids in the *dnaB* mutant. Furthermore, as described in the previous chapter, Z rings in *dna-1 Δspo0J* cells are capable of forming at midcell over single-lobed nucleoids, which, as seen here, have Noc association with the nucleoid. This suggests that Noc still localises around the DNA in a *spo0J* mutant even when initiation of replication is blocked. These observations argue against the possibility that the restoration of Z ring positioning in the *dna-1 spo0J* mutant occurs indirectly, by decreasing Noc function. Thus, the data suggests that Noc is still active in the *spo0J* mutant. If Noc is still active in the *spo0J* mutant, then the way in which Spo0J affects Z ring positioning is by changing nucleoid morphology which affects Noc distribution, but not so much its localisation to the DNA.

4.2.2 Examining Z ring positioning in the absence of all three proteins, Soj, Spo0J and Noc

4.2.2.1 *Characterization of Z ring positioning in dna-1 cells in the absence of soj, spo0J and noc at the non-permissive temperature*

As shown above, when initiation of replication is blocked Noc-YFP localizes to the nucleoid even in the absence of *spo0J*. This suggests that Noc is fully active under these conditions. If this is the case, then the absence of both *spo0J* and *noc* should have an additive effect on Z ring positioning when initiation of replication is blocked, such that even more Z rings form at midcell in a large portion of cells in a *noc spo0J* double mutant.

To investigate whether the deletion of both *spo0J* and *noc* has an additive effect on midcell Z ring assembly in the *dna-1* mutant at the non-permissive temperature, various strains were created. As a control, Z ring positioning analysis was also performed in the absence of *noc* and *soj* to show that Soj is not involved in these effects. To create the relevant strains, strains SU771 (*Δsoj*), SU772 (*dna-1 Δsoj*), SU769 (*Δspo0J*) and SU770 (*dna-1 Δspo0J*) were transformed with donor chromosomal DNA from strain SU533 (*Δnoc*) to create strains SU827 (*Δsoj Δnoc*), SU828 (*dna-1 Δsoj Δnoc*), SU829 (*Δspo0J Δnoc*) and SU830 (*dna-1 Δspo0J Δnoc*), respectively. Kanamycin- and chloramphenicol-resistant colonies were confirmed for temperature sensitivity. Deletion of *noc* and *spo0J* were confirmed via PCR.

All strains were grown vegetatively alongside control strains, wild-type (SU5) and *dna-1* (SU661), at 30°C to mid-exponential phase of growth, then shifted to the non-permissive temperature (48°C) for a further hour. Cells were then collected for IFM. Consistent with previous results, at the non-permissive temperature Z rings in wild-type and *dna-1* were predominantly located at midcell (87%) or acentrally (10%), respectively (Figure 4.2; Table 4.1). Z ring positioning in both *Δsoj Δnoc* and *Δspo0J Δnoc* in an otherwise wild-type background were essentially the same at the higher temperature, with the majority of Z rings forming at the cell centre (78% and 84%, respectively). Intriguingly, midcell Z ring positioning increased to wild-type levels when DnaB was inactive in the *spo0J noc* double mutant (81%), while Z ring

positioning was not greatly affected by the absence of *soj* in the *dnaA-1 Δsoj Δnoc* strain (47%). Thus, consistent with previous observations, Soj does not influence Z ring positioning. Importantly, these data show that Noc is still active in the *spo0J* mutant and suggests that Spo0J and Noc both contribute to the production of acentral Z rings when initiation of DNA replication is blocked.

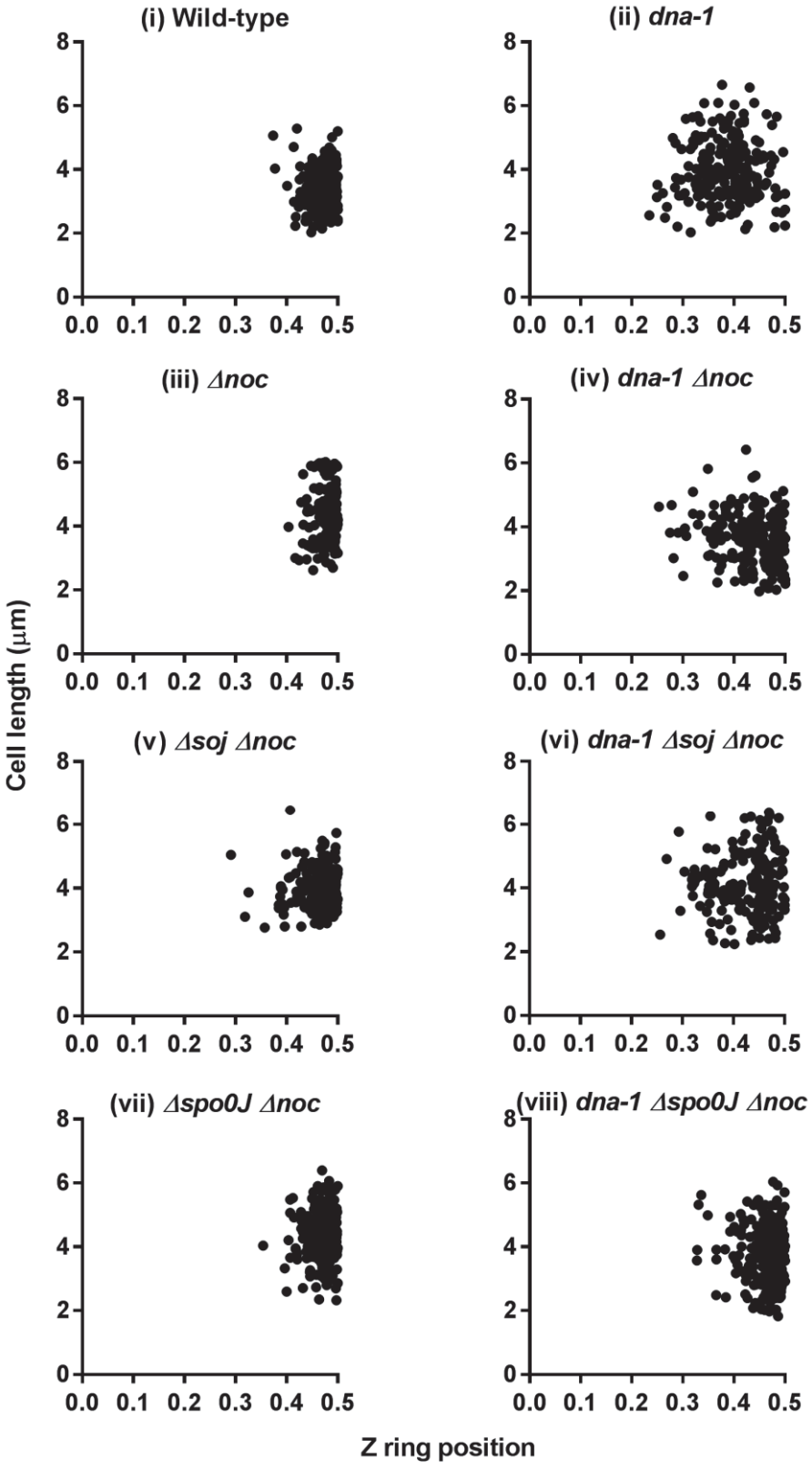

Figure 4.2: Z ring positioning in the individual mutants, *soj* or s*po0J*, in the *dna-1 Δnoc* mutation at the non-permissive temperature. Strains were grown in PAB at the permissive temperature (30°C) to mid-exponential phase of growth and then shifted to the non-

permissive temperature (48°C) for 60 minutes. Scatter plots showing Z ring positioning and average cell length (±SEM) of vegetatively grown fixed cells of (i) wild-type (SU5), (ii) *dna-1* (SU661), (iii) *Δnoc* (SU533), (iv) *dna-1 Δnoc* (SU802), (v) *Δsoj Δnoc* (SU829), (vi) *dna-1 Δsoj Δnoc* (SU830), (vii) *Δspo0J Δnoc* (SU827), and (viii) *dna-1 Δspo0J Δnoc* (SU828). Z ring position is determined by measuring the distance from the Z ring to the nearest cell pole and dividing this value by the cell length, with 0.5 being exactly midcell. A Z ring is considered to be at midcell if it was positioned within the range of 0.45-0.50, as this is where most Z rings form in the wild-type strain. n > 200. See Table 4.1 for midcell Z ring frequencies and average cell lengths (±SD) for each strain.

Table 4.1: Analysis of Z ring positioning in vegetative cells of the *dna-1* temperature-sensitive mutant in the absence of *noc*, *soj* and *spo0J* at 48°C. [a]

Strain	Average cell length (±SD) [a]	% Midcell Z rings [b]
Wild-type	3.44 ± 0.61	85%
dna-1	3.80 ± 0.88	10%
Δnoc	4.51 ± 0.87	86%
dna-1 Δnoc	3.61 ± 0.80	44%
Δsoj Δnoc	4.14 ± 0.63	78%
dna-1 Δsoj Δnoc	3.43 ± 0.67	47%
Δspo0J Δnoc	3.94 ± 0.85	84%
dna-1 Δspo0J Δnoc	3.44 ± 0.98	81%

[a] Table shows average cell length (±SD) and [b] percent of Z rings in the midcell range (0.45-0.5). Midcell is considered to be between 0.45 and 0.50 as this is where majority of Z rings form in wild-type cells. Scatter plots of Z ring positioning are depicted in Figure 4.2. See Figure 4.2 for strain growth conditions and midcell Z ring characterisation.

Since the involvement of Soj could be excluded in these experiments, it was decided that a similar result could be drawn by performing the experiments in outgrown spores of the triple mutant. Furthermore, performing these experiments allowed for examination of the nucleoid morphologies in relation to Z ring position. This was of interest because a deletion of *noc* has no observable effect on nucleoid morphology, but a deletion of *spo0J* does. However, the combined deletion of *noc* and *spo0J* may lead to further changes to nucleoid morphology, and this would provide insight to why a complete restoration of midcell Z rings to wild-type conditions is occurring in the absence of *spo0J* and *noc*. Therefore strains SU765 (*Δsoj-spo0J*) and SU766 (*dna-1 Δsoj-spo0J*) were transformed with chromosomal DNA from strain SU533 (*Δnoc*) to create strains SU803 (*Δsoj-spo0J Δnoc*) and SU804 (*dna-1 Δsoj-spo0J Δnoc*). Given the close proximity of these three genes on the genome, transformation via homologous recombination was completed on double antibiotic plates with 40% lower antibiotic concentration than standard to allow for growth of transformants. Chloramphenicol and tetracycline resistant strains were tested for temperature sensitivity (where relevant). Successful deletion of *noc*, as well as the absence of *soj-spo0J*, was confirmed via PCR. These strains were grown alongside control strains SU5 (wild-type) and SU661 (*dna-1*) to examine Z ring positioning and nucleoid morphology (discussed in next section). Both vegetatively-growing cells and outgrown spores were examined to ensure that the effect seen is consistent in both situations. However, since the results are the same in both cases, only the outgrown spore experiments will be described here.

Consistent with previous results, at the non-permissive temperature, Z rings formed either predominantly at the cell centre in wild-type cells (85%) or only 9% at midcell in the *dna-1* mutant strain (Figure 4.3; Table 4.2). The absence of *noc* in the wild-type background readily formed midcell Z rings (86%), however when combined with the temperature-sensitive *dna-1* mutant a partial restoration in midcell Z ring assembly was observed (44%), consistent with published data (Moriya et al, 2010). The combined deletion of *soj*, *spo0J* and *noc* in the wild-type background had no significant effect on Z ring positioning at the non-permissive temperature, with the majority of Z rings forming at the central position (85%). As was seen in the absence

of *spo0J* and *noc*, Z ring positioning was essentially completely restored (81%) to wild-type levels in the absence of all three proteins, Soj, Spo0J and Noc at the non-permissive temperature in the *dna-1* mutant (see Table 4.2). This further confirms that Spo0J and Noc prevent midcell Z ring assembly when initiation of DNA replication is blocked at the level of DnaB.

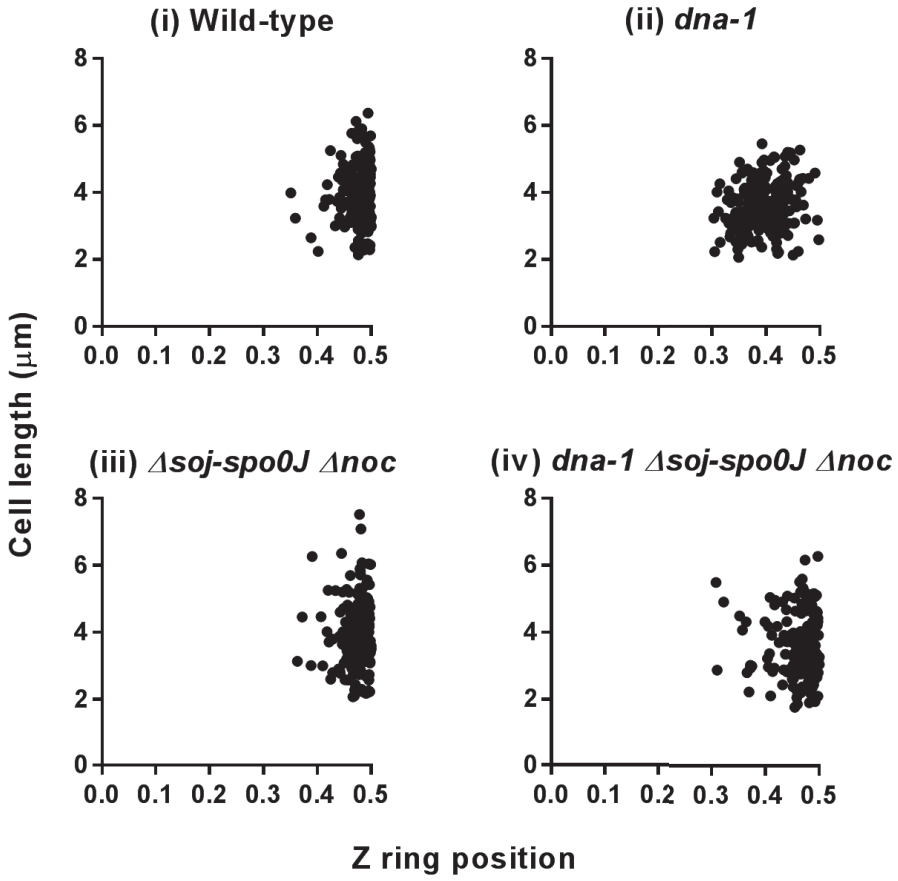

Figure 4.3: Z ring positioning when initiation of DNA replication is blocked during spore outgrowth in the *dna-1* temperature-sensitive mutation. Spores were germinated in GMD containing 0.02% xylose (v/v) for 20 minutes at the permissive temperature (34°C), then shifted to the non-permissive temperature (48°C) for a further 80 minutes (wild-type; SU5 and *dna-1*; SU661) or 95 minutes (*Δsoj-spo0J Δnoc*; SU803 and *dna-1 Δsoj-spo0J Δnoc*; SU804). Figure shows Z ring positioning in (i) wild-type, (ii) *dna-1*, (iii) *Δsoj-spo0J Δnoc*, and (iv) *dna-1 Δsoj-spo0J Δnoc*. Z ring position is determined by measuring the distance from the Z ring to the nearest cell pole and dividing this value by the cell length, with 0.5 being exactly midcell. A Z ring is considered to be at midcell if it was positioned within the range of 0.45-0.50, as this is where most Z rings form in the wild-type strain. n > 200. See Table 4.2 for midcell Z ring frequencies and average cell lengths (±SD) for each strain.

Table 4.2: Analysis of Z ring positioning in the *dna-1* temperature-sensitive mutation in the absence of *noc* and *soj-spo0J a*t 48°C.[a]

Strain	Average cell length (±SD) [a]	% Midcell Z rings [b]
Wild-type	4.43 ± 0.71	85%
dna-1	3.98 ± 0.66	9%
Δsoj-spo0J Δnoc	3.89 ± 0.76	85%
dna-1 Δsoj-spo0J Δnoc	3.71 ± 0.78	81%

[a] Table shows average cell length (±SD) and [b] percent of Z rings in the midcell range (0.45-0.5). Midcell is considered to be between 0.45 and 0.50 as this is where majority of Z rings form in wild-type cells. Scatter plots of Z ring positioning are depicted in Figure 4.3. See Figure 4.3 for strain growth conditions and midcell Z ring characterisation.

4.2.2.2 *Characterisation of Z ring positioning in the absence of soj, spo0J and noc in the presence of HPUra*

In the previous chapter, it was shown that, like Noc, Spo0J prevents a significant proportion of Z rings forming at midcell when entry into the round of DNA via is blocked by the addition of HPUra. However, as identified above, the combined absence of *noc* and *spo0J* in the temperature-sensitive mutant *dna-1* results in a complete restoration of midcell Z ring formation. Is this also true for the HPUra condition? Would Z rings form at the cell centre to wild-type levels like that seen in the *dna-1* mutant? If so, this would suggest that Spo0J and Noc are the only proteins responsible for preventing premature Z ring assembly during the initiation of DNA replication in *B. subtilis*.

To examine Z ring positioning when entry to DNA elongation is blocked, spores of the wild type strain (SU492; P_{xyl}-*ftsZ-yfp*) and test strain (SU767; P_{xyl}-*ftsZ-yfp Δsoj-spo0J Δnoc*) were used. As outlined in the previous chapter, to block entry solely to DNA elongation via the addition of HPUra, the spore outgrowth system must be used. Spores of the aforementioned strains were germinated and grown out at 34°C in GMD in the presence (and absence as a control) of HPUra (100 μM). GMD was also supplemented with xylose (0.02%) for Z ring visualisation. Consistent with previous results (see section 3.2.3.1, (Moriya et al, 2010), in the

wild-type strain in the absence of HPUra, Z rings formed readily at the cell centre (87%), while 23% formed at midcell when HPUra was added. As expected in the control experiment, in the absence of HPUra, Z rings readily formed at the cell center (80%) in the *Δsoj-spo0J Δnoc* triple mutant. Intriguingly, in the presence of HPUra (no replication), this same strain produced an identical number of midcell Z rings (80%), as if no inhibition to DNA replication initiation had been applied. In addition, this increase in midcell Z ring assembly was not due to DNA synthesis (see Chapter 3, section 3.2.5). These observations are similar to what was seen in the *dna-1* mutant. Thus, Spo0J and Noc are the only factors preventing Z ring assembly when the early stages of DNA replication are blocked.

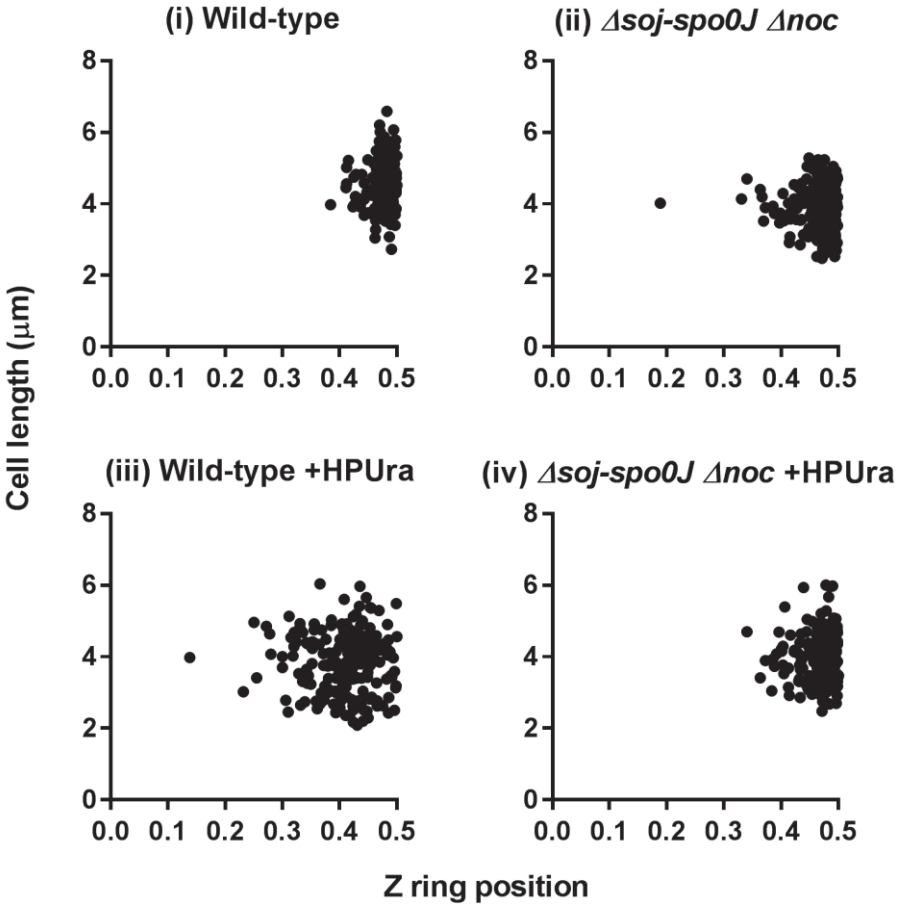

Figure 4.4: Z ring positioning when entry into DNA chain elongation is blocked during spore outgrowth in the +HPUra conditions. Wild-type and *Δsoj-spo0J Δnoc* spores were germinated in GMD containing 0.02% xylose (v/v), in the absence or addition of HPUra (100 μM) for 125 minutes and 140 minutes at 34°C, respectively. Figure shows scatter plots of Z ring positioning in (i) wild-type (SU492), (ii) *Δsoj-spo0J Δnoc* (SU767), (iii) wild-type +HPUra and (iv) *Δsoj-spo0J Δnoc* +HPUra. Z ring position is determined by measuring the distance from the Z ring to the nearest cell pole and dividing this value by the cell length, with 0.5 being exactly midcell. A Z ring is considered to be at midcell if it was positioned within the range of 0.45-0.50, as this is where most Z rings form in the wild-type strain. n > 200. See subsequent Table 4.3 for midcell Z ring frequencies and average cell lengths (±SD) for each sample.

Table 4.3: Analysis of Z ring positioning in outgrown spores in the absence of *soj-spo0J* and *noc* with the addition of HPUra.

Strain	Average cell length (±SD) [a]	% Midcell Z rings [b]
Wild-type	4.47 ± 0.74	87%
Δsoj-spo0J Δnoc	3.97 ± 0.55	80%
Wild-type +HPUra	4.43 ± 0.57	23%
Δsoj-spo0J Δnoc +HPUra	3.91 ± 0.54	80%

[a] Table shows average cell length (±SD) and [b] percent of Z rings in the midcell range (0.45-0.5). Midcell is considered to be between 0.45 and 0.50 as this is where majority of Z rings form in wild-type cells. Scatter plots of Z ring positioning are depicted in Figure 4.4. See Figure 4.4 for strain growth conditions and midcell Z ring characterisation.

4.2.3 Investigating nucleoid morphologies in the absence of *soj*, *spo0J* and *noc* when initiation of DNA replication is blocked

4.2.3.1 *Characterization of nucleoid morphology in the absence of soj, spo0J and noc*

Previously, it has been shown that a deletion of Noc does not impact nucleoid morphology (Moriya et al, 2010). However, to confirm that the Z ring positioning that are seen in the *spo0J noc* double mutant are not due to further nucleoid morphology changes, nucleoid morphologies were examined in the double mutant.

To examine nucleoid morphologies in the earliest block to initiation (*dna-1*), vegetative cells were grown at the non-permissive temperature, fixed with ethanol and DNA was stained with DAPI (Materials and Methods section 2.6.2). Consistent with previous results, *dna-1* demonstrated predominantly single-lobed nucleoid morphology (82%; Figure 4.5). Likewise, *dna-1 Δnoc* and *dna-1 Δsoj Δnoc* cells demonstrated little difference in nucleoid morphology profile in comparison to that of just *dna-1* cells, with single-lobed nucleoids being the predominant nucleoid morphology (80% and 84% single-lobed nucleoids, respectively; Figure 4.5). The frequency of single-lobed nucleoids in *dna-1 Δsoj-spo0J Δnoc* and *dna-1 Δspo0J Δnoc* cells on the other hand was almost halved (45% and 50% single-lobed nucleoids,

respectively), with an increase in spread (31% and 28%, respectively) or bilobed (24% and 22%, respectively) morphology. Importantly, this nucleoid morphology distribution is like that seen in *dna-1 Δsoj-spo0J* cells where nucleoids were seen to be predominantly either of bilobed (37%) or spread (22%) morphology (see Figure 3.4). In other words, a deletion of *noc* in the absence of *soj-spo0J* (or just *spo0J*) does not alter the nucleoid morphology profiles. This indicates that complete restoration of midcell Z rings to wild-type levels in the *noc spo0J* double deletion does not occur as a result of further changes to nucleoid morphology. Instead, Noc and Spo0J appear to act differently in the way they prevent midcell Z ring assembly; Noc actively prevents the Z ring from forming over the DNA, whereas Spo0J induces a change in nucleoid morphology. Thus combining the two, is sufficient to allow for wild-type levels of midcell Z ring assembly when initiation of DNA replication is blocked.

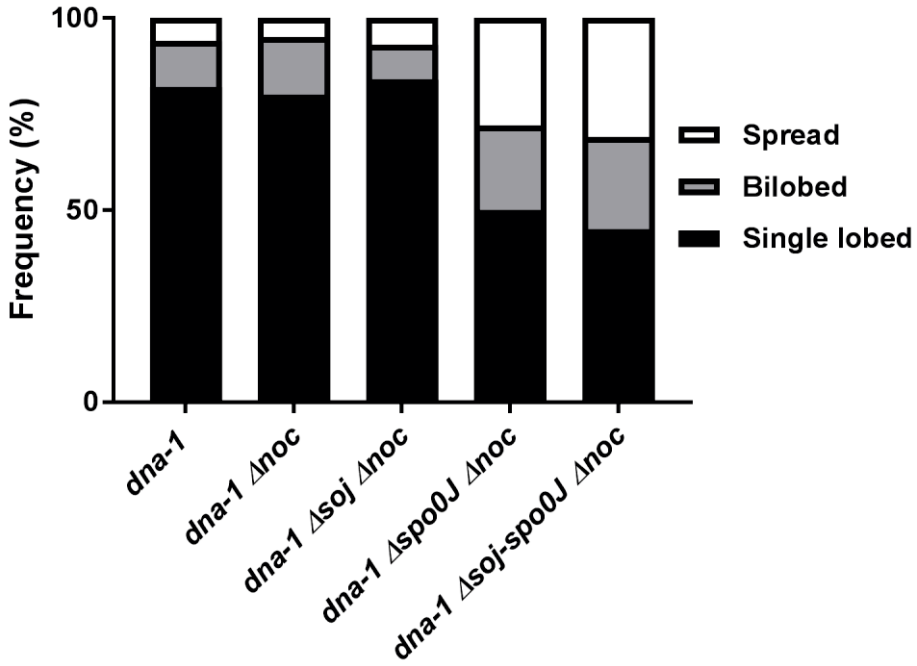

Figure 4.5: Nucleoid morphology in ethanol-fixed DAPI stained vegetative cells of the *dna-1* mutation in absence of *noc*, *soj* and/or *spo0J*. Strains were grown in PAB to mid-exponential point at the permissive temperature (30°C) and then shifted to the non-permissive temperature (48°C) for 60 minutes (n > 200).

To confirm that changes to nucleoid morphology in the combined absence of *noc* and *soj-spo0J* is not unique to the *dna-1* mutant, nucleoid morphologies were also examined in the HPUra condition. To examine nucleoid morphology, DNA of live outgrown wild-type and *Δsoj-spo0J Δnoc* spores were germinated and outgrown in GMD and HPUra (100 µM, where relevant) and stained with DAPI. Nucleoid morphologies were scored as above. A significant decrease in single-lobed nucleoids was observed in *Δsoj-spo0J Δnoc* +HPUra in comparison to wild-type +HPUra (53% in wild-type +HPUra versus 10% in *Δsoj-spo0J Δnoc* +HPUra; Figure 4.6). A significant increase in bilobed and spread nucleoids was instead observed, with relatively equal frequencies between the two morphologies (44% and 46%, respectively). Overall, the *soj-spo0J noc* triple mutant grown in the presence of HPUra does not significantly alter the nucleoid morphology relative to that of *soj-spo0J* only (see Figure 3.7).

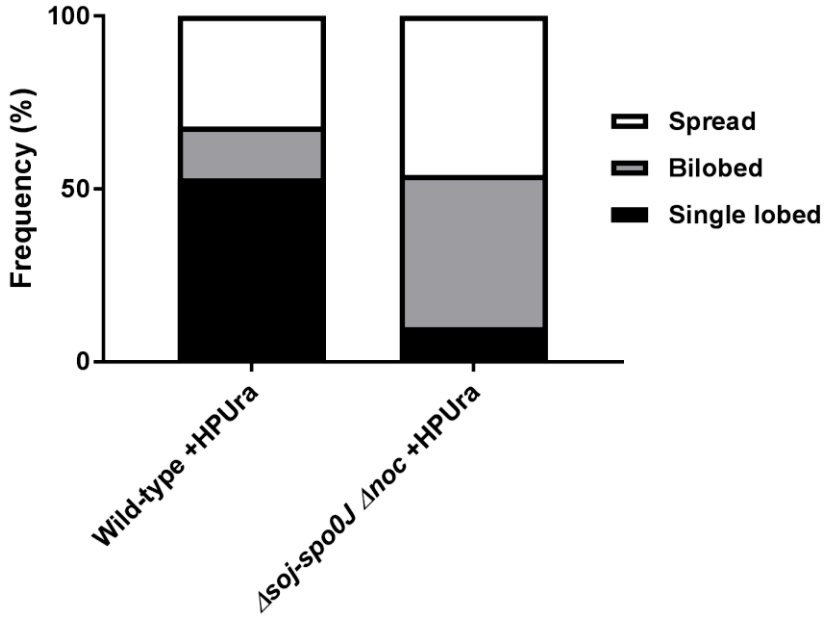

Figure 4.6: Nucleoid morphology in live DAPI-stained outgrown spores of wild-type and *Δsoj-spo0J Δnoc* in the presence of HPUra. Spores were germinated in GMD with the addition of HPUra (100 µM) for 125 minutes and 140 minutes at 34°C, respectively (n > 200). See Chapter 3, section 3.2.3.2 for the nucleoid morphology profile observed in *soj-spo0J* +HPUra for comparison.

4.2.3.2 *Co-visualisation of Z rings and nucleoids when initiation of DNA replication is blocked in the absence of soj, spo0J and noc.*

The data suggests that Z rings can form at midcell to the same extent as wild-type cells when DNA replication is inhibited in the absence of *noc* and *soj-spo0J* in both the *dna-1* mutation and the HPUra condition. Is there a change in the way the Z ring relates to the nucleoid in the *noc soj-spo0J* double mutant? To gain understanding where the Z ring formed relative to the DNA, Z rings were co-visualised with the nucleoid in live outgrown spores and localisation of the two was assessed. Donor chromosomal DNA of strain SU492 (*ftsZ-yfp*) was transformed into strains SU803 (*Δsoj-spo0J Δnoc*) and SU804 (*dna-1 Δsoj-spo0J Δnoc*) to create strains SU835 (*Δsoj-spo0J Δnoc ftsZ-yfp*) and SU836 (*dna-1 Δsoj-spo0J Δnoc ftsZ-yfp*), respectively. Spectinomycin resistant strains were confirmed for temperature sensitivity. Successful introduction of *ftsZ-yfp* was confirmed by testing the disruption of the *amyE* locus and visualising xylose induced fluorescence (see Materials and Methods 2.2.1). Table 4.4 shows the frequency distribution of Z ring positioning amongst the different nucleoid morphologies when initiation of DNA replication (*dna-1*) or entry to DNA chain elongation (+HPUra) is blocked either in the presence or absence of *soj-spo0J* and *noc*. Figure 4.7 shows representative images of the most common types of cells observed.

As expected, nucleoid morphology frequency profiles were consistent with previous results (see Chapter 3, sections 3.2.1.2 and 3.2.3.3). With regards to how the Z ring position correlated with each nucleoid morphology, very few Z rings formed at midcell in the predominantly single-lobed nucleoid population in the *dna-1* mutant, or all three morphologies in the HPUra-treated wild-type cells (see Sections 3.2.1.2 and 3.2.3.3, (Moriya et al, 2010). In the absence of all three genes, *soj, spo0J* and *noc*, Z rings are seen to readily form over the unreplicated nucleoids, predominantly of spread or bilobed morphology. In *dna-1 soj-spo0J noc*, a significant proportion of midcell Z rings formed over bilobed (20%, Table 4.4, Figure. 4.7 E ii) or spread nucleoids (24%, Table 4.4, Figure. 4.7 E iii). Thus, a deletion of *soj-spo0J* and *noc* in the *dna-1* mutant readily allows midcell Z ring formation over bilobed or spread nucleoids.

Table 4.4: Frequency of different nucleoid morphologies in the absence of *soj*, *spo0J* and *noc* in two blocks to initiation of DNA replication [a]

	Nucleoid morphology											
Z ring position	**Single-lobed**				**Bilobed**				**Spread**			
	dna-1	*dna-1 Δsoj-spo0J Δnoc*	Wild-type +HPUra	*Δsoj-spo0J Δnoc* +HPUra	*dna-1*	*dna-1 Δsoj-spo0J Δnoc*	Wild-type +HPUra	*Δsoj-spo0J Δnoc* +HPUra	*dna-1*	*dna-1 Δsoj-spo0J Δnoc*	Wild-type +HPUra	*Δsoj-spo0J Δnoc* +HPUra
Acentral Z ring (%)	**76**	**8**	**42**	**0**	**16**	**5**	10	10	4	6	**26**	**11**
Midcell Z ring over the nucleoid (%)	**0**	**14**	2	3	**0**	**20**	**5**	**32**	**2**	**24**	**7**	**31**
Midcell Z ring not over the nucleoid (%)	**2**	**15**	4	5	0	4	1	4	0	4	3	4

[a] Bolded numbers highlight significant differences in the conditions being compared, which are discussed further in text.

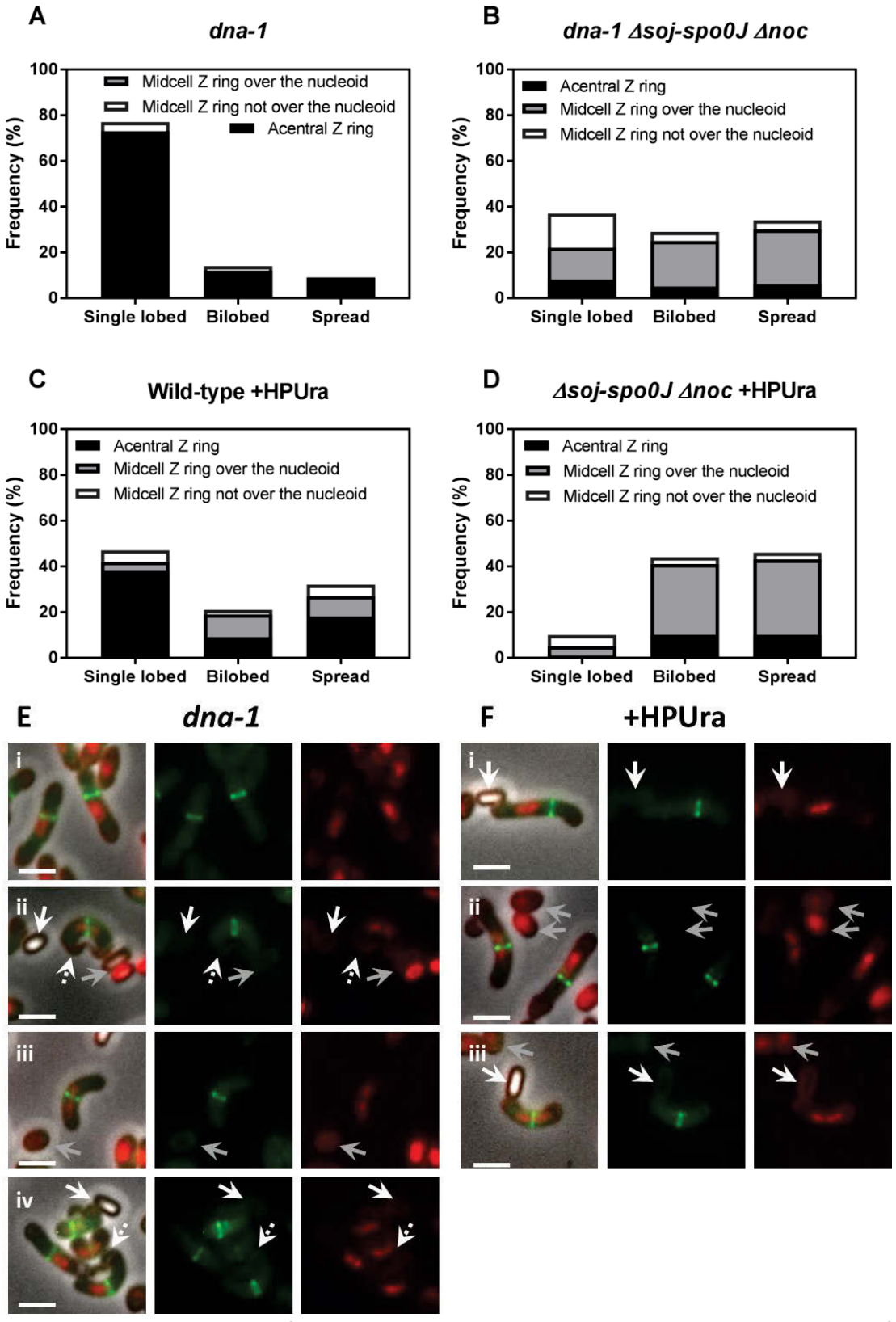

Figure 4.7: Co-visualization of the Z ring and nucleoids in live outgrown spores absent of *soj*, *spo0J* and *noc* when initiation of DNA replication is blocked at different stages. Spores were germinated in GMD with 0.02% xylose and 100 µM HPUra (where relevant) for (A and B) 20 minutes at permissive temperature (34°C) and then shifted to the non-permissive

temperature (48°C) for 60 minutes (wild-type), 70 minutes (*dna-1*), and 80 minutes (*Δsoj-spo0J Δnoc* and *dna-1 Δsoj-spo0J Δnoc*). (C and D) 125 minutes and 140 minutes at 34°C, respectively. (A - D) Histogram representation of Z ring position relative to different nucleoid type in (A) *dna-1 ftsZ-yfp,* (B) *dna-1 Δsoj-spo0J Δnoc ftsZ-yfp* (C) wild-type +HPUra and (D) *Δsoj-spo0J Δnoc* +HPUra. The height of each bar represents the frequency of each nucleoid type, showing the proportion of acentral Z rings (black), midcell Z rings over the nucleoid (grey) and midcell Z rings not over the nucleoid (white). (E and F) Representative images of predominant Z ring position and nucleoid type in (E) the *dna-1* mutation or (F) block to elongation via the addition of HPUra. Images show (E and F i) Z ring acentral to a single-lobed nucleoid, (E and F ii) central Z ring over bilobed nucleoid, (E and F iii) central Z ring over spread nucleoid, and (E iv) central Z ring not over a bilobed or single-lobed nucleoid. Arrows point to bright phase spores (white arrow), dark phase spores (grey arrow) and spore coats (white broken arrow). Images are DAPI pseudo-coloured in red (right), FtsZ-YFP pseudo-coloured in green (middle) and overlay of both with phase contrast (left). Scale bars are 2 μm.

Similarly, in the HPUra-treated triple deletion (*soj*, *spo0J* and *noc*) cells, the majority of nucleoids were either bilobed or spread with Z rings readily forming over these nucleoids at midcell. Midcell Z rings formed over bilobed (32%, Table 4.4, Figure. 4.7 F ii) or spread nucleoids (31%, Figure. 4.7 F iii) to almost equal levels. Similar to that of the *dna-1* background, very few single-lobed nucleoids were seen with Z rings forming either over the nucleoid or adjacent to a nucleoid that had moved off-centre. Thus, despite the absence of *noc* and *spo0J*, single-lobed nucleoids are generally associated with acentral Z rings.

Overall, these results show that the triple deletion of *soj-spo0J* and *noc* in the *dna-1* mutant and +HPUra-treated cells results in midcell Z ring formation over bilobed or spread nucleoids. Interestingly, most single-lobed nucleoids can still prevent midcell Z ring assembly, unless they have moved away from the cell center. Thus even in the absence of *soj-spo0J* and *noc,* there remains a unique factor that prevents Z rings from forming over the unreplicated nucleoid.

4.3 Discussion

Spo0J, as part of the ParABS system, plays an important role in the resolution and separation of sister chromosomes during the cell cycle (Ireton et al, 1994; Lee & Grossman, 2006; Marbouty et al, 2015; Wang et al, 2015). In Chapter 3, it was found that the absence of *spo0J* allows Z ring assembly at midcell when the early stages of DNA replication are blocked via *dna-1* or addition of HPUra. Furthermore, in these circumstances, midcell Z ring assembly appeared to correlate with a change in nucleoid morphology caused by the absence of *spo0J*. Thus the way in which the absence of *spo0J* appears to promote midcell Z ring positioning is through direct changes to nucleoid morphology that allows a decrease in DNA concentration at midcell. However, another possibility is that the absence of *spo0J* impacts the localization and/or function of Noc which normally binds the chromosome, thus affecting nucleoid occlusion and allowing for increased midcell Z ring assembly when the early stages of DNA replication are blocked. Here this latter possibility was investigated and found that Noc localisation, thus likely Noc activity, is not affected by the absence of *spo0J*. Furthermore, it was found that the combined deletion of *noc* and *spo0J* allows essentially wild-type levels of midcell Z ring assembly when the early stages of DNA replication are blocked. The implications of these findings in the context of the Ready-Set-Go model as well as the potential nucleoid occlusion function of Spo0J are discussed.

4.3.1 The complete restoration of midcell Z rings in *dna-1* and +HPUra in the absence of both *spo0J* and *noc* disproves the Ready-Set-Go model.

Tight coordination between the three key cellular processes (DNA replication. chromosome segregation and cell division) is essential for proper daughter cell generation. As such, eukaryotic cells have employed several stringent check points throughout the cell cycle to ensure the optimal conditions for progression to the next stage are met. If not, then the cell is restricted from progressing to the next stage (Elledge, 1996; Harashima et al, 2013; Hartwell & Weinert, 1989). The

eukaryotic can be broken down into four phases: The gap 1 (G1) phase, the synthesis (S) phase, the gap 2 (G2) phase and finally the mitosis (M) phase. Three major checkpoints exist within the cell cycle. One at G1 to assess DNA damage, one at G2 to ensure whole chromosome replication, and one at M ensuring that the sister chromatids are correctly attached to the spindle microtubules (Elledge, 1996; Harashima et al, 2013; Hartwell & Weinert, 1989).

In contrast, prokaryotes have long been thought to be significantly simpler in their architecture and cell cycle than that of the eukaryotic counterpart. Although clear coordination between DNA replication, chromosome segregation and cell division was evident in bacteria, there was no evidence of checkpoints or restriction points as seen in eukaryotic cells. That was up until a landmark study by Harry *et al.* that provided the first evidence of a DNA replication checkpoint linked to the progression of cell division in *B. subtilis* (Harry et al, 1999). It was found that if DNA initiation replication is blocked, Z rings would not form at the cell centre, suggesting that unless this initiation of DNA replication checkpoint is passed, then Z rings could not form at midcell. Continued work in this area found further evidence of a checkpoint system between DNA initiation replication and cell division where it was observed that the level of DNA initiation replication, up until DNA elongation, was coupled with the frequency of midcell Z rings (Moriya et al, 2010; Regamey et al, 2000). These collective observations thus led to the Ready-Set-Go model which postulates that the progression of initiation of DNA replication promotes Z ring formation at the cell centre (Moriya et al, 2010).

For years there was this idea that replication initiation was setting up the stage for the division site to form. However, the data presented here argues strongly against this idea of a checkpoint mechanism. As demonstrated in this chapter, Z ring positioning in the absence of *spo0J* and *noc* completely restores midcell Z ring assembly to wild-type levels regardless of the stage of initiation of DNA replication. This finding suggests that the progression of initiation of DNA replication is not linked to the maturation of the division site, and in turn, there is no checkpoint linking initiation of DNA replication and Z ring positioning. Instead there is always maximum potential for the Z ring to form at the midcell site, and the only factors

preventing utilization of the midcell site for Z ring assembly when initiation of DNA replication is blocked are Spo0J and Noc. Most importantly, at least in *Bacillus subtilis* and potentially other Firmicutes, there is no link between the stage of DNA replication and division site utilization. These findings are highly significant as they provide definite evidence that the Ready-Set-Go model, that is, the increase in midcell Z rings with the sequential progression of initiation, is incorrect.

An outstanding question that remains is what determines the division site if not initiation of DNA replication? Rodrigues *et al.* found that the Min system and Noc are not responsible for determining the division site in *B. subtilis*. When the nucleoids where allowed to resolve after a single round of DNA replication in the absence of both Noc and the Min system, Z rings still preferentially form at the cell centre. It was thus concluded that Min and Noc instead ensure the efficient utilisation of the midcell site at the right time (Rodrigues, 2011; Rodrigues & Harry, 2012). A similar midcell site control has been found in *E. coli* independent of that of SlmA, MinC and the SOS system (Cambridge et al, 2014). The data presented in this study suggests that there is some other factor independent of Spo0J, Noc and the early stages of DNA replication that defines the division site. For example, even in the earliest block to initiation (*dna-1* mutant), Z rings are able to effectively form at the cell centre to wild-type levels when *spo0J* and *noc* are absent. Additionally, in the absence of both *spo0J* and *noc* when initiation of DNA replication is blocked, a small number of cells (See Figure 4.7 E iv) are observed where Z rings have formed at the cell centre when the nucleoid had moved off centre, irrespective of its morphology (for example, bilobed nucleoid morphology). Overall, the data suggests that Spo0J and Noc do not determine the division site, and instead work in facilitating the efficient and timely use of the midcell "signpost". What defines the division site requires further investigations.

A question that also arises from the data presented here is how does the Min system play into this complete restoration of midcell Z ring assembly in the absence of *spo0J* and *noc*? The Min system, which is responsible for inhibiting Z ring assembly at the cell poles (Margolin & Rowlett, 2015), hence 'pushing' the Z ring towards the central position, is still active in these cells lacking *spo0J* and *noc* in this study, as there are

no polar Z rings observed. Is it possible that the loss of these two negative regulators (Spo0J and Noc), the Min system comes in to have a greater role in Z ring positioning? In other words, could there be a balancing act/homeostasis of the occlusive capabilities of the Min system and nucleoid occlusion (that is, Noc and Spo0J), such that the loss of *spo0J* and *noc* allows the Min system to 'push' the Z ring to the cell centre without inhibition? Indeed it has been found that when initiation of DNA replication was blocked in either the *dna-1* mutant or the thymineless condition, in the absence of both Noc and the Min system, less than 1% of Z rings formed at midcell. Instead Z rings formed acentrally (Rodrigues, 2011). This was in contrast with the principle of the Ready-Set-Go model which suggests that there should be some Z ring positioning potential with the absence of *noc.* The author thus speculated whether there were additional factors associated with the nucleoid independent of Noc. Given the data presented here, one such factor could be Spo0J. It would, therefore, be interesting to examine Z ring positioning when initiation of DNA replication is blocked in the absence of all three negative regulators (Min system, Noc and Spo0J). If removing all three components during a block to initiation of DNA replication still allows wild-type levels of Z ring positioning, then this would lend support to the idea of Spo0J playing a role in suppressing Z ring assembly during DNA initiation replication.

4.3.2 Noc-independent nucleoid occlusion

As examined in this chapter, in the *dna-1* mutant at the non-permissive temperature, Noc co-localisation with the nucleoid did not appear to be abolished regardless of the changes to nucleoid morphology seen in the absence of *spo0J*. However, this should in future be confirmed by comparing Noc localisation when Noc DNA-binding is lost. Nonetheless, the given results suggest that the effect Spo0J is having on Z ring positioning during initiation of DNA replication is separate to that of Noc. In addition, both blocks to initiation of DNA replication (*dna-1* temperature-sensitive mutant and addition of HPUra), not only resulted in a higher frequency of Z rings at midcell than that of individual mutants of *spo0J* or *noc*, but Z rings formed at midcell to essentially wild-type levels in the *spo0J noc* double mutant. These results suggest that during initiation of DNA replication there are two aspects required to prevent midcell Z ring

assembly: Noc and nucleoid morphology mediated by Spo0J. However, how nucleoid morphology in the absence of *spo0J* impacts Z ring positioning is unknown.

Although it was discussed in Chapter 3, it is worthwhile revisiting the idea of loss of chromosome inter-arm interactions in the absence of *spo0J*. The data suggests that when you lose these interactions you relieve the inhibition to midcell Z ring assembly. However, if the arms are together, it may activate an inhibitor of Z ring assembly. Whether this inhibitor is a protein or protein complex that requires the inter-arm interaction, or if it is solely about the DNA mass at the cell centre, is unknown but worthwhile exploring. Considering the former idea that inter-arm interactions allow for the production of an inhibitor, this data again raises the question of transertion. There is a possibility that, combined with the absence of *noc,* transertion activity between these bilobed or spread nucleoids and the cell membrane due the absence of *spo0J* is changed or relieved thus allowing Z rings to form at wild-type frequency over the unreplicated DNA at midcell.

Furthermore, such an inhibitor may be a Noc-independent nucleoid occlusion protein. Indeed the idea of a Noc-independent nucleoid occlusion protein has been put forward before. A study by Bernard *et al.* found that altering the nucleoid morphology by deleting *spo0J* during a replication fork arrest partially relieved this inhibition and allowed Z rings to form at midcell over the unreplicated DNA. The authors thus suggested that other Noc-independent nucleoid occlusion factors prevent Z rings from forming over unreplicated DNA in response to this replication roadblocks (Bernard et al, 2010). What was not considered however was that Spo0J could be this Noc-independent nucleoid occlusion protein.

4.3.2.1 *Could Spo0J have a nucleoid occlusion function?*

In the previous chapter, the possibility that perhaps Spo0J was affecting Z ring positioning by affecting Noc activity was raised (refer to Chapter 3, section 3.3.1.1). However, when initiation of DNA replication is blocked via *dnaA-1*, it was found that Noc localisation, and likely its binding and activity, is not affected in the absence of *spo0J*, as it still co-localises with the DNA. Instead it was found that regardless of the block to initiation of DNA replication, the combined absence of *spo0J* and *noc* results

in wild-type levels of midcell Z ring positioning. The findings presented here clearly demonstrate that there are two aspects to preventing Z ring assembly at the early stages of initiation of DNA replication. One is through Noc, and the other is through Spo0J. Thus the question then becomes, since Noc has been to some degree well described, how is Spo0J mediating this effect? Could Spo0J actually be a nucleoid occlusion protein?

This is an intriguing question; and there are several similarities between the two proteins to support this idea. Both Noc and Spo0J belong to the ParB family of proteins. Their genes are neighbours on the genome (the *soj-spo0J* operon and *noc* are separated by the *yyaB* gene), and their amino acid sequences are 35% identical. These two observations led to the hypothesis that they likely arose via gene duplication (Ogasawara & Yoshikawa, 1992; Sievers et al, 2002), potentially suggesting a level of redundancy between the two, an idea supported by finding that Noc is both involved in nucleoid occlusion and regulation of initiation of DNA replication in *S. aureus* (Pang et al, 2017). Noc binds specific locations along the chromosome with the exception of the terminus region (Wu et al, 2009), and prevents Z ring assembly over the unreplicated nucleoid with no effect to nucleoid morphology. Spo0J too binds to the chromosome in a specific manner although not to the same extent or to the same number of sites as Noc (74 Noc DNA-binding sites versus 10 Spo0J DNA-binding sites (Lin & Grossman, 1998; Wu et al, 2009)). It is, however, important to consider how nucleoid occlusion is defined. With the discovery of Noc and SlmA, a nucleoid occlusion protein has been defined by researchers as a DNA-binding protein analogous to Noc and SlmA that prevent Z ring formation over the nucleoid (Bernard et al, 2010; Wu & Errington, 2004). Spo0J does appear to fit this definition. The caveat however is that Spo0J also affects chromosome organisation, and how, if at all, this plays into the nucleoid occlusion function of Spo0J needs to be considered. Therefore, the potential nucleoid occlusion function of Spo0J is further explored in Chapter 5.

UTS
UNIVERSITY OF TECHNOLOGY SYDNEY

Chapter 5.
Investigating how Spo0J affects Z ring positioning when initiation of DNA of replication is blocked

i3 ithreeinstitute

5.1 Introduction

The chromosome organisation protein, Spo0J, has long been shown to be a multifaceted protein, with involvement in both the initiation of DNA replication and chromosome organisation in *B. subtilis* via its interaction with Soj and SMC, respectively. A clear observation made from the previous chapters is that Spo0J impacts nucleoid morphology to allow for an increase in midcell Z ring assembly when the initiation of DNA replication is blocked (either through the *dna-1* mutant or with HPUra treatment). Although the data points to the possibility that this is the only way in which Spo0J affects Z ring positioning, through its effect on nucleoid morphology, it is important to consider the possibility that it could still retain a nucleoid occlusion function. Unlike Noc, which does not impact nucleoid morphology, Spo0J could have a dual role; one in nucleoid morphology and the other in nucleoid occlusion, and its inhibitory effect on nucleoid occlusion could be partly masked by its effect on nucleoid morphology.

Because the function of Spo0J is so tightly linked to nucleoid morphology, likely through SMC, it is difficult to fully understand if Spo0J is a nucleoid occlusion protein because affecting the nucleoid morphology allows Z rings to form over the DNA at midcell. Therefore this link essentially masks the possible nucleoid occlusion function of Spo0J because it has such a huge impact on nucleoid morphology, which in turn impacts Z ring positioning. To dissect this role further, situations were identified in which the nucleoid morphology could be changed but without removing Spo0J within the cell.

One way to explore this is to generate point mutants in Spo0J that fail to recruit SMC thus affecting nucleoid morphology (Gruber & Errington, 2009). An alternative way to explore this is by removing SMC from the cell. In both situations, Spo0J is still present within the cell to perform, if it has one, its nucleoid occlusion function. Therefore, if Spo0J does have a nucleoid occlusion function, changing nucleoid morphology through means other than removing Spo0J, such as in the situations mentioned above, should not restore midcell Z ring assembly to the same degree as that of a *spo0J* null mutant.

Recently, Gruber *et al.* (2009) discovered point mutations in Spo0J which may aid in exploring the first possibility mentioned above. Through the selection of mutagenized cells that either retain or lose the pLOSS(*smc*$^{+}$) plasmid, Gruber *et al* elegantly identified point mutations separating the two functional domains of Spo0J: one that interacts with Soj and regulates initiation of DNA replication, and the other preventing SMC binding to the DNA and thus affecting chromosome organisation. Therefore, these point mutations were utilised in this chapter to explore the first situation described above. Additionally, Wang *et al* recently published a paper in which SMC was placed under an inducible degradation system to examine situations in which SMC no longer was present (Wang et al, 2014c). Strains and techniques from both studies were thus used in this chapter in order to further elucidate the potential nucleoid occlusion function of Spo0J during initiation of DNA replication.

5.2 Results

5.2.1 Investigating Z ring positioning in *spo0J* point mutations

5.2.1.1 *Construction and characterisation of spo0J point mutations*

a) Strain construction

To determine whether Spo0J may have a nucleoid occlusion role in addition to its role in chromosome organisation, six *spo0J* point mutation strains were used, three of which are defective in initiation of DNA replication (used as a control) and the other three defective in chromosome segregation (denoted henceforth as "*rep*" or "*seg*", respectively; (Gruber & Errington, 2009)). These were generously donated by Stephan Gruber and Jeff Errington (Newcastle University, UK). DNA from these strains was used to create strains containing the *spo0J* point mutants under control of the *soj-spo0J* native promoter, introduced into the *amyE* locus. The *spo0J* point mutations were introduced into a *Δspo0J* parent strain so that the ectopic *spo0J* point mutant was the only copy of *spo0J* within the genome. As such, donor chromosomal DNA from *spo0J*$^{rep1-3}$ (BSG253 to BSG255) and *spo0J*$^{seg1-3}$ (BSG256 to SG258) was transformed into recipient strains *Δspo0J* (SU769) and *dna-1 Δspo0J* (SU770) to create *Δspo0J spo0J*$^{rep1-3}$ and *spo0J*$^{seg1-3}$ (SU837 to SU842, respectively)

and *dnaA-1 ΔspoIIIJ spoIIIJ*$^{rep1-3}$ and *spoIIIJ*$^{seg1-3}$ (SU843 to SU848, respectively; see Materials and Methods Table 2.2). Transformants resistant to both chloramphenicol and kanamycin were further confirmed to possess the correct modifications via temperature sensitivity (where relevant), *amyE* locus disruption and PCR detection (data not shown; see Materials and Methods 2.2.1 and 2.5).

b) Sporulation characterisation

To further confirm that the relevant functions of SpoIIIJ were disrupted, strains were tested for their ability to sporulate (Figure 5.1). The point mutations affected in initiation of DNA replication (*spoIIIJ*^{rep}) are unable to sporulate due to over-initiation of DNA replication, while the chromosome segregation point mutations (*spoIIIJ*^{seg}) are unaffected in their ability to sporulate but show nucleoid morphology changes due to a loss in DNA binding and loss of SMC localisation at the origin (Gruber & Errington, 2009). Indeed, only the *spoIIIJ*^{rep} mutants were defective in sporulation, while the *spoIIIJ*^{seg} mutants were not, suggesting that the correct role of SpoIIIJ were affected.

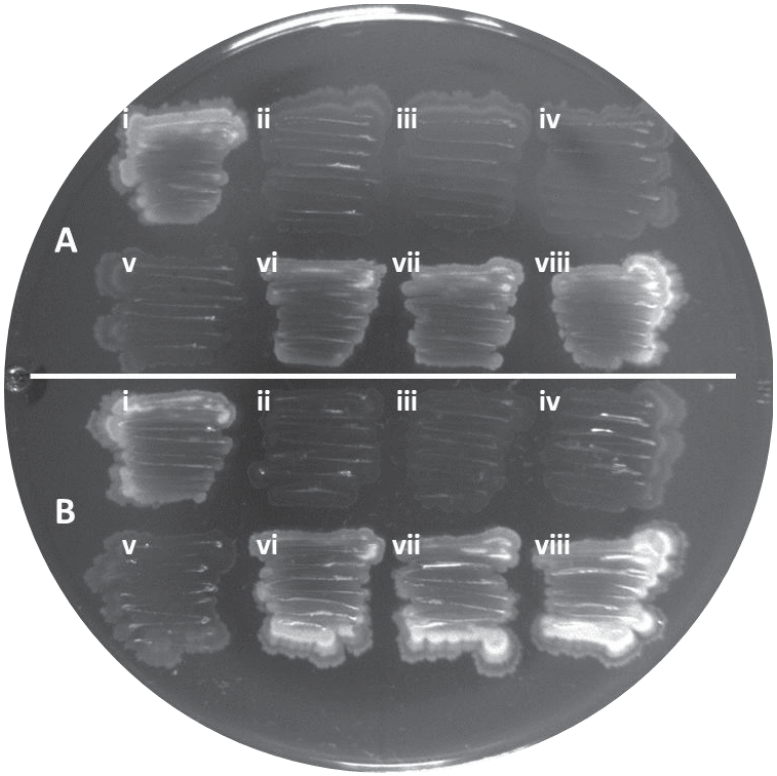

Figure 5.1: Sporulation ability of *spo0J* point mutations. Strains shown include (i) wild-type, (ii - iv) *spo0J*$^{rep1-3}$, (v) *Δspo0J* and (vi – viii) *spo0J*$^{seg1-3}$, and are of either the (A) non-temperature sensitive background (SU5; wild-type, or (B) temperature sensitive background (SU661; *dna-1*). Strains were grown on TBAB plates at 30°C for up to one week, until sporulation differences were observable on the plate. Translucent growth signifies no sporulation and hence cell death, while opaque growth demonstrates sporulation.

c) SMC condensin complex localisation characterisation

To ensure that these strains were behaving as previously reported, SMC localisation was also examined (Gruber & Errington, 2009). Spo0J bound at the *parS* sites adjacent to the *oriC* accounts for the majority of the recruitment of SMC condensin complex to the origin. This has been indicated by both SMC and ScpB co-localisation with Spo0J in exponentially growing cells (Gruber & Errington, 2009; Sullivan et al, 2009). As such, loss of *spo0J* leads to a significant reduction in SMC recruitment, with very few and/or faint SMC or ScpB foci observed. Therefore, it was important to confirm that SMC localisation was consistent with previously published observation in the conditions being tested here, that is, in the *dna-1* mutant. To confirm the loss

of SMC localization to the origin region in the chromosome segregation *spo0J* point mutations, strain SU852 (*scpB-yfp*; donated by D. Rudner; (Sullivan et al, 2009; Wang et al, 2015)), was used. This contains ScpB (one of three key components of the SMC condensin complex) tagged with a yellow fluorescent protein, which has been well characterised previously (Sullivan et al, 2009; Wang et al, 2015). Because the tagged version of ScpB is synthetically sick when combined with mutations in *spo0J* (Xindan Wang, personal communication), a second copy of *scpB* was additionally inserted in an ectopic region of the genome to overcome this. As such, chromosomal donor DNA of SU852 (*scpB-yfp)* and SU853 (*yhdG::scpAB*) was transformed into recipient strains wild-type (SU5), *dna-1* (SU661), *Δspo0J* (SU769), *dna-1 Δspo0J* (SU770), *Δspo0J spo0J*^{rep1} and *spo0J*^{seg2} (SU837 and SU841), and *dna-1 Δspo0J spo0J*^{rep1} and *spo0J*^{seg2} (SU843 and SU847). This created strains SU862 – SU869, respectively. Point mutation strains *spo0J*^{rep1} and *spo0J*^{seg2} were selected as representatives for each function of *spo0J*. These specific point mutation strains were selected above the others as these contained single point mutations within *spo0J*, while the other strains contained more than one point mutation within the gene (Gruber & Errington, 2009).

To visualise SMC localisation, specifically ScpB, the aforementioned strains were grown vegetatively at the non-permissive temperature to inactivate DnaB, and the samples collected for live-cell visualisation of ScpB-YFP. Distinct foci were observed overlaid with the nucleoid in both the *spo0J*$^{+}$ wild-type and *spo0J*$^{+}$ *dna-1* strains (Figure 5.2). As expected many foci can be seen in the wild-type cells undergoing active replication, and as expected a single focus is observed with that of the unreplicated nucleoid in *dna-1*. In contrast, no foci were visible in the absence of *spo0J* regardless of whether initiation of DNA replication was blocked. As expected, *spo0J*^{rep1} which appears to affect the DNA replication function of *spo0J* and not the chromosome segregation function, showed the distinct foci like that of the control strains. Also as expected, foci were absent in *spo0J*^{seg2} affecting chromosome organisation, suggesting a loss in SMC binding to DNA. However, a few faint foci were seen in these cells by observation (*spo0J*^{seg2}; denoted in Figure 5.2 by the white arrows) suggesting that SMC binding is not completely disrupted in this point

mutation, an observation also made by Gruber et al (Gruber & Errington, 2009). Overall, similar localisations of SMC were observed in these strains to that previously published (Gruber & Errington, 2009).

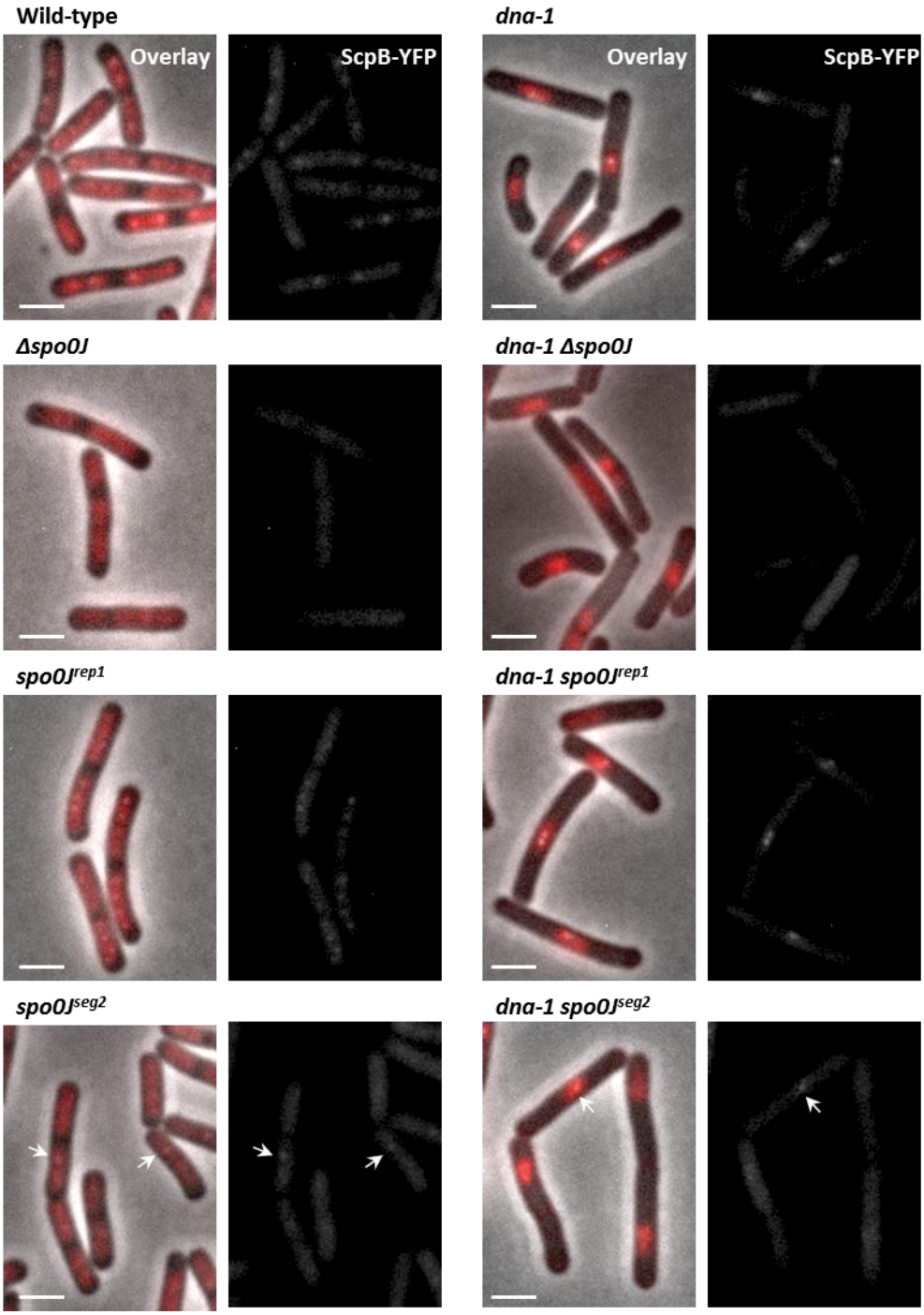

Figure 5.2: SMC and nucleoid co-visualisation in live *spo0J* point mutation vegetative cells at 48°C. Cells were grown vegetatively at 30°C to mid-exponential phase, and then shifted over to 48°C for 60 minutes to block initiation of DNA replication. Representative images above shown in each column: Overlay of phase-contrast, ScpB-YFP and DAPI (0.4 µg/mL), and ScpB-YFP only. White arrows denote potential ScpB-YFP foci in strains which are suggested to have lost SMC binding to DNA. Scale bar represents 2µm.

5.2.1.2 *Nucleoid morphology analysis of spo0J point mutations*

To examine whether these strains were affecting chromosome segregation, nucleoid morphology profiles were examined in the two classes of *spo0J* mutations (Figure 5.3). Only a small change in nucleoid morphology was observed in the *dna-1 spo0J*$^{rep1-3}$ mutants. This was somewhat expected as the DNA replication point mutations are thought to be defective in Spo0J interaction with Soj, and a deletion in *soj* in the *dna-1* mutant showed little difference in nucleoid morphology to that of the *dna-1* control. In contrast, in the chromosome organisation mutants (*spo0J*$^{seg1-3}$), there was an observable decrease in the predominant single-lobed nucleoid morphology from that seen in the *dna-1* Spo0J^{+} strain to a higher proportion of bilobed or spread nucleoids. These changes are reminiscent of the nucleoid morphology profile in the absence of *spo0J* when initiation of DNA replication is blocked. It was thus concluded that these mutants could be used to dissect the role of Spo0J in these studies.

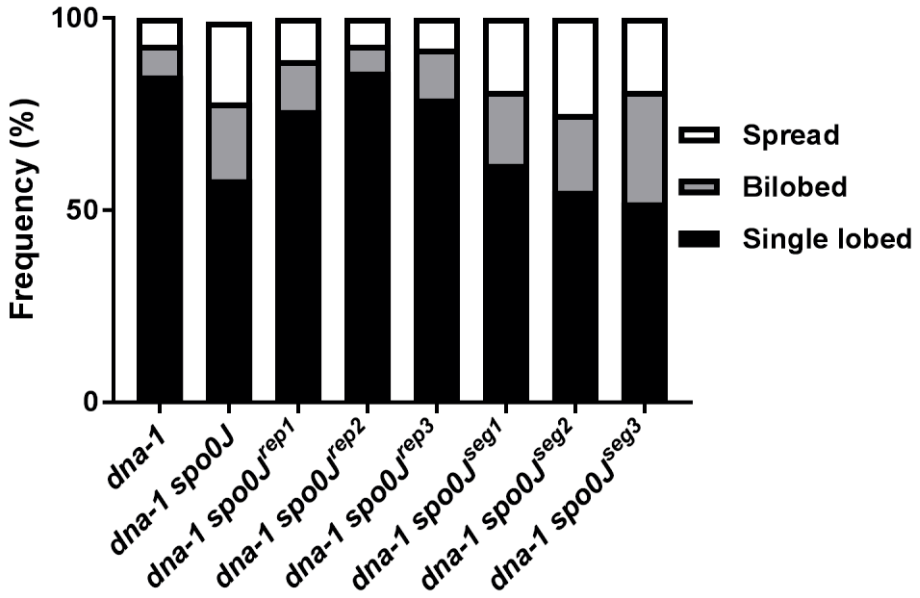

Figure 5.3: Nucleoid morphology in ethanol-fixed DAPI stained vegetative cells of *dna-1 spo0J* point mutation strains. Strains were grown in PAB to mid-exponential growth at the permissive temperature (30°C), shifted to the non-permissive temperature (48°C) for 60 minutes and then fixed and stained with DAPI. Bar graph shows the ratio of the three nucleoid morphology types in each strain. (n > 200).

5.2.1.3 *Z ring positioning analysis of spo0J point mutations*

To examine Z ring positioning in the six *spo0J* point mutations, Z rings were visualised in the following strains: wild-type (SU5), *dnaB-1*, *ΔspoJ*, *dnaB-1 ΔspoJ*, *spoJ*$^{rep1-3}$, *spoJ*$^{seg1-3}$, *dnaB-1 spoJ*$^{rep1-3}$ and *dnaB-1 spoJ*$^{seg1-3}$. All strains tested here for Z ring positioning in the *dnaB-1* mutant, as well as subsequent Z ring analysis experiments were tested at the permissive temperature to ensure all strains formed Z rings readily at the cell centre (data not shown). As expected, all strains formed Z rings predominantly at midcell like that of the wild-type. At the non-permissive temperature, in the wild-type and *spo0J* mutant, Z ring analysis (Table 5.1) revealed that the frequency of midcell Z rings is consistent with previous results (83% and 74% for wild-type and *spo0J*, respectively). Similarly, both *dnaB-1* and *dnaB-1 spo0J* strains formed Z rings at midcell to frequencies consistent with previous observations (9.5% and 39% midcell Z rings, respectively).

To dissect how Spo0J is affecting Z ring assembly, Z ring positioning was examined in the six point mutations. If the role of Spo0J in preventing Z ring assembly at midcell can be solely attributed to nucleoid morphology, then mutants in *spo0J* that affect SMC recruitment should have the same Z ring positioning phenotype as the *spo0J* null. Interestingly however, as seen in Table 5.1, none of the point mutations restored Z ring positioning in the *dnaB* mutant to the same extent as found in the complete absence of *spo0J*. All point mutations caused mid-range frequencies of midcell Z rings (~20%), in between the two control ranges of 9.5% and 39% (*dnaB-1* and *dnaB-1 spo0J*, respectively). In other words, there was essentially a two-fold difference in the frequency of midcell between the *spo0J* point mutations and *spo0J* null. This result argues that even when similar nucleoid morphologies are generated as that of a *spo0J* deletion strain, it is not sufficient to achieve the same midcell Z ring frequency as that of the *spo0J* null.

Table 5.1: Z ring positioning in *spo0J* point mutations at the non-permissive temperature (48°C).

Function	Strain	% Midcell Z rings [a]
Control	Wild-type	83 ±1
	dna-1	10 ±0.5
	Δspo0J	74 ±1
	dna-1 Δspo0J	39 ±1
DNA replication	*spo0J*^{rep1}	80 ±1
	spo0J^{rep2}	79 ±2
	spo0J^{rep3}	78 ±1
	dna-1 spo0J^{rep1}	20 ±0.5*
	dna-1 spo0J^{rep2}	19 ±2^*
	dna-1 spo0J^{rep3}	22 ±1.5
Chromosome organisation	*spo0J*^{seg1}	76 ±0.5
	spo0J^{seg2}	74 ±1
	spo0J^{seg3}	75 ±1.5
	dna-1 spo0J^{seg1}	22 ±2^
	dna-1 spo0J^{seg2}	19 ±0*
	dna-1 spo0J^{seg3}	17 ±1*

[a] All strains were grown vegetatively at 30°C in PAB to mid-exponential phase, shift to the non-permissive temperature (48°C) for 1 hour before being collected for IFM and subsequent Z ring analysis. Percentages shown are representative of two replicates. n >100 cells in each sample and replicate. Scatter plots not shown. ^Statistical significance to *dna-1*; *Statistical significance when compared with *dna-1 Δspo0J*. The Kolmogorov-Smirnoff test was used here and throughout this thesis, however, results from only these two comparisons are shown here for simplicity and for discussion in-text.

5.2.1.4 *Investigating Z ring positioning in the spo0J point mutations when noc is absent*

In section 5.2.1.3, it was shown that when initiation of DNA replication was blocked in the *dna-1* mutant, neither of the classes of *spo0J* mutants restored midcell Z ring formation to the same level as seen in the complete absence of *spo0J.* Instead, midcell Z ring frequencies of all six point mutations were around ~20 %, compared to the 40% of *dna-1 spo0J.* The range in which midcell Z ring frequencies were to fall to test the hypothesis was quite narrow (9.5% in *dna-1* vs. 39% in *dna-1 spo0J*). However, as shown in Chapter 4 (see section 4.2.2), when initiation of DNA replication is blocked in the absence of both *spo0J* and *noc*, there is complete restoration of Z ring positioning to wild type midcell Z ring frequencies (80%). Therefore, by exploring Z ring positioning in the *spo0J* point mutations when combined with a deletion of *noc* provides a greater phenotypic range of midcell Z ring frequencies to occur (e.g. ~10% in *dna-1* vs 81% in *dna-1 spo0J noc*), thus giving more confidence that Spo0J could indeed have a nucleoid occlusion function. Therefore, Z ring positioning of one point mutation of each class of *spo0J* mutation (*seg*^{1} and *rep*^{2}) was tested in the absence of *noc* in the *dna-1* mutant at the non-permissive temperature.

To examine Z ring positioning in the two *spo0J* point mutants (*spo0J*^{rep1} and *spo0J*^{seg2}) in the absence of *noc* and when initiation of DNA replication is blocked, donor chromosomal DNA from strain SU656 (*Δnoc*) was introduced into recipient strains *Δspo0J spo0J*^{rep1} and *spo0J*^{seg2} (SU837 and SU841), and *dna-1 Δspo0J spo0J*^{rep1} and *spo0J*^{seg2} (SU843 and SU847). This created strains *Δnoc Δspo0J spo0J*^{rep1} and *spo0J*^{seg2} (SU870 and SU871), and *dna-1 Δnoc Δspo0J spo0J*^{rep1} and *spo0J*^{seg2} (SU872 and SU873). Transformants resistant to kanamycin, chloramphenicol and tetracycline were further confirmed for *noc* and *spo0J* deletion via PCR and *dnaB* temperature sensitivity (where relevant). Before Z ring positioning was examined, nucleoid morphologies were first examined as a control. As expected, characterisation of nucleoid morphologies was consistent with previous results, such that the deletion of *noc* did not alter the nucleoid morphologies of the point mutation strains (Figure 5.4). The DNA replication initiation point mutation (*dna-1 noc spo0J*^{rep1}), affecting the

DNA replication function of Spo0J showed a similar nucleoid morphology profile to that of *dna-1* highlighting that this function of Spo0J is not involved in chromosome organisation. On the other hand, the chromosome segregation point mutation (*dna-1 noc spo0J*^{seg2}) confirmed the expected chromosome organisation changes with a profile similar to that of *dna-1 noc spo0J.*

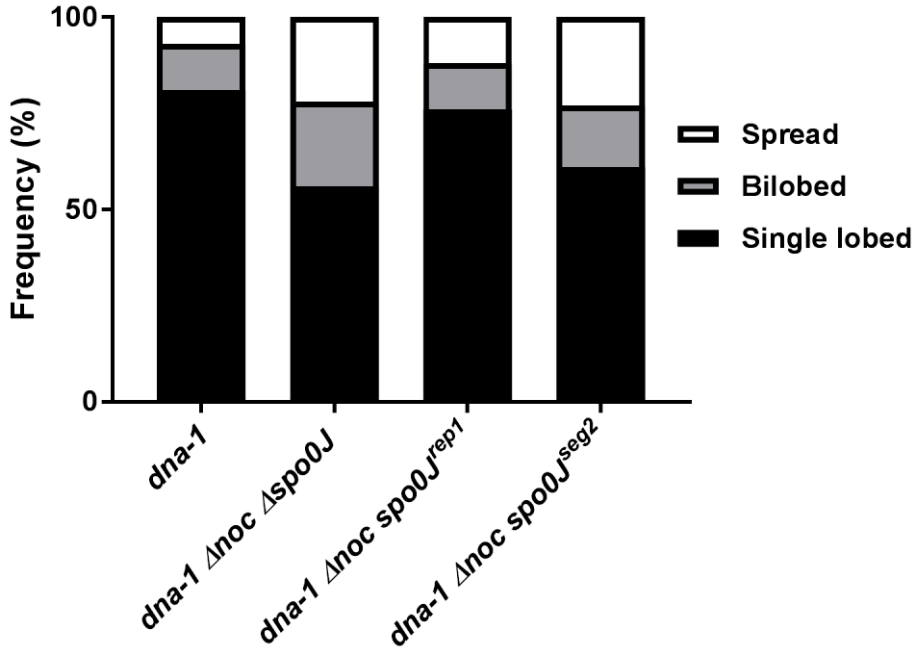

Figure 5.4: Nucleoid morphology in ethanol-fixed DAPI stained vegetative cells of *dna-1 Δnoc spo0J* point mutation strains. Strains were grown in PAB to the mid-exponential phase of growth at the permissive temperature (30°C), shifted to the non-permissive temperature (48°C) for 60 minutes and then fixed and stained with DAPI. Bar graph shows the ratio of the three classes of nucleoid morphology in each strain (n > 200).

In regards to Z ring positioning, control strains including wild-type, *dna-1*, *noc spo0J* and *dna-1 noc spo0J* displayed Z ring positioning profiles consistent with previous results (Figure 5.5 and Table 5.2, see also Chapter 4, section 4.2.3.1), such that Z ring predominantly formed at the cell centre in the control strains, with the exception of *dna-1* which had only 10% midcell Z rings. When replication is not blocked, both point mutation strains (*noc spo0J*^{rep1} and *noc spo0J*^{seg2}) had a preference for midcell Z ring formation (79% and 80%, respectively). When initiation of DNA replication was blocked via *dna-1* however, both *spo0J* point mutation strains (*dna-1 noc spo0J*^{rep1} and *dna-1 noc spo0J*^{seg2}) showed an increase in midcell Z ring frequencies (53% and 59%, respectively), however not to the extent of that of the double deletion, in which Z ring positioning was restored to wild-type levels (81%). As hypothesised, the additional loss of *noc* in the point mutations is not sufficient to restore Z ring positioning to that of a *Δspo0J* mutant. This data demonstrates that abolishing either role of Spo0J is not sufficient to allow for complete restoration of midcell Z ring assembly, especially in the *spo0J*^{seg2} mutant in which nucleoid morphologies are affected to the same extent as that of a *spo0J* null. Thus Spo0J could indeed have a nucleoid occlusion function.

Table 5.2: Analysis of Z ring positioning in the *dna-1* temperature-sensitive *spo0J* point mutants in the absence of noc at 48°C.

Strain	Average cell length (±SD) [a]	% Midcell Z rings [b]
Wild-type	3.83 ±0.91	88%
dna-1	3.23 ±0.60	10%
Δnoc Δspo0J	3.73 ±0.67	86%
dna-1 Δnoc Δspo0J	3.32 ±0.96	81%
Δnoc spo0J^{rep1}	3.81 ±0.74	79%
dna-1 Δnoc spo0J^{rep1}	**3.53 ±0.93**	**53%**
Δnoc spo0J^{seg2}	3.66 ±0.69	80%
dna-1 Δnoc spo0J^{seg2}	**3.40 ±0.99**	**59%**

[a] Table shows average cell length (±SD) and [b] percent of Z rings in the midcell range (0.45-0.5). Midcell is considered to be between 0.45 and 0.50 as this is where majority of Z rings form in wild-type cells. Scatter plots of Z ring positioning are depicted in Figure 5.5. See Figure 5.5 for strain growth conditions and midcell Z ring characterisation. See Table 4.1 for comparative midcell Z ring positioning in strains *dna-1 Δnoc* and *dna-1 Δnoc Δsoj.*

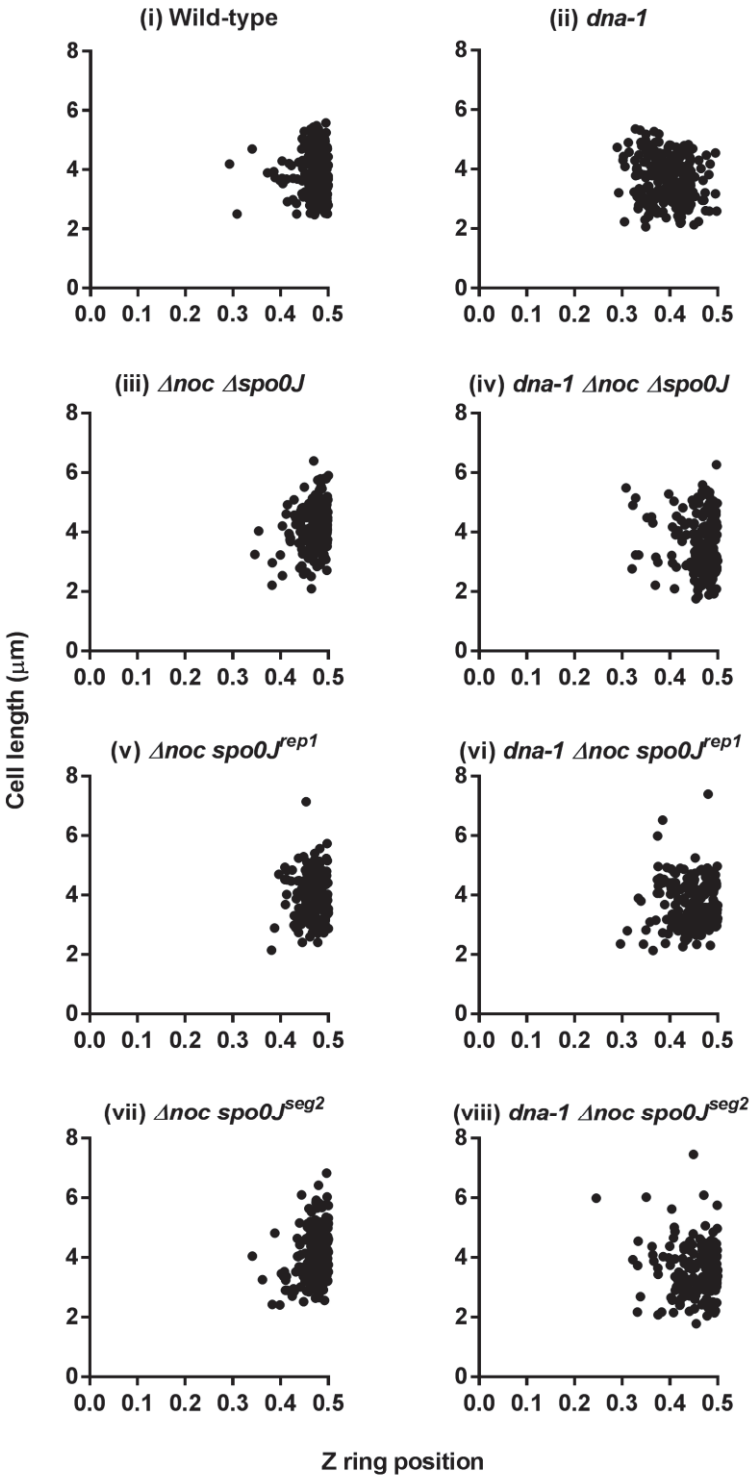

Figure 5.5: Z ring positioning scatter plot in *spo0J* point mutations when initiation of DNA replication is blocked and *noc* is absent. Strains were grown vegetatively at 30°C to mid-exponential phase, shifted to 48°C for 60 minutes, before being collected and prepared for IFM and Z ring analysis. Scatter plots showing Z ring positioning and average cell length (±SEM) of vegetatively grown fixed cells of (i) wild-type (SU5), (ii) *dna-1* (SU661), (iii) *Δnoc Δspo0J* (SU827), (iv) *dna-1 Δnoc Δspo0J* (SU828), (v) *Δnoc spo0J*^{rep1} (SU870), (vi) *dna-1 Δnoc*

spo0J^{rep1} (SU872)**,** (vii) *Δnoc spo0J*^{seg2} (SU871)*,* and (viii) *dna-1 Δnoc spo0J*^{seg2} (SU873). Z ring position is determined by measuring the distance from the Z ring to the nearest cell pole and dividing this value by the cell length, with 0.5 being exactly midcell. A Z ring is considered to be at midcell if it was positioned within the range of 0.45-0.50, as this is where most Z rings form in the wild-type strain. n > 200. See Table 5.2 for midcell Z ring frequencies and average cell lengths (±SD) for each strain.

5.2.2 Z ring positioning analysis in the absence of SMC

5.2.2.1 *Characterisation of the SMC-degron system*

As detailed in section 5.2.1.2, when initiation of DNA replication was blocked in the *spo0J* point mutations, midcell Z ring positioning was not restored to the same level as the *spo0J* mutant, despite the fact that nucleoid morphologies of the *spo0J*^{seg} mutants were the same as that of the *spo0J* mutant. An independent way to confirm that Spo0J could have an effect on Z ring positioning beyond its role in initiation and segregation, nucleoid morphologies were changed by abolishing SMC during a block to initiation of DNA replication via the inactivation of DnaB.

Loss of SMC in *B. subtilis* leads to synthetically sick cells (Britton et al, 1998; Gruber & Errington, 2009), such that the deletion of *smc* is not lethal, but instead leads to non-lethal growth impairments (Nijman, 2011). Therefore, to overcome this, conditional mutants of *smc* must be used. Two referenced methods to explore *smc*- situations are via either the use of a temperature sensitive *smc* mutant or inducible degradable alleles of SMC. As documented in Wang *et al.* 2014, both systems are equally valid to carry out *smc*- investigations, where both systems lead to similar phenotypes (Wang et al, 2014c). In our investigations, the *dnaB* mutant is also temperature sensitive, therefore the *smc*(ts) mutant was incompatible with our *dnaB*(ts) mutant when considering the conditional control experiments. Hence the SMC-degron system was used. The SMC-degron strain contains the xylose-inducible *E. coli* adaptor protein SspB which targets SsrA-tagged proteins (in this case SMC possesses the SsrA tag) to the ClpXP protease leading to degradation of the SsrA-tagged protein (Wang et al, 2014c).

To create the SMC-degron strains to examine Z ring positioning, chromosomal DNA from donor strain SU849 (donated by Xindan Wang and David Rudner), was introduced into recipient strains wild-type (SU5) and *dnaB-1* (SU661) to create strains *smc-ssrA* (SU850) and *dnaB-1 smc-ssrA* (SU851). Kanamycin and erythromycin resistant strains were also checked for temperature sensitivity (where relevant), PCR detection and loss of viability on agar plates containing the inducer xylose (1% v/v; data not shown).

To keep the experimental conditions consistent, vegetative growth conditions were used in which the four strains of interest (wild-type, *dnaB-1*, *smc-ssrA* and *dnaB-1 smc-ssrA*) were grown at 30°C to mid-exponential stage and shifted to 48°C for a further hour before being collected for IFM. Fifteen minutes prior to the shift to the non-permissive temperature, the media was supplemented with xylose (1% v/v) to induce the degradation of SMC. Additional samples were also collected at this point for Western blotting and immunodetection (data not shown) to confirm that SMC is degraded to the maximum level.

When cells were examined under the microscope, abnormal growth was observed such that a significant portion (27%) of the cells had an unusual and obvious bulging formation at one end (Figure 5.6). A portion of the cells had also lysed. This effect was also observed in the non-temperature sensitive strain at the higher temperature suggesting that it was not the combination of *dnaB-1* and *smc-ssrA*, but the duration of incubation to induce SMC depletion that was causing this abnormal phenotype. The conditions of the experiment could not however be altered as it was necessary to ensure that SMC was degraded before inducing DnaB inactivation to be able to conclude that any changes to Z ring positioning in these cells was due solely to the absence of SMC and not the combined gradual inactivation of both DnaB and SMC.

In an attempt to overcome this issue, the spore outgrowth system was used. Spores of these strains were germinated and grown out in GMD in the presence or absence of xylose at 34°C for 20 minutes before being shifted to 48°C for a further 90 minutes and collected for IFM. Additional samples were also collected at this point to ensure SMC degradation.

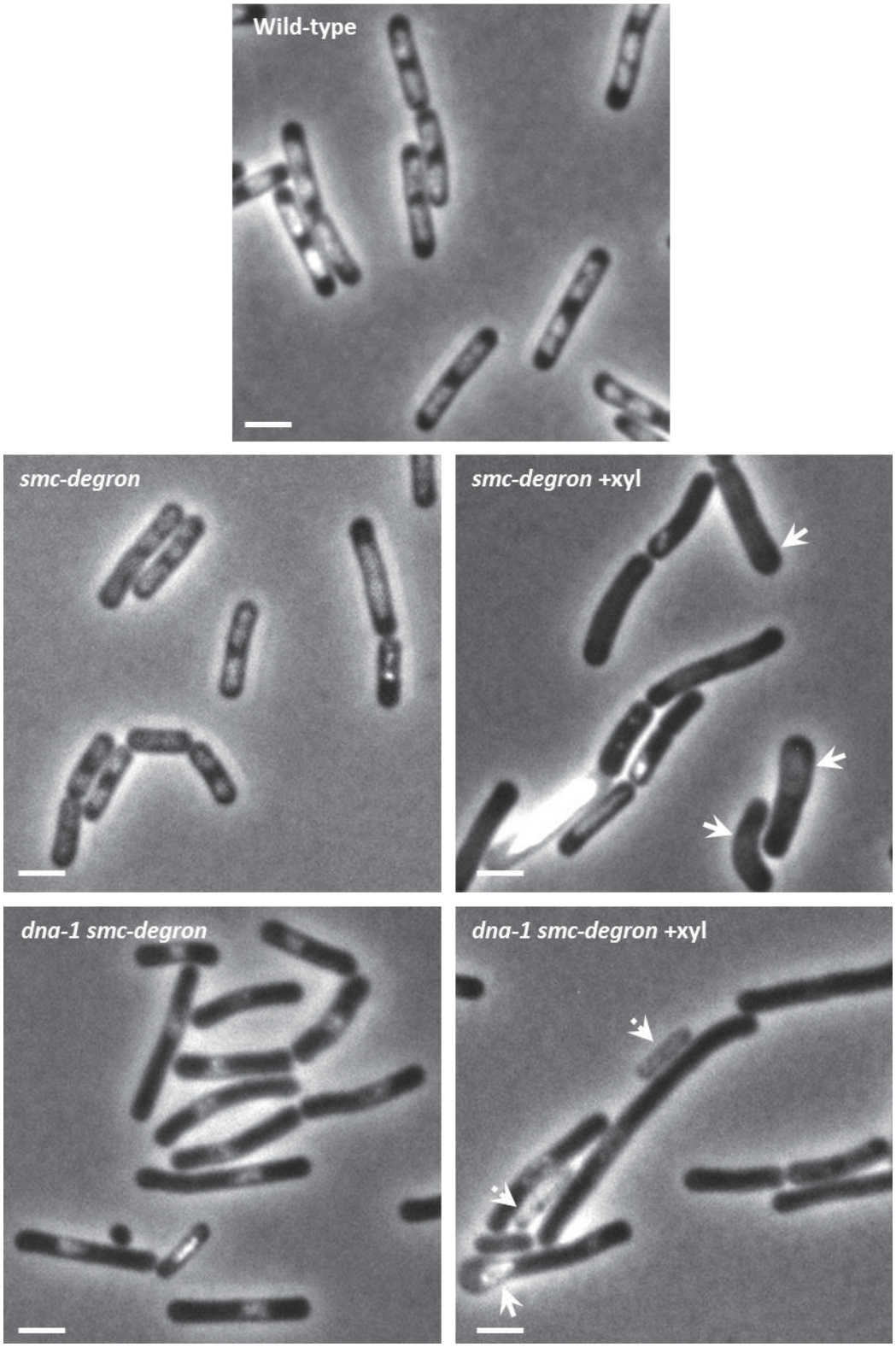

Figure 5.6: Different cell morphologies observed when SMC is depleted and initiation of DNA replication is inhibited by the *dna-1* mutation. DAPI and phase-contrast overlaid images are shown. Cells were grown vegetatively in PAB at 30°C to mid-exponential phase before being shifted to 48° for 1 hour and collected for live visualisation. Those denoted with

"+xyl" had 1% (v/v) xylose added to the media 15 minutes prior to the shift to 48°C. White broken arrows denote cell lysis and white full arrows denote cell bulging. Scale bar represents 2μm.

In the presence of 1% (v/v) xylose, Western blot analysis (See Materials and Methods 2.8) confirmed that *smc-ssrA* and *dna-1 smc-ssrA* contained approximately 10% of the SMC present in the same strains grown in the absence of xylose. This is shown in Figure 5.7. This is the maximum level of degradation of SMC possible (personal communication with Xindan Wang). Overall, inducing SMC degradation via the addition of xylose at the onset of spore germination depletes SMC to the maximum level and is appropriate for use in examining the effect of Z ring positioning when SMC is depleted and initiation of DNA replication is blocked.

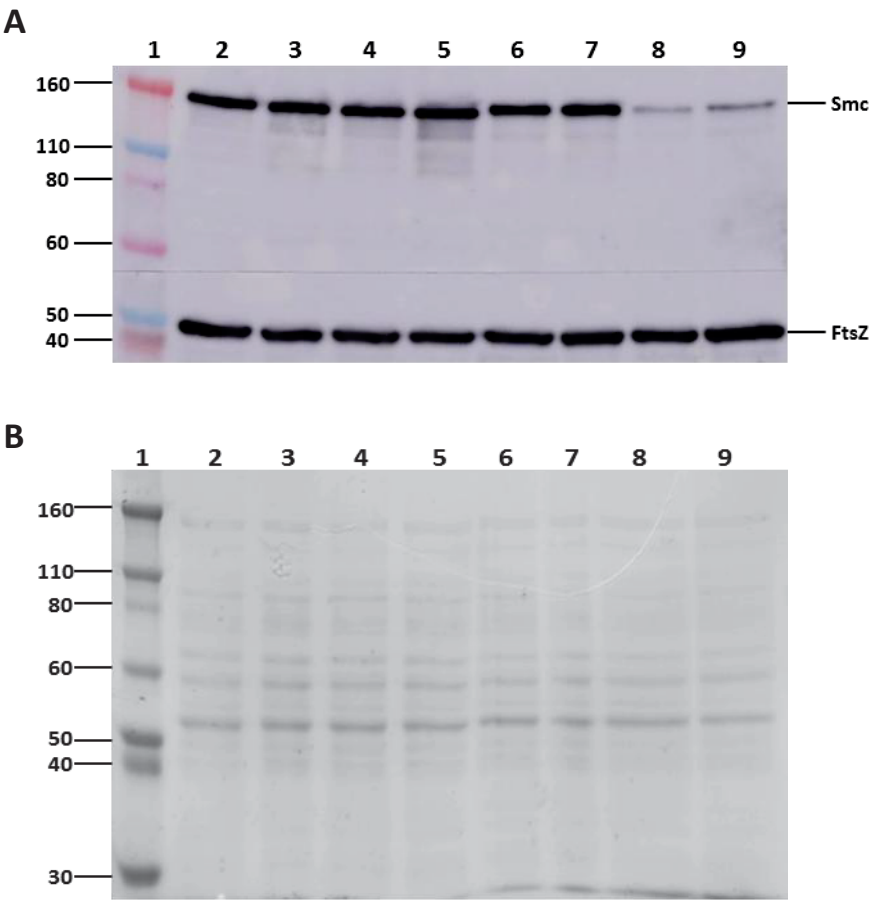

Figure 5.7: Western analysis of SMC levels in the wild-type and SMC-depletion germinated spore cells. Spores were germinated in GMD at 34°C for 20 minutes, and then shifted to 48°C for a further 90 minutes before being collected and cell lysates prepared. Spores were grown in the absence or presence of xylose (1% v/v). (A) Immunoprobing for protein detection using anti-*smc* antibodies (1:10,000) and anti-FtsZ (1:10,000) as a normalizing control; and (B) The corresponding Coomassie-stained protein gel to demonstrate equal loading of samples. The lanes in both A and B pertain to: **(1)** molecular weight markers with the numbers on the side indicating protein sizes in kDa; **(2)** the wild-type strain (SU5); **(3)** the *dna-1* mutant (SU661); **(4)** the wild-type strain in the presence of xylose (SU5); **(5)** the *dna-1* mutant (SU661) in the presence of xylose; **(6)** the wild-type strain containing the *smc-degron* system (SU850); **(7)** the *dna-1* mutant strain containing the *smc-degron* system (SU851); **(8)** the wild-type strain containing the *smc-degron* system in the presence of xylose (SU850); **(9)** the *dna-1* mutant strain containing the *smc-degron* system in the presence of xylose (SU851).

5.2.2.2 *Nucleoid morphology*

Like Spo0J, loss of SMC has been shown to result in morphological changes to the nucleoid. Therefore, to confirm that such changes are also occurring in the absence of SMC following induced degradation of SMC, nucleoid morphologies were examined. Nucleoid morphologies of fixed outgrown spores under the same conditions were also observed (Figure 5.8). Consistent with previous findings, *dna-1* cells possessed predominantly single-lobed nucleoids. Similarly, *dna-1 smc-ssrA* displayed mostly single-lobed nucleoids. Examining the changes to nucleoid morphology when initiation of DNA replication is blocked and SMC is degraded (*dna-1 smc-ssrA*) however revealed a significant decrease in single-lobed nucleoids towards more predominant population of bilobed or spread nucleoids, even more so than that seen in the absence of *spo0J*. This trend is the same as that seen in *dna-1 spo0J* highlighting that similar changes to the nucleoid are occurring in the absence of either *smc* or *spo0J.*

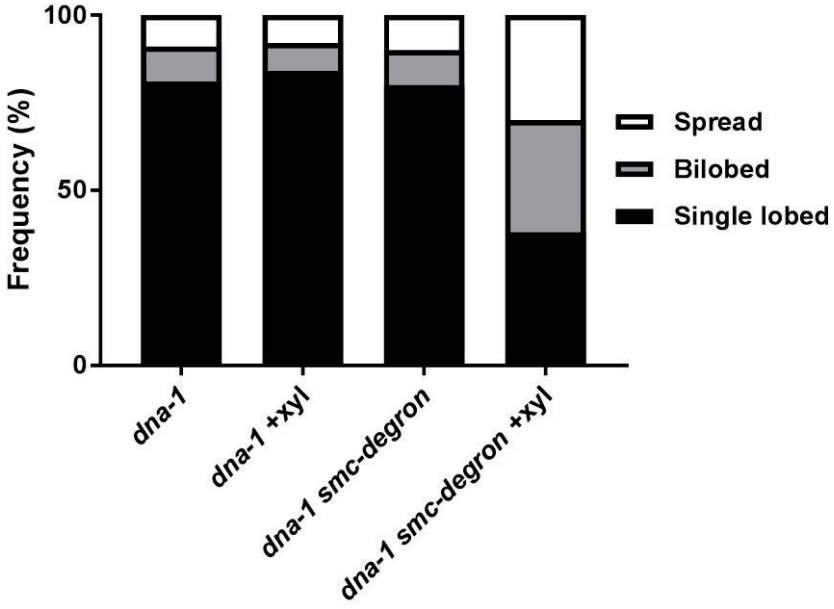

Figure 5.8: Nucleoid morphology in ethanol-fixed, DAPI stained, SMC-depletion germinated spore cells. Spores were germinated in GMD at 34°C for 20 minutes, and then shifted to 48°C for a further 90 minutes before being collected and prepared for fixation. Spores were grown in the absence or presence of xylose (1% v/v). Bar graph shows the ratio of the three nucleoid morphology types in each strain. (n > 200). See Chapter 3, section 3.2.2 for the nucleoid morphology profile observed in *dna-1 spo0J*.

5.2.2.3 *Z ring positioning*

To ensure that the addition of the SMC-degron system into the genome was not having any adverse effects to the strains, two controls were performed. Firstly, it was tested whether the addition of xylose to germinating spores not containing the SMC-degron did not affect Z ring positioning. Indeed, in the wild-type or *dna-1* cells, the addition of xylose did not affect Z ring positioning (wild-type: +xylose 89%, - xylose 87%; *dna-1:* +xylose 10%, - xylose 10% midcell Z rings; Figure 5.9 i – iv, Table 5.3). Secondly, it was tested whether the strains containing the SMC-degron were not affected in Z ring positioning if the system was not induced (no addition of xylose). Again, Z ring positioning was as expected in both strains if xylose was omitted (*smc-ssrA* 80%, and *dna-1 smc-ssrA* 11% midcell Z rings; Figure 5.9 v and vi).

In the presence of xylose to induce the degradation of SMC, a small decrease in midcell Z ring frequency was observed in *smc-ssrA* when grown in the presence of xylose (71%; Figure 5.9 vii). This decrease was expected, as like that in the absence of *spo0J*, there is a significant increase in the occurrence of minicells, indicative of Z ring mispositioning in a proportion of the cell population. Most interestingly, Z ring positioning is only partially restored (22%; Figure 5.9 viii) when SMC is degraded and initiation of DNA replication is blocked via *dna-1.* These results suggest that the low frequency of SMC localisation in the *dna-1 spo0J*^{seg2} mutant seen in section 5.2.1.3 cannot explain why so few midcell Z rings form in these cells. Furthermore, considering the *dna-1* mutant at the non-permissive temperature, the degradation of SMC does not lead to the same level of midcell Z ring frequency as seen in the absence of Spo0J (22% versus 40% midcell Z rings, respectively). This suggests that the 40% midcell Z rings observed in the *dna-1 Δspo0J* mutant results from the absence of *spo0J* and might not be just the loss of SMC recruitment. Furthermore, during the block to initiation of DNA replication, nucleoid morphology has changed in the absence of *smc* to the same extent as that of a *spo0J* null yet midcell Z rings are not restored to the same level. Could this be because Spo0J is still present in these cells in the absence of *smc*?

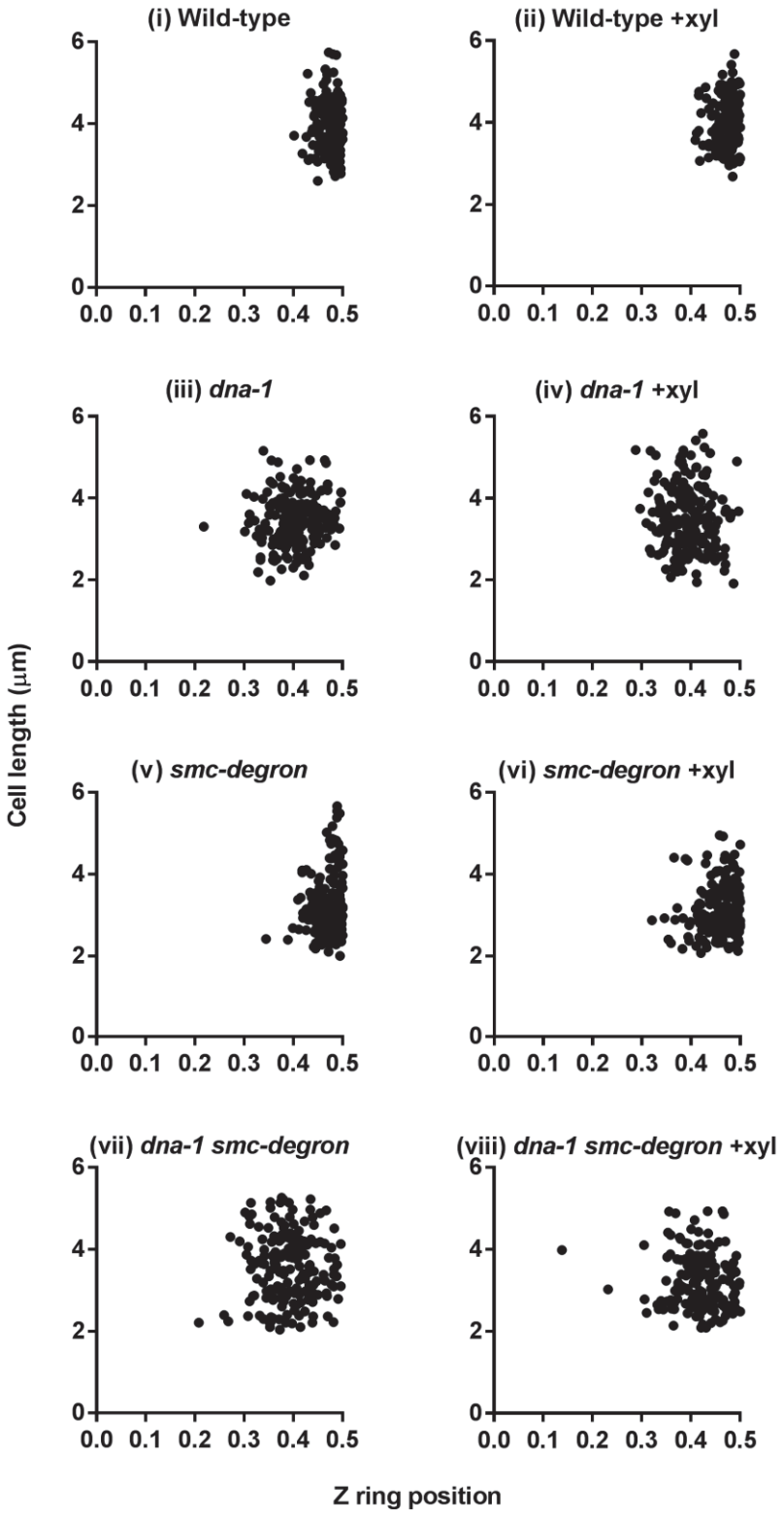

Figure 5.9: Z ring positioning when initiation of DNA replication is blocked during spore outgrowth in the *dna-1* temperature-sensitive SMC-depleted mutant. Spores were germinated in GMD in the absence or presence of xylose (1% v/v) for 20 minutes at the permissive temperature (34°C), then shifted to the non-permissive temperature (48°C) for a

further 90 minutes before being collected for IFM. Scatter plots showing Z ring positioning and average cell length (±SEM) of vegetatively grown fixed cells of (i) wild-type (SU5), (ii) wild-type + xylose, (iii) *dna-1* (SU661), (iv) *dna-1* + xylose, (v) *smc-degron* (SU850), (vi) *smc-degron* + xylose**,** (vii) *dna-1 smc-degron* (SU851)*,* and (viii) *dna-1 smc-degron* + xylose. Z ring position is determined by measuring the distance from the Z ring to the nearest cell pole and dividing this value by the cell length, with 0.5 being exactly midcell. A Z ring is considered to be at midcell if it was positioned within the range of 0.45-0.50, as this is where most Z rings form in the wild-type strain. n > 200. See Table 5.3 for midcell Z ring frequencies and average cell lengths (±SD) for each strain.

Table 5.3: Analysis of Z ring positioning in the *dna-1* temperature-sensitive SMC-depleted mutant at the non-permissive temperature.

Strain [a]	Average cell length (±SD) [b]	% Midcell Z rings [c]
Wild-type	3.30 ±0.42	87%
Wild-type +xyl	3.28 ±0.49	89%
dna-1	3.23 ±0.61	10%
dna-1 +xyl	3.21 ±0.66	10%
smc-degron	3.10 ±0.50	80%
smc-degron +xyl	3.13 ±0.68	71%
dna-1 smc-degron	3.28 ±0.70	11%
dna-1 smc-degron +xyl	3.25 ±0.70	22%

[a] Addition of xylose (denoted by +xyl) was used to induce the degradation of SMC where relevant. [b] Table shows average cell length (±SD) and [b] percent of Z rings occurring into the midcell range (0.45-0.5); [c] Midcell is considered to fall between 0.45 and 0.50 as this is where majority of Z rings form in wild-type germinated spore cells. Scatter plots of Z ring positioning are depicted in Figure 5.9. See Figure 5.9 for strain growth conditions and midcell Z ring characterisation.

5.3 Discussion

The previous chapters of this thesis have shown that during initiation of DNA replication, the absence of *spo0J* leads to an increase in midcell Z ring assembly. These regulatory effects on Z ring positioning are in addition to the nucleoid occlusion activity of Noc. Interestingly, the restoration of midcell Z ring assembly in the absence of *spo0J* when initiation of DNA replication is inhibited coincided with a change in nucleoid morphology to one of a bilobed or spread morphology. These observations raise the question whether these changes to nucleoid morphology are the sole reason for the increase in midcell Z rings, or could Spo0J possess an additional nucleoid occlusion function beyond its role in chromosome organisation? To explore this, mutants of *spo0J* that are specifically defective in SMC recruitment created by Gruber *et al.* were studied (Gruber & Errington, 2009). It was found that although these mutants produce similar nucleoid morphologies to that of the *spo0J* null, they were unable to restore midcell Z ring frequencies to the same level as a *spo0J* null suggesting that the nucleoid occlusion role of Spo0J is not only through its role in chromosome segregation through recruitment of SMC. As an additional test for this hypothesis that Spo0J could have an additional role in nucleoid occlusion beyond its role in changing nucleoid morphology, Z ring positioning was examined during the degradation of SMC. Under these conditions it was found that degradation of SMC produced nucleoid morphologies that were more severe than that of the *spo0J* null; that is, a higher frequency of bilobed or spread nucleoids. Even though these nucleoid morphology results were consistent with a decrease in DNA at midcell, Z rings still could not readily form at midcell in the absence of SMC thus suggesting that Spo0J has an additional role in nucleoid occlusion that is independent of its role in changing chromosome organisation through SMC.

5.3.1 Further testing the nucleoid occlusion function of Spo0J

The data presented in this chapter supports the idea that Spo0J has a nucleoid occlusion function. Interestingly if it does indeed have this role, it is different from the one of Noc because Spo0J is multifaceted in its function within the cell.

Unmasking this potential role of Spo0J has been difficult because of this multifaceted nature of Spo0J, but now we have data to support the idea of an additional nucleoid occlusion role for Spo0J. However, further experiments are required to provide support for this hypothesis. These are discussed below.

5.3.1.1 *Test a SMC-degron noc null strain*

Although the difference in midcell Z ring frequency in the *dna-1* mutant is two-fold between the *spo0J* null and when SMC is depleted (40% and 22% midcell Z rings, respectively), it would be ideal to validate these results in a range in which midcell Z ring frequencies can fall. Therefore the priority experiment to perform to further validate that the degradation of SMC indeed does not affect Z ring positioning to the same extent is to examine a combined *Δnoc smc-degron* strain in the *dna-1* mutant background. Like the point mutations in section 5.2.1.4, the deletion of *noc* from the *dna-1 smc-degron* strain would provide this greater range. If like the point mutations (*spo0J*$^{seg1\text{-}3}$), Z ring positioning is not restored to the same levels as that of the *spo0J noc* double knockout (80% midcell Z rings), then it would lend further support for the idea that Spo0J has a nucleoid occlusion function in addition to its effect on nucleoid morphology.

There is however a caveat to the SMC-degron system used here. A small level of SMC remained in the cells after maximum induction of degradation. Ideally, these experiments should be complemented with situations in which SMC is completely removed or inactivated, for example via a temperature sensitive mutant of SMC treated with HPUra (Wang et al, 2014c).

5.3.1.2 *Over-expression of Spo0J*

Over-expression of a protein of interest is one of the most common ways to gain insight into whether that protein may play a role in a key cellular process such a cell division. For example, Wu et al first gave reason to suggest that Noc plays a role in cell division regulation due to observed cell filamentation when Noc was over-expressed (Wu & Errington, 2004). If, like Noc, Spo0J is indeed possesses a nucleoid occlusion function, then a similar approach can be used to explore this aspect of Spo0J. As such, to investigate whether Spo0J does play a role in cell division, cell

morphology effects when Spo0J is over-expressed should be examined. Since Spo0J is well conserved and over-expression of ParB (Spo0J) in *Mycobacterium tuberculosis* has shown a clear defect in cell cycle progression (Maloney et al, 2009), it is likely that over-expression of Spo0J in *B. subtilis* wild-type cells would have a similar effect. However to more specifically validate the nucleoid occlusion function of Spo0J, effects to cell division and Z ring positioning should be examined in the thymineless block to initiation of DNA replication. The thymineless condition is one of the blocks to initiation of DNA replication that was investigated in previous studies leading to the Ready-Set-Go model (Moriya et al, 2010). This condition blocks initiation of DNA replication at the point of complete replisome assembly and at the start of DNA synthesis. This condition when examining Z ring positioning allows for almost wild-type levels of midcell Z ring assembly (Moriya et al, 2010). If Spo0J is acting as a nucleoid occlusion protein then over-expression of Spo0J in this condition in vegetatively growing cells should result in acentral Z rings and filamentous cells. However, there are caveats in that Spo0J plays a role in chromosome organisation and initiation of DNA replication. Therefore, it would be ideal to perform the over-expression using a combination of the point mutations used in this chapter. This would result in Spo0J mutant that lacks either of its known roles, and thus only maintaining its potential nucleoid occlusion role. Would this Spo0J mutant result in cell division inhibition? If so, this would support the idea that Spo0J has an additional role in nucleoid occlusion beyond its role in nucleoid morphology.

5.3.1.3 *Identify Spo0J point mutations that affect its predicted nucleoid occlusion function*

The potential nucleoid occlusion function of Spo0J can be investigated through identifying point mutations that lose this function. Several methods are commonly used to introduce mutations into a gene of interest including the use of mutator strains (Muteeb & Sen, 2010), error-prone PCR (McCullum et al, 2010), transposon mutagenesis (Wilson & Szurmant, 2011) or UV irradiation (Tanooka et al, 1978) to name a few. To screen for these point mutations, a similar approach to that described by Adams *et al.* can be used (Adams et al, 2015). A double deletion of *noc* and *minCD* in *B. subtilis* is temperature sensitive such that the strain can grow at the

permissive temperature (30°C) but unable to grow at 48°C. If Spo0J does have a nucleoid occlusion function like Noc, then it can be hypothesised that a point mutation of *spo0J* affecting this nucleoid occlusion function combined with a deletion of *minCD* will lead to a similar temperature sensitive phenotype. If such a point mutation is successfully identified then during initiation of DNA replication, no significant changes to nucleoid morphology should be observed, such that nucleoids remain in a single-lobed morphology, however, Z rings should be able to form over these nucleoids irrespective of the morphology.

5.3.1.4 *Identify potential interaction proteins*

A caveat of the above suggestion is the assumption that the nucleoid occlusion function is encoded on Spo0J. However it is possible that the potential nucleoid occlusion function of Spo0J is indirect such that Spo0J recruits a novel nucleoid occlusion protein to its location on the DNA. In turn, loss of Spo0J results in loss of recruitment of this third unidentified interaction partner. There are a vast number of *in vitro, in vivo* and *in silico* methods used to identify unknown interaction proteins (Blikstad & Ivarsson, 2015; Zhou et al, 2016). If this were to be successful, not only would it identify another regulatory role for Spo0J, but also identify a novel potential nucleoid occlusion protein.

UNIVERSITY OF TECHNOLOGY SYDNEY

Chapter 6.
General Discussion

ithreeinstitute

Correct positioning of the division machinery in coordination with DNA replication and segregation is of utmost importance for all organisms. Therefore, it is of no surprise that this has been an area of great interest over the past few decades. What still eludes us however is how do bacteria precisely position the Z ring at midcell? This thesis investigates a long-standing model of how Z ring positioning is linked to DNA replication initiation. Through the study of Spo0J, a potential new role for Spo0J in the regulation of Z ring positioning has been revealed, highlighting its multifaceted role in chromosome replication, segregation and cell division. In addition, these investigations into the regulatory role of Spo0J in Z ring positioning have brought into question the validity of this long-standing model linking DNA replication initiation and Z ring positioning.

6.1 Z ring positioning is not linked to the early stages of DNA replication

Research over the past two decades looking into how bacteria position their division site lead to the idea that there is a link between the early stages of DNA replication and Z ring positioning in *B. subtilis* (Harry et al, 1999; Moriya et al, 2010; Regamey et al, 2000). These observations led to the Ready-Set-Go model proposing that the progression of initiation of DNA replication, leading up to the assembly of the replication machinery, coincides with an increase in potential to form a Z ring at midcell (Moriya et al, 2010). Importantly, this is observed only when the nucleoid occlusion protein, Noc, is absent. Furthermore, different nucleoid morphologies (including single-lobed and bilobed nucleoids) were observed in the four DNA replication inhibition treatments used to support this model and these were seen to correlate with the formation of Z rings at midcell. That is, Z rings were able to more readily form at the cell centre when the nucleoid had a bilobed or spread morphology. However, in one of the replication blocks applied to study this link, the temperature-sensitive *dna-1* mutant, never results in Z rings at midcell irrespective of the nucleoid morphology. This observation suggested that mechanisms apart from Noc were at play to prevent Z rings from forming over the unreplicated nucleoid.

Collectively, the leading question was how does this link between DNA replication and positioning the division site at midcell come about? Given the changes to nucleoid morphology and the close relationship between DNA replication and chromosome segregation, it was likely that Soj and Spo0J could play into this link.

For many years it has been known that ParB (Spo0J) of the ParABS system plays a role in initiation of DNA replication and chromosome segregation in a number of bacteria (Badrinarayanan et al, 2015; Donczew et al, 2016; Donovan et al, 2010; Livny et al, 2007; Mierzejewska & Jagura-Burdzy, 2012; Ptacin et al, 2010). Interestingly, by studying Spo0J in this work, this thesis has provided unforeseen insights into how Z ring positioning may be regulated in *B. subtilis*. Initial investigations presented in Chapter 3 revealed that Spo0J does contribute to preventing midcell Z ring assembly during the early stages of DNA replication, and that this effect correlated with changes to nucleoid morphology. A question arising from these findings was whether the increase in frequency of midcell Z rings was due to changes in Noc localisation and therefore a result of relieving Noc-mediated nucleoid occlusion. However Noc localisation investigations in Chapter 4 found that during a block to initiation of DNA replication, in the absence of *spo0J*, Noc nonetheless localised with the DNA, suggesting that Noc localisation and, by extension, Noc activity, was not affected when initiation of DNA replication was blocked in the absence of s*po0J*. It was thus questioned whether the impact Noc and Spo0J were having on Z ring positioning during DNA initiation replication was additive, therefore bringing the Ready-Set-Go model and the idea of cell cycle checkpoints linking the progression of initiation to Z ring positioning into question.

Indeed, one of the most important advancements in knowledge arising from this research is that Z ring positioning is not linked to the early stages of DNA replication: Z rings can form at midcell regardless of the block to the initiation stage. For years it has been proposed that Z ring positioning was linked to the initiation stage of DNA replication, an attractive idea paralleling the checkpoints found in the eukaryotic cell cycle. There were multiple studies supporting these ideas through investigating the relationship between different replication blocks, nucleoid morphology and Z ring positioning (Harry et al, 1999; Moriya et al, 2010; Regamey et al, 2000). However,

this thesis provides conclusive evidence that there is no such link and that it can potentially be explained by the effect of two proteins, Noc and Spo0J. Chapter 4 results showed that deleting both *spo0J* and *noc*, the effect of the early versus late stage of initiation potentiating the midcell site for Z ring formation is abolished, and instead Z rings are able to form at midcell to wild-type levels at both the early and late stages of DNA replication initiation. Overall, it was found that, at least in *B. subtilis*, Noc and Spo0J are all that are required to prevent Z rings assembly at the cell centre when the early stages of DNA initiation replication are blocked. These findings change our perception of the bacterial cell cycle.

Could this observation also hold true in other bacteria? A link between DNA replication and midcell Z ring assembly has similarly been suggested in *E. coli.* Cambridge *et al.* found when DNA synthesis was blocked, midcell Z ring assembly was also inhibited (Cambridge et al, 2014). Importantly, this midcell Z ring inhibition occurred in a SlmA-, MinC- and SOS-independent manner. Could there be a SlmA-independent inhibitory factor in *E. coli* that prevents Z rings from forming over the unreplicated nucleoid? Although *E. coli* does not have a Spo0J homologue, it is possible that there are other factors within the bacterium that affect nucleoid morphology in a similar manner to Spo0J, for example the *E. coli* Muk proteins (Danilova et al, 2007; Nicolas et al, 2014; Rybenkov et al, 2014).

While the findings presented in this thesis suggest that there is no link between Z ring positioning and the early stages of DNA replication initiation, it does not rule out the possibility that there is a link between Z ring formation and DNA replication initiation. Arjes *et al.* supports this idea having found that Z ring formation (not positioning) does require DNA replication initiation. It was seen that blocking DNA replication in both *B. subtilis* and *S. aureus* leads to an irrecoverable arrest in division, and vice versa (Arjes et al, 2014). Combining the findings of both this study and Arjes *et al.* it appears that blocking DNA replication leads to the loss of information about forming the Z ring, however, this information is not positional. So how is the positional cue or the signpost for Z ring assembly determined? The data presented in this study suggest that firstly, Noc and Spo0J do not define the signpost but instead block its use, and secondly, if there is a signpost then it is not defined by

the early stages of initiation of DNA replication. Given that the earliest block to initiation of DNA replication (*dna-1*) allows for complete midcell Z ring assembly when *spo0J* and *noc* are absent, then it would suggest that the positional signpost for Z ring assembly is determined prior to this early stage of initiation of DNA replication. This raises the question of what defines the signpost. For example, there could be some unknown factor related to the absolute first stage of initiation of DNA replication where the initiator protein DnaA is recruited to *oriC* and the double stranded DNA begins to unwind. Another example could be that the signpost is determined in the previous round of division. This idea has been speculated on previously with the observation that, following DNA replication, sister origins bi-directionally segregate to the future division site (Wang et al, 2014b). Thus it is possible that when the new sister origins arrive at the ¼ and ¾ positions, they identify the next division site. How this site is determined by the chromosomes, how the origins know to position themselves there, and whether this creates the signpost for Z ring assembly is yet to be extensively explored.

6.2 Potential roles for Spo0J in the regulation of Z ring positioning

The data presented in this study suggest a role for Spo0J in regulating Z ring positioning during the early stages of DNA replication. One of the key pieces of data that supports this potential regulatory role for Spo0J is that in the *spo0J noc* double mutant, Z ring assembly occurs at midcell to wild-type levels regardless of what stage of initiation of DNA replication is blocked. That is, deletion of *noc* only allows for partial increase in midcell Z ring assembly, and the further deletion of *spo0J* allows for complete restoration of midcell Z ring assembly creating an additive effect. How Spo0J is functioning to do so is unclear, however, there are two possibilities to consider: Spo0J is either a nucleoid occlusion protein, or it is aiding an unknown nucleoid occlusion effect.

6.2.1 Is Spo0J a nucleoid occlusion protein?

Spo0J has been shown to have two separate functions within the cell: initiation of DNA replication and chromosome segregation (Autret et al, 2001; Lee & Grossman, 2006; Ogura et al, 2003). These two functions appear to reside in two separate domains of the protein, identified through point mutations (Gruber & Errington, 2009). The data from Chapters 3 and 4 are consistent with the idea that the absence of Spo0J changes the nucleoid morphology and it is that change that allows the Z ring to form at the midcell. How is Spo0J changing the nucleoid morphology? It is possible that it does so through its chromosome segregation partner, SMC, which is known to exhibit the same, if not more severe nucleoid morphology changes (Britton et al, 1998; Gruber et al, 2014; Wang et al, 2014c). This is the simplest explanation, but it could not be ruled out that Spo0J has an additional role in affecting Z ring positioning. To dissect this question, the point mutations separating the two functions of Spo0J were utilised (Gruber & Errington, 2009).

The results demonstrated that when initiation of DNA replication was blocked, the chromosome segregation point mutant of *spo0J* elicited the same nucleoid morphology as that as a *spo0J* null mutant. However changing the nucleoid morphology was not sufficient to restore midcell Z ring assembly to the same extent as that of the *spo0J* null. To further support this finding, Z ring positioning was also examined when initiation of DNA replication was blocked in SMC-depleted outgrown spores. Like the *spo0J* point mutations, nucleoid morphologies were significantly affected in SMC depleted cells; however, midcell Z ring assembly was again not restored to that of a *spo0J* null mutant. Collectively, the results presented in Chapter 5 support the idea that Spo0J has a function in addition to changing nucleoid morphology that is required to inhibit midcell Z ring assembly when initiation of DNA replication is blocked, and this function could be nucleoid occlusion.

Noc is thus far the only known nucleoid occlusion protein in *B. subtilis*. However the data presented in this study lead to the possibility that Spo0J too is a nucleoid occlusion protein. Indeed there are distinct similarities between Noc and Spo0J which suggest that Spo0J may have some nucleoid occlusion function. These include

sequence identity, DNA-binding affinity and nucleoprotein complex formation (Adams et al, 2014; Graham et al, 2014; Murray et al, 2006). However, the number and spread of binding sites between the two proteins is significantly different, with over 70 Noc DNA-binding sites in comparison to 10 Spo0J DNA-binding sites, eight of which are concentrated near the origin of replication (Lin & Grossman, 1998). Therefore, if Spo0J does have a nucleoid occlusion function, it is likely different to Noc (for example, Spo0J might act specifically around the origin region), and requires further investigation. For example, as suggested in Chapter 5, over-expression of *spo0J* may lead to cell division inhibition and filamentation, paralleling that seen in the over-expression of *noc.* Alternatively, exploration of specific point mutations of *spo0J* may allow for isolation of this nucleoid occlusion function within the protein. If so, when initiation of DNA replication is blocked, the point mutation should allow for increase in midcell Z ring assembly to the same level as that of a *spo0J* null strain.

6.2.2 Is Spo0J masking an unexplored aspect of how the chromosome impacts Z ring positioning?

Recent work has shown that Spo0J has a clear role in organising the origin (Marbouty et al, 2015; Wang et al, 2017; Wang et al, 2015; Wang et al, 2014c). Indeed, in this study when *spo0J* is absent in the *dna-1* mutation, significantly more bilobed nucleoids are observed and so are more midcell Z rings observed. Interestingly, Wang *et al.* demonstrated that these bilobes in the *dna-1* mutation represent two arms of the chromosome (Wang et al, 2017). Whether these bilobes are observed by Wang et al are the same as seen here in this study in the *dna-1 spo0J* needs to be tested, however assuming that they are, then this suggests that there is something about this morphology that is important in Z ring positioning. In other words, arm resolution allows for midcell Z ring assembly. It is possible that Spo0J could play a role in Z ring positioning by affecting some aspect of how the chromosome arms are held together during initiation of DNA replication. If so, then loss of Spo0J may lead to loss of chromosome arm interactions required for gene clustering, interacting proteins, protein complex formation or some other form of activity at the origin

inhibiting early midcell Z ring formation. For instance, it could be potentially relieving an inhibitory effect of transertion by changing the way in which transertion activity is generated from the nucleoid. Instead of this transertion activity being concentrated in one area, for example, between a single-lobed nucleoid and the membrane, this activity could be split into two distinct regions corresponding with the nucleoid bilobes and it is this that allows for the Z ring to assemble at midcell.

The transertion theory of the coupling of transcription, translation and subsequent insertion of nascent proteins into the membrane, remains an interesting one that has yet to be explored extensively. A leading area of the chromosome likely to play into transertion is the origin of replication due to very high levels of transcription in the region (Davies & Lewis, 2003; Karlin et al, 2001; Woldringh, 2002). Indeed ribosomal and translation-transcription genes in *B. subtilis* predicted to have high levels of expression can be mapped to the 20% origin-proximal region (Davies & Lewis, 2003; Karlin et al, 2001). It is important to note that ribosomal activity largely remains localised to its region of transcription and translation, thus creating a region of high protein concentration or crowding (Campos & Jacobs-Wagner, 2013; Montero Llopis et al, 2010). Interestingly, these gene locations mirror that of the *parS* sequences to which Spo0J binds, spreads and bridges neighbouring DNA to form nucleoprotein complexes (Graham et al, 2014). Albeit highly speculative, it is possible to draw comparison to the Woldringh's transertion theory whereby Spo0J may be required to draw in and bridge the DNA into gene clusters at *oriC* involved in high levels of local protein production at *oriC.* This would thus create an area of protein crowding to inhibit Z ring assembly. This idea is supported by data in this study with the observed bilobed nucleoids, and loss of centralized positioning of *oriC* when Spo0J is absent (Chapter 3). Thus when initiation of DNA replication is blocked in the absence of *spo0J*, this area of high transcription and translation activity is no longer positioned at the cell centre and the subsequent protein crowding is lost with the formation of bilobed or spread nucleoids, thus allowing midcell Z ring assembly.

To examine the possible involvement of Spo0J and *oriC* in such a process, it would be interesting to examine Z ring positioning in mutants where the origin has been relocated elsewhere on the chromosome, for example, to the terminus region. This

would decrease the level of transertion activity at the origin, and, therefore, would allow for more Z rings to form at the cell centre when initiation of DNA replication is blocked. Alternatively, it would be intriguing to examine whether over-expression of an origin-proximal highly transcribed gene is able to supersede the effects of a *spo0J* null strain when initiation of DNA replication is blocked. For example, the HPUra condition in the absence of *spo0J* leads to a significant increase in midcell Z rings (57%) and bilobed nucleoids. Would over-expression of an origin-proximal highly transcribed gene supersede this and create an inhibitory effect such that there is a decrease in midcell Z rings (less than 57%) and more single-lobed nucleoids? If so, this would support the idea of transertion and localised protein crowding around the DNA creating a Z ring inhibitory zone.

It is clear that Spo0J is a multifaceted protein; however, investigation into this protein has revealed that there is more about the chromosome and Spo0J in regulating cell division than originally thought. Further investigation into Spo0J is an exciting prospect and is likely to continue to provide unforeseen insights into how bacteria regulate their cell cycle.

References

Abeles AL, Friedman SA, Austin SJ (1985) Partition of unit-copy miniplasmids to daughter cells: III. The DNA sequence and functional organization of the P1 partition region. *Journal of molecular biology* **185:** 261-272

Adams DW, Errington J (2009) Bacterial cell division: assembly, maintenance and disassembly of the Z ring. *Nat Rev Micro* **7:** 642-653

Adams DW, Wu LJ, Errington J (2014) Cell cycle regulation by the bacterial nucleoid. *Curr Opin Microbiol* **22:** 94-101

Adams DW, Wu LJ, Errington J (2015) Nucleoid occlusion protein Noc recruits DNA to the bacterial cell membrane. *The EMBO journal* **34:** 491-501

Arjes Heidi A, Kriel A, Sorto Nohemy A, Shaw Jared T, Wang Jue D, Levin Petra A (2014) Failsafe Mechanisms Couple Division and DNA Replication in Bacteria. *Current Biology* **24:** 2149-2155

Autret S, Nair R, Errington J (2001) Genetic analysis of the chromosome segregation protein Spo0J of Bacillus subtilis: evidence for separate domains involved in DNA binding and interactions with Soj protein. *Molecular microbiology* **41:** 743-755

Badrinarayanan A, Le TBK, Laub MT (2015) Bacterial chromosome organization and segregation. *Annual review of cell and developmental biology* **31:** 171-199

Bailey MW, Bisicchia P, Warren BT, Sherratt DJ, Mannik J (2014) Evidence for divisome localization mechanisms independent of the Min system and SlmA in Escherichia coli. *PLoS genetics* **10:** e1004504

Bakshi S, Choi H, Mondal J, Weisshaar JC (2014) Time-dependent effects of transcription- and translation-halting drugs on the spatial distributions of the Escherichia coli chromosome and ribosomes. *Molecular microbiology* **94:** 871-887

Bakshi S, Choi H, Weisshaar JC (2015) The spatial biology of transcription and translation in rapidly growing Escherichia coli. *Frontiers in microbiology* **6:** 636

Bates D, Kleckner N (2005) Chromosome and Replisome Dynamics in E. coli: Loss of Sister Cohesion Triggers Global Chromosome Movement and Mediates Chromosome Segregation. *Cell* **121:** 899-911

Bazill GW, Gross JD (1972) Effect of 6-(p-hydroxyphenyl)-azouracil on B. subtilis DNA polymerases. *Nature: New biology* **240:** 82-83

Beattie TR, Reyes-Lamothe R (2015) A Replisome's journey through the bacterial chromosome. *Frontiers in microbiology* **6**

Berkmen MB, Grossman AD (2007) Subcellular positioning of the origin region of the Bacillus subtilis chromosome is independent of sequences within oriC, the site of replication initiation, and the replication initiator DnaA. *Molecular microbiology* **63:** 150-165

Bernard R, Marquis KA, Rudner DZ (2010) Nucleoid occlusion prevents cell division during replication fork arrest in Bacillus subtilis. *Molecular microbiology* **78:** 866-882

Bernhardt TG, de Boer PAJ (2005) SlmA, a Nucleoid-Associated, FtsZ Binding Protein Required for Blocking Septal Ring Assembly over Chromosomes in E. coli. *Molecular cell* **18:** 555-564

Blikstad C, Ivarsson Y (2015) High-throughput methods for identification of protein-protein interactions involving short linear motifs. *Cell communication and signaling : CCS* **13:** 38

Britton RA, Lin DC-H, Grossman AD (1998) Characterization of a prokaryotic SMC protein involved in chromosome partitioning. *Genes & development* **12:** 1254-1259

Broedersz CP, Wang X, Meir Y, Loparo JJ, Rudner DZ, Wingreen NS (2014) Condensation and localization of the partitioning protein ParB on the bacterial chromosome. *Proceedings of the National Academy of Sciences of the United States of America* **111:** 8809-8814

Bruand C, Ehrlich SD, Janniere L (1995) Primosome Assembly Site in Bacillus subtilis. *The EMBO journal* **14:** 2642-2650

Buss J, Coltharp C, Huang T, Pohlmeyer C, Wang SC, Hatem C, Xiao J (2013) In vivo organization of the FtsZ-ring by ZapA and ZapB revealed by quantitative super-resolution microscopy. *Molecular microbiology* **89:** 1099-1120

Buss J, Coltharp C, Shtengel G, Yang X, Hess H, Xiao J (2015) A multi-layered protein network stabilizes the Escherichia coli FtsZ-ring and modulates constriction dynamics. *PLoS genetics* **11:** e1005128

Buss JA, Peters NT, Xiao J, Bernhardt TG (2017) ZapA and ZapB form an FtsZ-independent structure at midcell. *Molecular microbiology* **104:** 652-663

Bussiere DE, Bastia D (1999) Termination of DNA replication of bacterial and plasmid chromosomes. *Molecular microbiology* **31:** 1611-1618

Cabre EJ, Monterroso B, Alfonso C, Sanchez-Gorostiaga A, Reija B, Jimenez M, Vicente M, Zorrilla S, Rivas G (2015) The Nucleoid Occlusion SlmA Protein Accelerates the Disassembly of the FtsZ Protein Polymers without Affecting Their GTPase Activity. *PloS one* **10:** e0126434

Cambridge J, Blinkova A, Magnan D, Bates D, Walker JR (2014) A replication-inhibited unsegregated nucleoid at mid-cell blocks Z-ring formation and cell division independently of SOS and the SlmA nucleoid occlusion protein in Escherichia coli. *Journal of bacteriology* **196:** 36-49

Campos M, Jacobs-Wagner C (2013) Cellular organization of the transfer of genetic information. *Current Opinion in Microbiology* **16:** 171-176

Chen BW, Lin MH, Chu CH, Hsu CE, Sun YJ (2015) Insights into ParB spreading from the complex structure of Spo0J and parS. *Proceedings of the National Academy of Sciences of the United States of America* **112:** 6613-6618

Cho H, Bernhardt TG (2013) Identification of the SlmA active site responsible for blocking bacterial cytokinetic ring assembly over the chromosome. *PLoS genetics* **9:** e1003304

Cho H, McManus HR, Dove SL, Bernhardt TG (2011) Nucleoid occlusion factor SlmA is a DNA-activated FtsZ polymerization antagonist. *Proceedings of the National Academy of Sciences of the United States of America* **108:** 3773-3778

Cozzarelli NR (1977) The mechanism of action of inhibitors of DNA synthesis. *Annual review of biochemistry* **46:** 641-668

Daniel RA, Errington J (2003) Control of cell morphogenesis in bacteria: Two distinct ways to make a rod-shaped cell. *Cell* **113:** 767-776

Danilova O, Reyes-Lamothe R, Pinskaya M, Sherratt D, Possoz C (2007) MukB colocalizes with the oriC region and is required for organization of the two Escherichia coli chromosome arms into separate cell halves. *Molecular microbiology* **65:** 1485-1492

Davies KM, Lewis PJ (2003) Localization of rRNA synthesis in Bacillus subtilis: characterization of loci involved in transcription focus formation. *Journal of bacteriology* **185:** 2346-2353

de Boer PAJ (2010) Advances in understanding E. coli cell fission. *Current Opinion in Microbiology* **13:** 730-737

de Boer PAJ, Crossley RE, Rothfield LI (1989) A division inhibitor and a topological specificity factor coded for by the minicell locus determine proper placement of the division septum in E. coli. *Cell* **56:** 641-649

Di Ventura B, Knecht B, Andreas H, Godinez WJ, Fritsche M, Rohr K, Nickel W, Heermann DW, Sourjik V (2013) Chromosome segregation by the Escherichia coli Min system. *Molecular Systems Biology* **9:** 686

Donczew M, Mackiewicz P, Wrobel A, Flardh K, Zakrzewska-Czerwinska J, Jakimowicz D (2016) ParA and ParB coordinate chromosome segregation with cell elongation and division during Streptomyces sporulation. *Open biology* **6:** 150263

Donovan C, Schwaiger A, Kramer R, Bramkamp M (2010) Subcellular localization and characterization of the ParAB system from Corynebacterium glutamicum. *Journal of bacteriology* **192:** 3441-3451

Du S, Lutkenhaus J (2014) SlmA antagonism of FtsZ assembly employs a two-pronged mechanism like MinCD. *PLoS genetics* **10:** e1004460

Duderstadt KE, Mott ML, Crisona NJ, Chuang K, Yang H, Berger JM (2010) Origin Remodeling and Opening in Bacteria Rely on Distinct Assembly States of the DnaA Initiator. *Journal of Biological Chemistry* **285:** 28229-28239

Duggin IG, Wake RG, Bell SD, Hill TM (2008) The replication fork trap and termination of chromosome replication. *Molecular microbiology* **70:** 1323-1333

Elledge SJ (1996) Cell cycle checkpoints: preventing an identity crisis. *Science* **274:** 1664-1672

Fernandez-Fernandez C, Gonzalez D, Collier J (2011) Regulation of the Activity of the Dual-Function DnaA Protein in Caulobacter crescentus. *PloS one* **6:** e26028

Fleurie A, Lesterlin C, Manuse S, Zhao C, Cluzel C, Lavergne J-P, Franz-Wachtel M, Macek B, Combet C, Kuru E, VanNieuwenhze MS, Brun YV, Sherratt D, Grangeasse C (2014) MapZ marks the division sites and positions FtsZ rings in Streptococcus pneumoniae. *Nature* **516:** 259-262

Funnell BE (1988) Participation of Escherichia coli integration host factor in the P1 plasmid partition system. *Proceedings of the National Academy of Sciences of the United States of America* **85:** 6657-6661

Glaser P, Sharpe ME, Raether B, Perego M, Ohlsen K, Errington J (1997) Dynamic, mitotic-like behavior of a bacterial protein required for accurate chromosome partitioning. *Genes & development* **11:** 1160-1168

Graham TGW, Wang X, Song D, Etson CM, van Oijen AM, Rudner DZ, Loparo JJ (2014) ParB spreading requires DNA bridging. *Genes & development* **28:** 1228-1238

Grainge I, Bregu M, Vazquez M, Sivanathan V, Ip SC, Sherratt DJ (2007) Unlinking chromosome catenanes in vivo by site-specific recombination. *The EMBO journal* **26:** 4228-4238

Grainge I, Lesterlin C, Sherratt DJ (2011) Activation of XerCD-dif recombination by the FtsK DNA translocase. *Nucleic acids research* **39:** 5140-5148

Griffith KL, Grossman AD (2008) Inducible protein degradation in Bacillus subtilis using heterologous peptide tags and adaptor proteins to target substrates to the protease ClpXP. *Molecular microbiology* **70:** 1012-1025

Gruber S, Errington J (2009) Recruitment of Condensin to Replication Origin Regions by ParB/SpoOJ Promotes Chromosome Segregation in B. subtilis. *Cell* **137:** 685-696

Gruber S, Veening JW, Bach J, Blettinger M, Bramkamp M, Errington J (2014) Interlinked sister chromosomes arise in the absence of condensin during fast replication in B. subtilis. *Current biology : CB* **24:** 293-298

Haeusser DP, Margolin W (2016) Splitsville: structural and functional insights into the dynamic bacterial Z ring. *Nature reviews Microbiology* **14:** 305-319

Hajduk IV, Rodrigues CDA, Harry EJ (2016) Connecting the dots of the bacterial cell cycle: Coordinating chromosome replication and segregation with cell division. *Seminars in Cell & Developmental Biology* **53:** 2-9

Harashima H, Dissmeyer N, Schnittger A (2013) Cell cycle control across the eukaryotic kingdom. *Trends in cell biology* **23:** 345-356

Harry E, Monohan L, Thompson L (2006) Bacterial Cell Division: The Mechanism and Its Precision. *International Review of Cytology* **253:** 27-94

Harry EJ (2001) Coordinating DNA replication with cell division: lessons from outgrowing spores. *Biochimie* **83:** 75-81

Harry EJ, Pogliano K, Losick R (1995) Use of immunofluorescence to visualize cell-specific gene expression during sporulation in Bacillus subtilis. *Journal of bacteriology* **177:** 3386-3393

Harry EJ, Rodwell J, Wake RG (1999) Co-ordinating DNA replication with cell division in bacteria: a link between the early stages of a round of replication and mid-cell Z ring assembly. *Molecular microbiology* **33:** 33-40

Hartwell LH, Weinert TA (1989) Checkpoints: controls that ensure the order of cell cycle events. *Science* **246:** 629-634

Hensel Z, Weng X, Lagda AC, Xiao J (2013) Transcription-factor-mediated DNA looping probed by high-resolution, single-molecule imaging in live E. coli cells. *PLoS biology* **11:** e1001591

Hiraga S (2000) Dynamic Localization of Bacterial and Plasmid Chromosomes. *Annual Review of Genetics* **34:** 21-59

Holečková N, Doubravová L, Massidda O, Molle V, Buriánková K, Benada O, Kofroňová O, Ulrych A, Branny P (2015) LocZ Is a New Cell Division Protein Involved in Proper Septum Placement in Streptococcus pneumoniae. *mBio* **6**

Ireton K, Gunther NW, 4th, Grossman AD (1994) spo0J is required for normal chromosome segregation as well as the initiation of sporulation in Bacillus subtilis. *J Bacteriol* **176:** 5320-5329

Jin DJ, Cagliero C, Zhou YN (2013) Role of RNA polymerase and transcription in the organization of the bacterial nucleoid. *Chemical reviews* **113:** 8662-8682

Jun S, Mulder B (2006) Entropy-driven spatial organization of highly confined polymers: Lessons for the bacterial chromosome. *Proceedings of the National Academy of Sciences of the United States of America* **103:** 12388-12393

Junier I, Boccard F, Espéli O (2014) Polymer modeling of the E. coli genome reveals the involvement of locus positioning and macrodomain structuring for the control of chromosome conformation and segregation. *Nucleic acids research* **42:** 1461-1473

Kaguni JM (2006) DnaA: Controlling the Initiation of Bacterial DNA Replication and More. *Annual Review of Microbiology* **60:** 351-371

Kaimer C, Schenk K, Graumann PL (2011) Two DNA Translocases Synergistically Affect Chromosome Dimer Resolution in Bacillus subtilis. *Journal of bacteriology* **193:** 1334-1340

Karlin S, Mrazek J, Campbell A, Kaiser D (2001) Characterizations of highly expressed genes of four fast-growing bacteria. *Journal of bacteriology* **183:** 5025-5040

Katayama T, Ozaki S, Keyamura K, Fujimitsu K (2010) Regulation of the replication cycle: conserved and diverse regulatory systems for DnaA and oriC. *Nature Reviews Microbiology* **8:** 163-170

Kretschmer S, Schwille P (2014) Toward Spatially Regulated Division of Protocells: Insights into the E. coli Min System from in Vitro Studies. *Life* **4:** 915-928

Le TBK, Imakaev MV, Mirny LA, Laub MT (2013) High-Resolution Mapping of the Spatial Organization of a Bacterial Chromosome. *Science* **342:** 731-734

Le TBK, Laub MT (2014) New approaches to understanding the spatial organization of bacterial genomes. *Current Opinion in Microbiology* **22:** 15-21

Lee PS, Grossman AD (2006) The chromosome partitioning proteins Soj (ParA) and Spo0J (ParB) contribute to accurate chromosome partitioning, separation of replicated sister origins, and regulation of replication initiation in Bacillus subtilis. *Molecular microbiology* **60:** 853-869

Lemon KP, Grossman AD (2000) Movement of replicating DNA through a stationary replisome. *Molecular cell* **6:** 1321-1330

Lemon KP, Kurtser I, Grossman AD (2001) Effects of replication termination mutants on chromosome partitioning in Bacillus subtilis. *Proceedings of the National Academy of Sciences of the United States of America* **98:** 212-217

Lewis PJ (2001) Bacterial chromosome segregation. *Microbiology* **147:** 519-526

Lin DC-H, Grossman AD (1998) Identification and Characterization of a Bacterial Chromosome Partitioning Site. *Cell* **92:** 675-685

Livny J, Yamaichi Y, Waldor MK (2007) Distribution of Centromere-Like parS Sites in Bacteria: Insights from Comparative Genomics. *Journal of bacteriology* **189:** 8693-8703

Lutkenhaus J, Pichoff S, Du S (2012) Bacterial cytokinesis: From Z ring to divisome. *Cytoskeleton* **69:** 778-790

Maloney E, Madiraju M, Rajagopalan M (2009) Overproduction and localization of Mycobacterium tuberculosis ParA and ParB proteins. *Tuberculosis* **89 Suppl 1:** S65-69

Marbouty M, Le Gall A, Cattoni DI, Cournac A, Koh A, Fiche JB, Mozziconacci J, Murray H, Koszul R, Nollmann M (2015) Condensin- and Replication-Mediated Bacterial Chromosome Folding and Origin Condensation Revealed by Hi-C and Super-resolution Imaging. *Molecular cell* **59:** 588-602

Margalit DN, Romberg L, Mets RB, Hebert AM, Mitchison TJ, Kirschner MW, RayChaudhuri D (2004) Targeting cell division: Small-molecule inhibitors of FtsZ GTPase perturb cytokinetic ring assembly and induce bacterial lethality. *Proceedings of the National Academy of Sciences of the United States of America* **101:** 11821-11826

Margolin W, Rowlett VW (2015) The Min system and other nucleoid-independent regulators of Z ring positioning. *Frontiers in microbiology* **6**

Marston AL, Errington J (1999) Dynamic Movement of the ParA-like Soj Protein of B. subtilis and Its Dual Role in Nucleoid Organization and Developmental Regulation. *Molecular cell* **4:** 673-682

McCullum EO, Williams BA, Zhang J, Chaput JC (2010) Random mutagenesis by error-prone PCR. *Methods in molecular biology* **634:** 103-109

Mierzejewska J, Jagura-Burdzy G (2012) Prokaryotic ParA–ParB–parS system links bacterial chromosome segregation with the cell cycle. *Plasmid* **67:** 1-14

Monahan LG, Hajduk IV, Blaber SP, Charles IG, Harry EJ (2014) Coordinating Bacterial Cell Division with Nutrient Availability: a Role for Glycolysis. *mBio* **5**

Montero Llopis P, Jackson AF, Sliusarenko O, Surovtsev I, Heinritz J, Emonet T, Jacobs-Wagner C (2010) Spatial organization of the flow of genetic information in bacteria. *Nature* **466:** 77-81

Moriya S, Rashid RA, Rodrigues CDA, Harry EJ (2010) Influence of the nucleoid and the early stages of DNA replication on positioning the division site in Bacillus subtilis. *Molecular microbiology* **76:** 634-647

Murray H, Errington J (2008) Dynamic Control of the DNA Replication Initiation Protein DnaA by Soj/ParA. *Cell* **135:** 74-84

Murray H, Ferreira H, Errington J (2006) The bacterial chromosome segregation protein Spo0J spreads along DNA from parS nucleation sites. *Molecular microbiology* **61:** 1352-1361

Muteeb G, Sen R (2010) Random mutagenesis using a mutator strain. *Methods in molecular biology* **634:** 411-419

Nicolas E, Upton AL, Uphoff S, Henry O, Badrinarayanan A, Sherratt D (2014) The SMC Complex MukBEF Recruits Topoisomerase IV to the Origin of Replication Region in Live Escherichia coli. *mBio* **5**

Nijman SM (2011) Synthetic lethality: general principles, utility and detection using genetic screens in human cells. *FEBS letters* **585:** 1-6

Niki H, Jaffé A, Imamura R, Ogura T, Hiraga S (1991) The new gene mukB codes for a 177 kd protein with coiled-coil domains involved in chromosome partitioning of E. coli. *The EMBO journal* **10:** 183-193

Norris V (1995) Hypothesis: chromosome separation in Escherichia coli involves autocatalytic gene expression, transertion and membrane-domain formation. *Molecular microbiology* **16:** 1051-1057

Norris V, Madsen MS (1995) Autocatalytic gene expression occurs via transertion and membrane domain formation and underlies differentiation in bacteria: a model. *Journal of molecular biology* **253:** 739-748

Ogasawara N, Yoshikawa H (1992) Genes and their organization in the replication origin region of the bacterial chromosome. *Molecular microbiology* **6:** 629-634

Ogura Y, Ogasawara N, Harry EJ, Moriya S (2003) Increasing the Ratio of Soj to Spo0J Promotes Replication Initiation in Bacillus subtilis. *Journal of bacteriology* **185:** 6316-6324

Okumura H, Yoshimura M, Ueki M, Oshima T, Ogasawara N, Ishikawa S (2012) Regulation of chromosomal replication initiation by oriC-proximal DnaA-box clusters in Bacillus subtilis. *Nucleic acids research* **40:** 220-234

Pang T, Wang X, Lim HC, Bernhardt TG, Rudner DZ (2017) The nucleoid occlusion factor Noc controls DNA replication initiation in Staphylococcus aureus. *PLoS genetics* **13:** e1006908

Pichoff S, Lutkenhaus J (2001) Escherichia coli Division Inhibitor MinCD Blocks Septation by Preventing Z-Ring Formation. *Journal of bacteriology* **183:** 6630-6635

Pomerantz RT, O'Donnell M (2007) Replisome mechanics: insights into a twin DNA polymerase machine. *Trends in microbiology* **15:** 156-164

Ptacin JL, Lee SF, Garner EC, Toro E, Eckart M, Comolli LR, Moerner WE, Shapiro L (2010) A spindle-like apparatus guides bacterial chromosome segregation. *Nature cell biology* **12:** 791-798

Reeve JN, Mendelso.Nh, Coyne SI, Hallock LL, Cole RM (1973) Minicells of Bacillus subtilis. *Journal of bacteriology* **114:** 860-873

Regamey A, Harry EJ, Wake RG (2000) Mid-cell Z ring assembly in the absence of entry into the elongation phase of the round of replication in bacteria: co-ordinating chromosome replication with cell division. *Molecular microbiology* **38:** 423-434

Rodrigues C (2011) Establishing how Bacterial Cells Position the Division Site University of Technology Sydney, Sydney, Australia

Rodrigues CDA, Harry EJ (2012) The Min System and Nucleoid Occlusion Are Not Required for Identifying the Division Site in Bacillus subtilis but Ensure Its Efficient Utilization. *PLoS genetics* **8:** e1002561

Rybenkov VV, Herrera V, Petrushenko ZM, Zhao H (2014) MukBEF, a Chromosomal Organizer. *Journal of molecular microbiology and biotechnology* **24:** 371-383

Sambrook J, Fritsch EF, Maniatis T (1989) *Molecular cloning : a laboratory manual*, Cold Spring Harbor, N.Y.: Cold Spring Harbor Laboratory.

Scholefield G, Whiting R, Errington J, Murray H (2011) Spo0J regulates the oligomeric state of Soj to trigger its switch from an activator to an inhibitor of DNA replication initiation. *Molecular microbiology* **79:** 1089-1100

Shih Y-L, Zheng M (2013) Spatial control of the cell division site by the Min system in Escherichia coli. *Environmental Microbiology* **15:** 3229-3239

Sievers J, Raether B, Perego M, Errington J (2002) Characterization of the parB-Like yyaA Gene of Bacillus subtilis. *Journal of bacteriology* **184:** 1102-1111

Sivanathan V, Emerson JE, Pages C, Cornet F, Sherratt DJ, Arciszewska LK (2009) KOPS-guided DNA translocation by FtsK safeguards Escherichia coli chromosome segregation. *Molecular microbiology* **71:** 1031-1042

Smits WK, Goranov AI, Grossman AD (2010) Ordered association of helicase loader proteins with the Bacillus subtilis origin of replication in vivo. *Molecular microbiology* **75:** 452-461

Sullivan NL, Marquis KA, Rudner DZ (2009) Recruitment of SMC by ParB-parS Organizes the Origin Region and Promotes Efficient Chromosome Segregation. *Cell* **137:** 697-707

Sun Q, Margolin W (1998) FtsZ dynamics during the division cycle of live Escherichia coli cells. *Journal of bacteriology* **180:** 2050-2056

Sun Q, Margolin W (2004) Effects of perturbing nucleoid structure on nucleoid occlusion-mediated toporegulation of FtsZ ring assembly. *Journal of bacteriology* **186:** 3951-3959

Szwedziak P, Wang Q, Bharat TAM, Tsim M, Löwe J (2015) Architecture of the ring formed by the tubulin homologue FtsZ in bacterial cell division. *eLife* **3:** e04601

Tan CM, Therien AG, Lu J, Lee SH, Caron A, Gill CJ, Lebeau-Jacob C, Benton-Perdomo L, Monteiro JM, Pereira PM, Elsen NL, Wu J, Deschamps K, Petcu M, Wong S, Daigneault E, Kramer S, Liang L, Maxwell E, Claveau D, Vaillancourt J, Skorey K, Tam J, Wang H, Meredith TC, Sillaots S, Wang-Jarantow L, Ramtohul Y, Langlois E, Landry F, Reid JC, Parthasarathy G, Sharma S, Baryshnikova A, Lumb KJ, Pinho MG, Soisson SM, Roemer T (2012) Restoring Methicillin-Resistant Staphylococcus aureus Susceptibility to β-Lactam Antibiotics. *Science Translational Medicine* **4:** 126ra135

Tanooka H, Munakata N, Kitahara S (1978) Mutation induction with UV- and X-radiations in spores and vegetative cells of Bacillus subtilis. *Mutation research* **49:** 179-186

Teather RM, Collins JF, Donachie WD (1974) Quantal Behavior of a Diffusible Factor Which Initiates Septum Formation at Potential Division Sites in Escherichia coli. *J Bacteriol* **118:** 407-413

Thanbichler M, Viollier PH, Shapiro L (2005) The structure and function of the bacterial chromosome. *Current Opinion in Genetics & Development* **15:** 153-162

Tonthat NK, Milam SL, Chinnam N, Whitfill T, Margolin W, Schumacher MA (2013) SlmA forms a higher-order structure on DNA that inhibits cytokinetic Z-ring formation over the nucleoid. *Proceedings of the National Academy of Sciences of the United States of America* **110:** 10586-10591

Traag B, van Wezel G (2008) The SsgA-like proteins in actinomycetes: small proteins up to a big task. *Antonie van Leeuwenhoek* **94:** 85-97

Treuner-Lange A, Aguiluz K, van der Does C, Gómez-Santos N, Harms A, Schumacher D, Lenz P, Hoppert M, Kahnt J, Muñoz-Dorado J, Søgaard-Andersen L (2013) PomZ, a ParA-like protein, regulates Z-ring formation and cell division in Myxococcus xanthus. *Molecular microbiology* **87:** 235-253

Veening JW, Murray H, Errington J (2009) A mechanism for cell cycle regulation of sporulation initiation in Bacillus subtilis. *Genes & development* **23:** 1959-1970

Veiga H, Jorge AM, Pinho MG (2011) Absence of nucleoid occlusion effector Noc impairs formation of orthogonal FtsZ rings during Staphylococcus aureus cell division. *Molecular microbiology* **80:** 1366-1380

Velten M, McGovern S, Marsin S, Ehrlich SD, Noirot P, Polard P (2003) A Two-Protein Strategy for the Functional Loading of a Cellular Replicative DNA Helicase. *Molecular cell* **11:** 1009-1020

Vollmer W (2006) The prokaryotic cytoskeleton: a putative target for inhibitors and antibiotics? *Applied Microbiology and Biotechnology* **73:** 37-47

Wang W, Li GW, Chen C, Xie XS, Zhuang X (2011) Chromosome organization by a nucleoid-associated protein in live bacteria. *Science* **333:** 1445-1449

Wang X, Brandao HB, Le TB, Laub MT, Rudner DZ (2017) Bacillus subtilis SMC complexes juxtapose chromosome arms as they travel from origin to terminus. *Science* **355:** 524-527

Wang X, Le TB, Lajoie BR, Dekker J, Laub MT, Rudner DZ (2015) Condensin promotes the juxtaposition of DNA flanking its loading site in Bacillus subtilis. *Genes & development* **29:** 1661-1675

Wang X, Montero Llopis P, Rudner DZ (2014a) Bacillus subtilis chromosome organization oscillates between two distinct patterns. *Proceedings of the National Academy of Sciences of the United States of America* **111:** 12877-12882

Wang X, Montero Llopis P, Rudner DZ (2014b) Bacillus subtilis chromosome organization oscillates between two distinct patterns. *Proceedings of the National Academy of Sciences* **111:** 12877-12882

Wang X, Rudner DZ (2014) Spatial organization of bacterial chromosomes. *Current Opinion in Microbiology* **22:** 66-72

Wang X, Tang OW, Riley EP, Rudner DZ (2014c) The SMC condensin complex is required for origin segregation in Bacillus subtilis. *Current biology : CB* **24:** 287-292

White K, Sueoka N (1973) Temperature-sensitive DNA synthesis mutants of Bacillus subtilis--appendix: theory of density transfer for symmetric chromosome replication. *Genetics* **73:** 185-214

Willemse J, Borst JW, de Waal E, Bisseling T, van Wezel GP (2011) Positive control of cell division: FtsZ is recruited by SsgB during sporulation of Streptomyces. *Genes & development* **25:** 89-99

Wilson AC, Szurmant H (2011) Transposon-mediated random mutagenesis of Bacillus subtilis. *Methods in molecular biology* **765:** 359-371

Wolanski M, Donczew R, Zawilak-Pawlik A, Zakrzewska J (2015) oriC-encoded instructions for the initiation of bacterial chromosome replication. *Frontiers in microbiology* **5**

Wolański M, Jakimowicz D, Zakrzewska-Czerwińska J (2014) Fifty Years after the Replicon Hypothesis: Cell-Specific Master Regulators as New Players in Chromosome Replication Control. *Journal of bacteriology* **196:** 2901-2911

Woldringh CL (2002) The role of co-transcriptional translation and protein translocation (transertion) in bacterial chromosome segregation. *Molecular microbiology* **45:** 17-29

Wu L, Franks A, Wake R (1995) Replication through the terminus region of the Bacillus subtilis chromosome is not essential for the formation of a division septum that partitions the DNA. *Journal of bacteriology* **177:** 5711-5715

Wu LJ, Errington J (2004) Coordination of cell division and chromosome segregation by a nucleoid occlusion protein in Bacillus subtillis. *Cell* **117:** 915-925

Wu LJ, Ishikawa S, Kawai Y, Oshima T, Ogasawara N, Errington J (2009) Noc protein binds to specific DNA sequences to coordinate cell division with chromosome segregation. *The EMBO journal* **28:** 1940-1952

Zhou M, Li Q, Wang R (2016) Current Experimental Methods for Characterizing Protein-Protein Interactions. *ChemMedChem* **11:** 738-756